DEVELOPMENT OF MULTI-FUNCTIONALIZED POLYMERIC CARRIERS FOR DELIVERY OF ANTICANCER DRUG COMBINATIONS

DUONG HOANG HANH PHUOC

NATIONAL UNIVERSITY OF SINGAPORE

2013

DEVELOPMENT OF MULTI-FUNCTIONALIZED CARRIERS FOR DELIVERY OF ANTICANCER DRUG COMBINATIONS

DUONG HOANG HANH PHUOC

(B. Eng., HOCHIMINH UNIVERSITY OF TECHNOLOGY, VIETNAM)

A THESIS SUBMITTED

FOR THE DEGREE OF DOCTOR OF PHILOSOPHY

DEPARTMENT OF CHEMICAL & BIOMOLECULAR ENGINEERING

NATIONAL UNIVERSITY OF SINGAPORE

2013

DECLARATION

I hereby declare that the thesis is my original work and it has been written by me in its entirety. I have duly acknowledged all the sources of information which have been used in the thesis.

This thesis has also not been submitted for any degree in any university previously.

Duong Hoang Hanh Phuoc

29 November 2013

ACKNOWLEDGEMENTS

First of all, I would like to express my deepest and most sincere gratitude to my supervisor, Professor Yung Lin Yue Lanry, for his endless help, support, guidance, and patience. Without his extremely generous help and support, it would have been impossible for me to accomplish my PhD study. I deeply appreciate him for giving me not only a lot of opportunities to learn but also freedom to try and explore new ideas. I am grateful to his advice, encouragement and care not only in research works but also in personal matters. I am privileged to have him, not just as a great and thoughtful supervisor, but as a good friend as well.

I would like to thank all friends and fellow graduate students in Prof. Yung's and Prof. Tong's lab, past and present, especially Ms Tan Weiling, Dr Deny Hartono, Miss Fong Kah Ee, Dr Zhao Shuang, Dr Luo Jingnan for their unconditional help and encouragement. I would like to convey my thanks to all lab technologists and friends from Chemical & Biomolecular Engineering Department of NUS whom I had worked closely with during my PhD study. I would like to express my thanks to Mdm Li Xiang for all her help, care and positive encouragement.

I would like to acknowledge National University of Singapore for giving me a research scholarship to pursue my PhD study.

Last but not least, I would like to express my most sincere appreciation to my family members for all their constant love, encouragement and support. My gratitude also goes to all other friends that had supported me in many ways during my PhD study.

TABLE OF CONTENTS

SUMMARY

Cancer is a major public health problem as one of the leading in causes of burden and causes of death diseases with more than one death by cancer among 8 deaths by all causes in global. The cancer mortality is even much higher in Singapore with more than 25% of deaths by cancer among all deaths. It is due to the lack of new generation of anticancer drugs with high chemotherapeutic effectiveness and low side-effects. Therefore, investigation of drug delivery systems using polymeric micelles as carriers with the enhancement in therapeutic efficacy, high selectivity and binding affinity to cancer cells has been aimed in this project for different cancer treatments.

Most of current clinical therapies are not sufficient to cancer treatments due to the non-specific delivery of therapeutic agents to healthy cells and the less penetration of therapeutic agents into cancer cells. The first objective of this work is to develop an effective system for anticancer drug delivery. The system has been developed for physically encapsulating of hydrophobic drugs because most of anticancer drugs are hydrophobic in nature. Self-assembled polymeric micelles based on biodegradable amphiphilic copolymer poly(D,L-lactide-co-glycolide)-poly(ethylene glycol)(PLGA-PEG) have been multi-functionalized using folate targeting moiety (FOL) and a cell penetrating peptide (TAT) to enhance the tumor targeting ability and the cellular uptake of carriers. The concentration of FOL and TAT combined modification on the carrier surface has been optimized.

Another strategy to reduce toxic side effects of chemotherapy is the treatment by combining different classes of chemotherapeutic drugs. Besides the reduction of side effects, enhancement in therapeutic efficacy can also be achieved at synergistic treatment combinations. Therefore, targeting delivery of combinations of two classes of anticancer drugs has been developed based on the optimized FOL/TAT-modified micellar system in the earlier study to further improve the treatment efficacy. The synergism in combination therapy depends on many factors such as the therapeutic mechanism of the drugs, the respond of certain cell lines to drugs, the combination ratio. A combined chemo-drug system for cancer treatments based on an antitumor antibiotic agent (doxorubicin, DOX) and a mitotic inhibitor agent (paclitaxel, PTX); and a combined system of PTX and a hormone drug (tamoxifen, TAM) for breast cancer treatment have been investigated.

Although PLGA-PEG micellar system can be used successfully in encapsulation of hydrophobic anticancer drugs, it is not suitable for encapsulation of platinum-based anticancer drugs due to the low hydrophobic interactions between the drugs and the hydrophobic core of micelles. Another suitable micellar system for targeting delivery of a platinum drug (cisplatin, CDDP) has been demonstrated using the polymer-drug complex system based on poly(ethylene glycol)-poly(glutamic acid) (PEG-PGA) and folate-PEG-PGA (FOL-PEG-PGA). Moreover, this system shows potentially for encapsulation of positive charged drug due to the negative charged of the PGA block. Targeting delivery of DOX has been studied using this micellar system as a high DOX loading system due to the electrostatic interaction between DOX and PGA. Further enhancement in cancer

treatment efficacy has been investigated by the targeting delivery of CDDP and DOX simultaneously for advanced solid cancer treatments.

This is the first study that has utilized the combined advantages of (1) synergistic effect of combined drugs, (2) polymeric carrier for drug delivery with sustained release and biocompatibility properties, (3) carrier modifications with targeting moiety to enhance the delivery selectivity and/or with penetrating peptide to enhance the uptake. The comparisons between the co-delivery of two single drug-loaded carrier systems and the delivery of dual-drugs-loaded carrier system using different pair of drugs have been investigated.

LIST OF TABLES

LIST OF FIGURES

CHAPTER 1. Introduction

1.1 Background

1.1.1 Cancer

Cancer is a major public health problem because it is one of the leading causes of burden and causes of death diseases. Although cancer disease has been exiting for many centuries, it becomes a more and more common disease all over the world. As reported by World Health Organization, there were 12.4 million new cancer cases and 7.6 million cancer deaths in 2008 [1]. With the increase in the global population, the number of new cases of cancer has been increased from 5.9 million in 1975 to 12.4 million in 2008 as shown in Figure 1.1. It was estimated by the International Agency for Research on Cancer (IARC) that the new cancer incidence was expected to rise from 12.4 million in 2008 to 26.4 million in 2030 with the growth in the world population from 6.7 billion in 2008 to 8.3 billion by 2030.

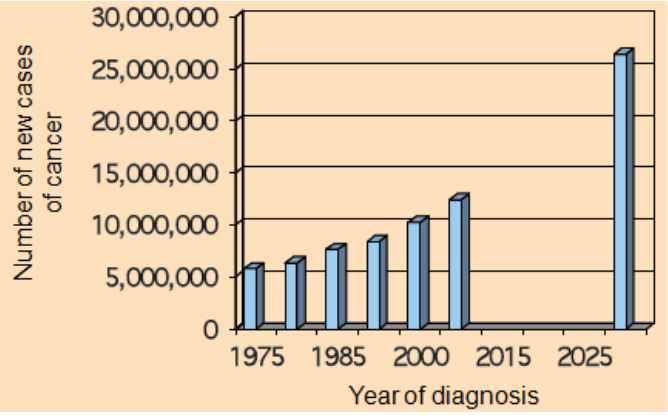

Figure 1.1 Estimated global cancer incidence, 1975-2030 [1].

Due to the huge worldwide health burden of cancer, the ultimate efforts of scientists, researchers and society have been put on the improvement of diagnostic devices and treatments over decades. Cancer therapy can be listed into three methods including surgery, radiation therapy and chemotherapy. In chemotherapy, the severe side-effects and less effectiveness of anticancer drugs are still present. Therefore, the focus in anticancer drug research has been increasing recently. As can be seen in industry therapeutic area (Figure 1.2), the research focus was shifted from hypertension therapy in 2001 to cancer in 2010.

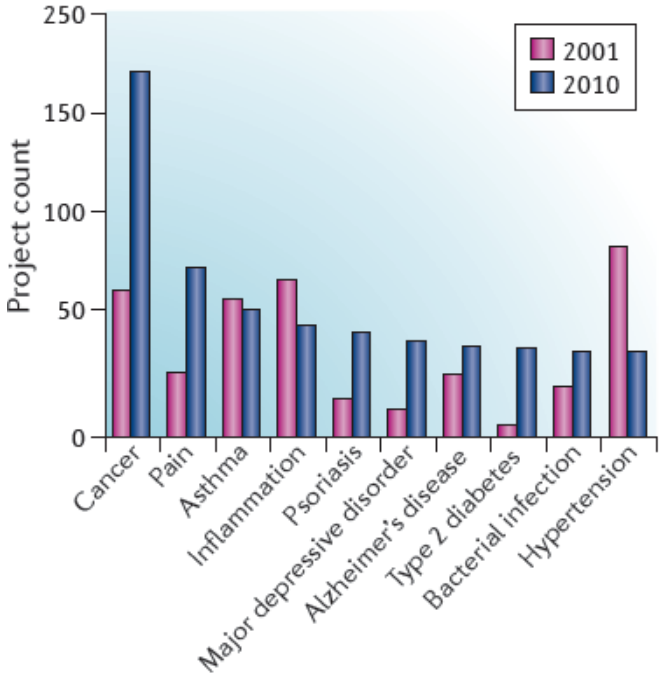

Figure 1.2 Changes in therapeutic area focus from 2001 to 2010 [2].

With the mission on enhancing cancer therapeutic efficacy around the world, many new anticancer drugs have been discovered every year with the enhancement in treatment effectiveness. Clearly, the trends in cancer mortality rates of both male and female in the United States and Singapore have been declined as shown in Figure 1.3. It can be seen

that the incidence rates of male keep almost unchanged recently while the incidence rates of female increase. Although the incidence rates increase in general, the declining in the mortality rates are still observed. In addition, the 5-year relative survival ratios gradually

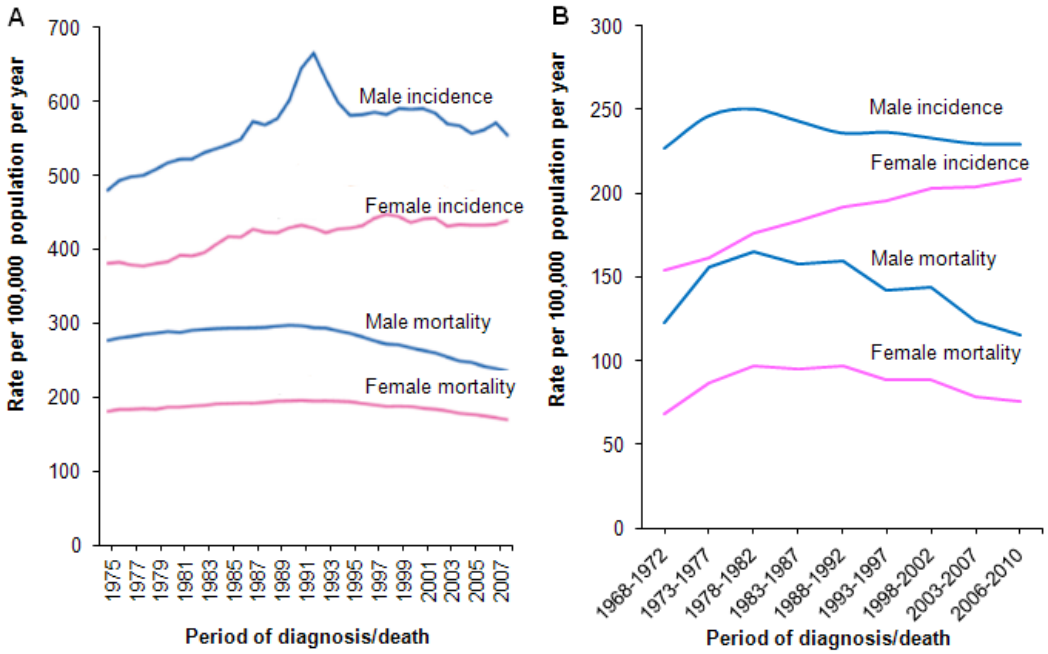

Figure 1.3 Trends in cancer incidence and mortality by gender: (A) United States, 1975-2008 [3]; (B) Singapore, 1968-2010 [4, 5].

increase for both genders in the period of 1973-2007 in Singapore (Figure 1.4) [4]. The 5-year relative survival ratios of male and female cancer patients in Singapore improve from 13.6% and 28.3% in the period of 1973-1977 to 44.6% and 57.5% in 2003-2007, respectively. These observations indicate the valuable contribution of the global effort in enhancing the cancer therapeutic effectiveness to eliminating cancer as a major health problem. Although many new anticancer drugs have been developed, cancer death is still rated as one of the most death disease, even more than HIV/AIDS with approximate one in every eight deaths of all causes in global and more than 25% deaths of all causes in Singapore (Figure 1.5).

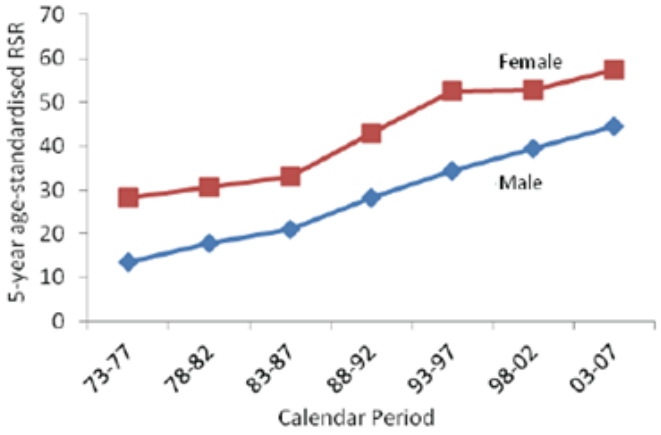

Figure 1.4 Trends in 5-year relative survival ratio, Singapore, 1973-2007 [4].

Therefore, a continued focus on investigating new generation anticancer agents is needed to increase the effectiveness of anticancer agents while reducing the side effects to increase the quality of cancer patient's life.

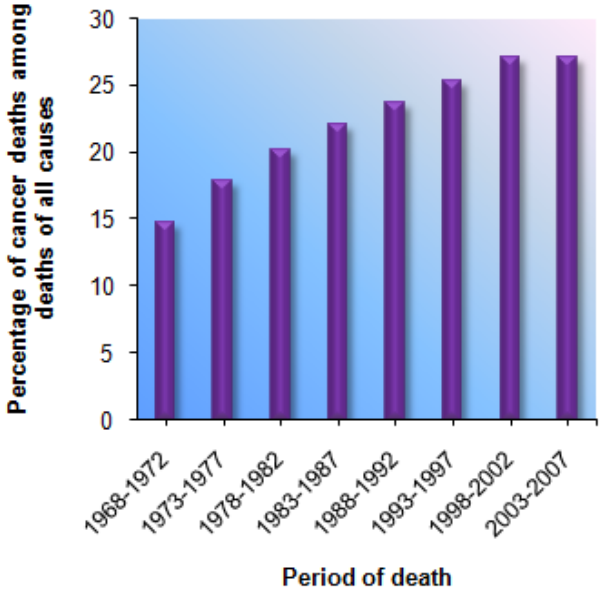

Figure 1.5 Trends in the percentage of cancer deaths among deaths of all causes, Singapore, 1968-2007 [4].

1.1.2 Limitation of traditional chemotherapeutic technology for cancer treatments

Chemotherapy is a common method for cancer treatments and is the most effective method for metastatic cancer treatments. However, the traditional chemotherapeutic drugs, which are small-molecules and toxic drugs, remain low success rate due to their delivered blindly to healthy tissues which lead to severe harmful side-effects, limited accessibility of drugs to the tumor tissue, their intolerable toxicity, development of multi-drug resistance, and the dynamic heterogeneous biology of the growing tumors [6, 7]. Therefore, chemotherapeutic systems using biocompatible nanocarriers have been developed as an emerging platform to deliver the anticancer drugs selectively to tumor cells. Doxil is the first drug-loaded carrier that was approved in 1995 using polyethylene glycol (PEG) modified-liposome to encapsulate doxorubicin (DOX). DOX is an effective anticancer drug that can be used effectively for many cancer treatments. However, DOX also causes severe side-effects that result in the serious heart damage to cancer patients. By encapsulating DOX into a nanocarrier, the serious heart damage incidence of this system (Doxil) treated patients has been reduced by 3 times compared with that of traditional DOX treated patients [8].

1.1.3 Requirements for an ideal drug delivery system

In order to overcome the limitations of the traditional chemotherapeutic technology and more effective in cancer therapy, anticancer drugs should be delivered in high molecular carrier systems that (1) are hydrophilic [9], biocompatible and non toxic; (2) exhibit prolonged circulation in the blood stream by having molecular weights and sizes of more

than 50,000 and 6 nm, respectively [9, 10]; (3) have sustained delivery property; and (4) have higher selectivity and affinity to tumor cells than healthy cells.

1.2 Hypotheses

The key hypotheses of this work are defined as such:

(1) To meet the specialized requirements of drug delivery system, it has been hypothesized that hydrophobic drugs can be physically loaded into PEG-PLGA micelles and the resultant drug-loaded micelles exhibit suitable properties for drug delivery.

(2) Multi-modification of micelles with different moieties which are specially used for drug delivery systems can increase the treatment efficacy of the resultant micelles compared to that of single-moiety modified one.

(3) It has been further hypothesized that the drug delivery system is more effective when synergistic combinations of anticancer drugs are co-encapsulated into the micelles.

(4) Polymeric micelles can also be used as carriers for hydrophilic drug delivery if the drugs and polymers exhibit specific chemical interactions.

1.3 Objectives and scope of the study

The objectives of this thesis are to investigate and demonstrate polymeric micellar drug delivery systems for cancer therapy to address the limitations of the traditional chemotherapeutic technology. In addition, the newly developed systems in this study have also been aimed to maximize the therapeutic effect and to satisfy the requirements

for an ideal drug delivery system as mentioned above. Therefore, multifunctional delivery systems (Figure 1.6) which are aimed for working in a synergistic manner have been investigated in this work. These multifunctional systems contain three main design components: a platform material (polymer micelle), encapsulated active agents (anti-cancer drugs), and functional ligands.

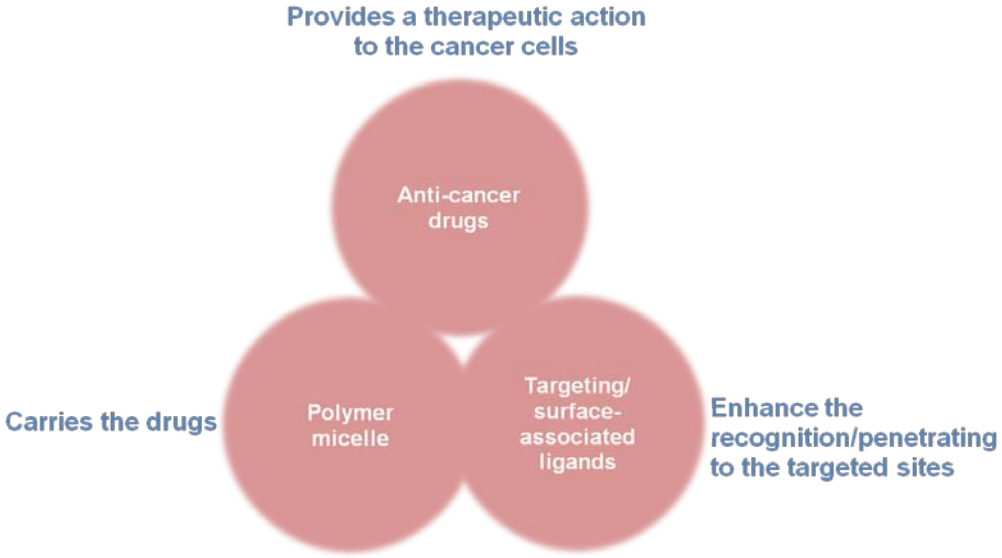

Figure 1.6 Schematic of multifunctional drug delivery system.

The specific aims of this research include:

(1) Development a carrier system for hydrophobic drug delivery for enhanced delivery of anticancer drugs to cancer cells, prolonged the circulation and sustained release. Self-assembled polymeric micelles based on biodegradable copolymer poly(D,L-lactide-co-glycolide)-poly(ethylene glycol)(PLGA-PEG) have been chosen due to the well-known bioavailability of PLGA and PEG polymers. This system has been multi-functionalized using folate targeting moiety (FOL) and cell penetrating peptide TAT to enhance the tumor targeting ability

and the cellular uptake. Optimization has been carried to investigate the suitable concentration of FOL and TAT combined modification on the carrier surface.

(2) Investigation the synergistic effect of combined chemotherapy of doxorubicin (DOX) and paclitaxel (PTX). Firstly, the effects of combined DOX and PTX at various ratios have been studied to investigate the synergistic regime. Secondly, the effect of co-delivery of the two drugs encapsulated separately into the mentioned TAT/FOL modified system has been investigated. Finally, the simultaneously encapsulation of the two drugs into the TAT/FOL modified micelle have been demonstrated.

(3) Study the dual-functionalized micellar system for synergistic delivery of two anticancer drugs for breast cancer treatment. Tamoxifen (TAM), a hormone drug, prevents the effects of estrogen to breast cancer cells [11]. PTX, a chemo-drug, kills cancer cells by promoting microtubule assembly from tubulin dimmers, stabilizes microtubules by preventing depolymerization [12]. Therefore, combined treatment of TAM and PTX has been investigated using TAT/FOL modified micellar system to demonstrate the enhancement of the system by utilizing the synergistic effect of the combination of two drugs and the enhancement in tumor accumulation via TAT/FOL modification for breast cancer treatment.

(4) Design a drug delivery system with high drug loading ability for the chemotherapy using a platinum-based drug and DOX. Cisplatin (CDDP) is a powerful drug for various cancer treatments but it exhibits serious side effects including acute and chronic nephrotoxicity, myelosuppression [13]. Therefore, delivery of CDDP using a carrier is essential. In addition, a non-platinum based drug (DOX) has been combined with CDDP to enhance the therapeutic efficacy based on the synergistic effect of the combined treatment. Combined treatment of CDDP and DOX has been demonstrated using the polymer-drug complex system based on poly(ethylene glycol)-poly(glutamic acid) (PEG-PGA) and folate-PEG-PGA (FOL-PEG-PGA) polymers.

CHAPTER 2. Literature Review

2.1 Cancer treatment

Cancer, medically termed as malignant neoplasm, is a class of disease in which abnormal cells divide without control, invade other near end tissues and finally metastasis via blood and lymph node vessels to other organs as insulated in Figure 2.1 [14]. Cancer is normally caused by the genetic mutation in transformed cells and exhibits in many types mainly including carcinoma, sarcoma, leukemia, glioma, lymphoma and myeloma.

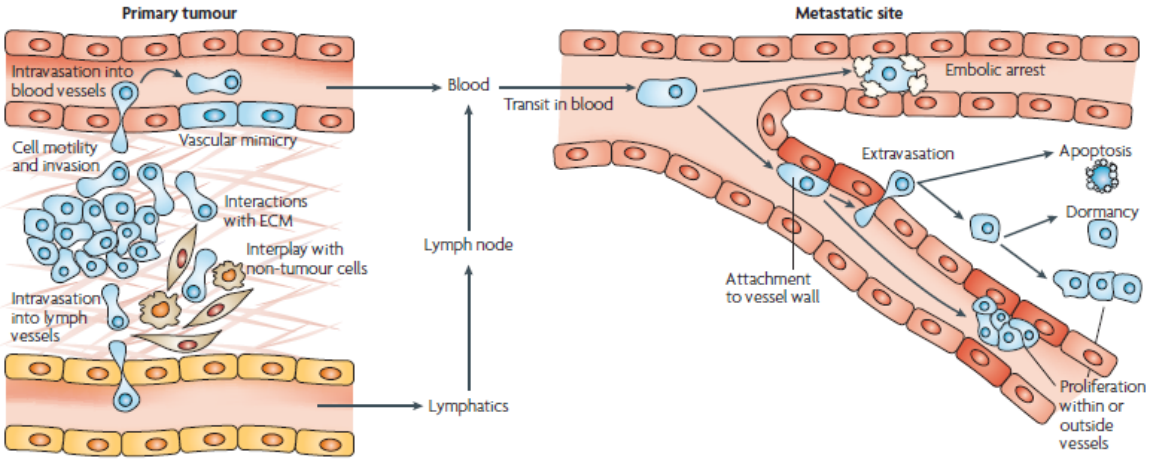

Figure 2.1 Development of cancer from the primary tumor to metastatic site [14].

Cancer can be treated by several methods depends on the type, the location and the stage of the disease and the patient's conditions. Common methods for cancer treatment are surgery, radiation therapy, immunotherapy, hormone therapy and chemotherapy. Surgery is the oldest known method that can be used to remove the cancer without affecting the normal tissues if the cancer has not spread to other parts of the body. However, the patient has to experience the physical pain and the high danger of infections. The patient

may also suffer from the rapid growth of the remaining cancer cells which can cause metastatic cancer if the cancer cells have not been removed completely by the surgery. In radiation therapy, cancer cells are destroyed by high energy particles or waves. It is one of the common and valuable tools for the treatment of local and regional cancer, similar to surgery. Immunotherapy, also called as biologic therapy, is a therapeutic strategy including monoclonal antibodies, non-specific immunotherapies and cancer vaccines. It is designed to boost the patient's immune system to work harder or smarter to attack cancer cells. It can be used to destroy cancer cells, stop or slow the growth of cancer cells, reduce the spreading speed of cancer cells. It is likely to be effective for treating of the early stage cancer with less toxicity to patient's body. Hormone therapy treats the cancer cells by altering the growth and activity of hormones in the body that inhibits the growth of cancer cells. Hormone therapy is commonly used to treat breast cancer [15-20] and prostate cancer [21-23]. Chemotherapy is an effective method using chemotherapeutical agents to treat cancer that has spread or metastasized because the medicines can travel throughout the entire body. Chemotherapy usually treats cancer via damaging to DNA or RNA of cancer cells. Although hundreds of chemotherapeutical agents have been developed for clinical use, their applications are still limited due to the serious side-effect to normal tissues, poor water-solubility, and short circulation time.

2.2 Traditional cancer chemotherapy technology

Traditional cancer chemotherapy is the treatment using one or more small-molecule anticancer drugs which aim to destroy the rapidly dividing cells via their specific mechanisms to the cells. Chemotherapeutic drugs are very strong to fight against a

spectrum of cancers from the early stage to the metastatic stage due to their broad range of mechanism to cancer cells (Table 2.1) **[24]**. Although the mechanisms of action are different among them, they all rely on the rapid and uncontrolled proliferation and division properties of cancer cells. They attack the cell division and apoptosis pathways.

Table 2.1 Anticancer therapeutic and their mechanism of action [24].

Compound	Mechanism of action
Amethopterin/methotrexate	Inhibits dihydrofolate reductase, blocking thymidine synthesis and, in turn, DNA and protein synthesis
Cisplatin/carboplatin/tetraplatin/oxaliplatin	Platinum-based compounds, adduct formation leading to DNA cross linking, inducing apoptosis
Daunorubicin/adriamycin/doxorubicin/ mitoxanthrone/actinomycin/idarubicin	DNA intercalating compounds, blocking polymerase activity, inhibiting DNA replication, inducing apoptosis
Etoposide	Forms a ternary complex with topoisomerase II and DNA, leading to errors in synthesis, inducing apoptosis
Fluorouracil	Pyrimidine analog, inhibiting DNA synthesis, induces p53-dependent apoptosis
Hydroxyurea	Inhibits ribonucleoside reductase, inhibiting DNA synthesis, inducing apoptosis
Mercaptopurine	Purine analog, inhibiting DNA synthesis, inducing apoptosis
Paclitaxel/ Taxol/ Docetaxel	Binds β-tubulin, forming highly stable microtubules that resist depolymerization, preventing cell division and inducing apoptosis
Tamoxifen	Selective estrogen response modifier (SERM), used against estrogen-sensitive breast tumors, competitively inhibits estrogen binding, slowing cell proliferation
Vinblastine/vincristine/vindesine	Binds tubulin, inducing self-association and depolymerizes pre-existing microtubules, inducing apoptosis
Camptothecin	inhibits the catalytic activity of mammalian DNA topoisomerase I, inhibiting DNA synthesis and inducing DNA strand breaks, leading to apoptosis

Unfortunately, besides the remarkable achievement of chemotherapy in cancer treatment, there are still many uncontrollable in the typical chemotherapy factors that challenge the treatment efficacy. Due to the small size with inability to target selectively to tumor cells (Figure 2.2), traditional chemotherapeutic drugs attack the proliferation of normal cells that causes toxic to healthy tissues with serious side-effects including hair loss, appetite loss, nausea, vomiting, anemia, nerve damage, memory loss, and permanent organ damage to heart, lung, liver and kidneys [25-29]. In addition, treatments using these small-molecule anticancer drugs exhibit some difficulties such as poor solubility [30],

sensitivity to degradation, instability, rapid clearance, and fast development of multiple-drug resistance (MRD).

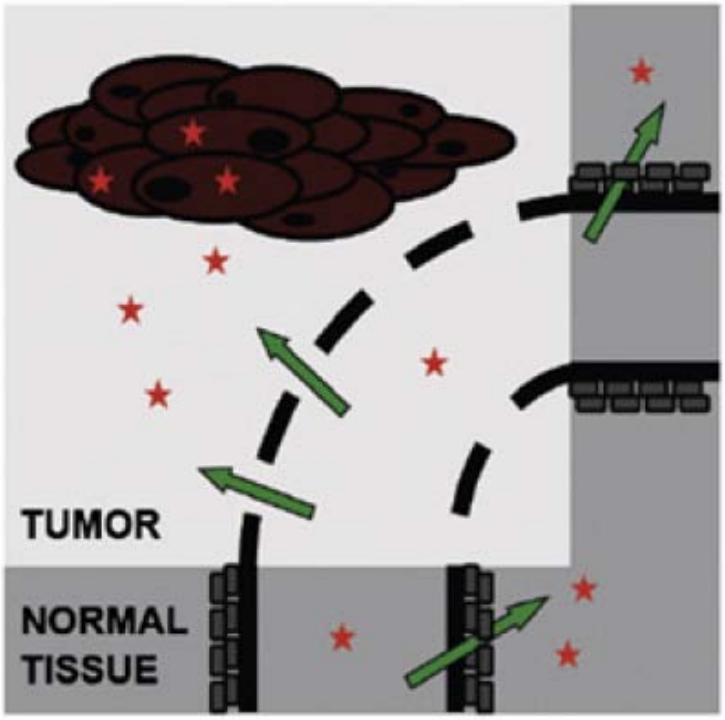

Figure 2.2 Schematic representation of the delivery mechanism of small-molecule drugs to tumors [31].

2.3 Drug delivery technology

To overcome the limitations of the typical chemotherapy, drug delivery systems have been developed to generate new therapeutic systems with better treatment efficacy and lower side effects. Numerous drug delivery systems (Figure 2.3) have been developed with different designs including liposomes, micelles, nanoparticles, polymer-drug conjugates, dendrimer, silica nanoparticle, carbon nanotubes, and metallic particles [8, 32-38]. Although the designs and materials of these delivery systems are different, they are all developed based on the same aims which are able to deliver the right dose of drugs

in the active condition to the targeted tissues without causing side-effects or drug resistance to tumor cells.

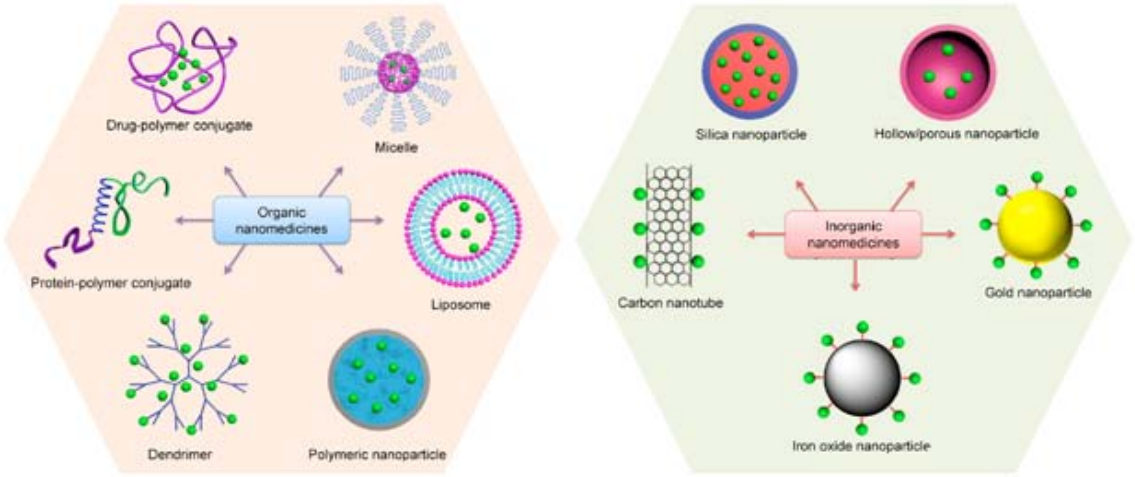

Figure 2.3 Schematic of organic and inorganic drug delivery systems for cancer diagnosis and therapy [39].

The existing challenges of drug delivery system are to design suitable carriers that can efficiently encapsulate anticancer drugs, overcome drug-resistance, and increase selectivity of drugs towards cancer cells while eliminating their toxicity to normal tissues. To efficiently encapsulate drugs into a carrier, the selection of the carrier must be strongly based on the properties of the anti-cancer agents such as size, hydrophilicity, and other chemical properties. Moreover, the association between drugs and the carrier also determines the release rate of drugs inside the tumor cells. Once the drug-loaded carrier in the blood stream, the system is usually be taken up by liver, spleen and other parts of the reticuloendothelial (RES) system. The taken up rate of the system by RES depend on its surface properties. The more hydrophobic system is preferentially taken up by the liver, the spleen and lungs [40]. At the tumor level, the accumulation mechanism of the

drug-loaded carrier system relies on the diffusion or convection across the leaky tumor vasculature. As presented in Figure 2.4, drug-loaded carriers with nano-size have higher accumulation into cancer tissues by the enhanced permeability and retention (EPR) effect due to the leaky blood vessels and the dysfunctional lymphatic drainage of tumors [41-44]. The uptake of a drug delivery system can also be enhanced by decorating the carrier with specific ligands. In addition other important properties of carriers have also been considered for designing a drug delivery system including biocompatibility and low toxicity.

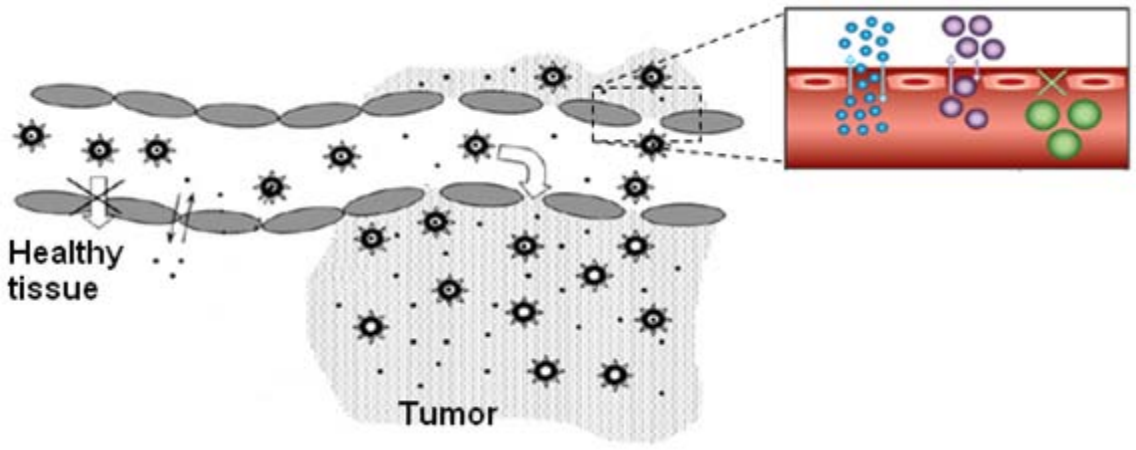

Figure 2.4 Schematic of delivery mechanism of drug-loaded carriers to tumor cells [42, 45].

Compared with small-molecule drugs, the nanoparticulate drug delivery technology exhibits more favorable properties such as (1) prolonged systemic circulation, (2) sustained drug release, (3) higher accumulation into cancer tissues and (4) overcoming multiple drug resistance. Therefore, cancer chemotherapy using nanoparticulate drug delivery system has been expected to result in higher treatment efficacy with lower side-effects. The first drug-loaded carrier (Doxil) was approved in 1995 using polyethylene

glycol (PEG) modified-liposome to encapsulate DOX. Doxil was designed with 100 nm size, hence it is delivered selectively to tumor tissues while excluding from the healthy tissues. By encapsulating DOX into nano-carriers, the serious side-effects caused by the toxicity of DOX have been reduced. As the result, the heart damage incidence of Doxil treated patients has been reduced by 3 times compared with that of traditional DOX treated patients [8].

2.4 Common carriers for anticancer drug delivery

2.4.1 Liposomes

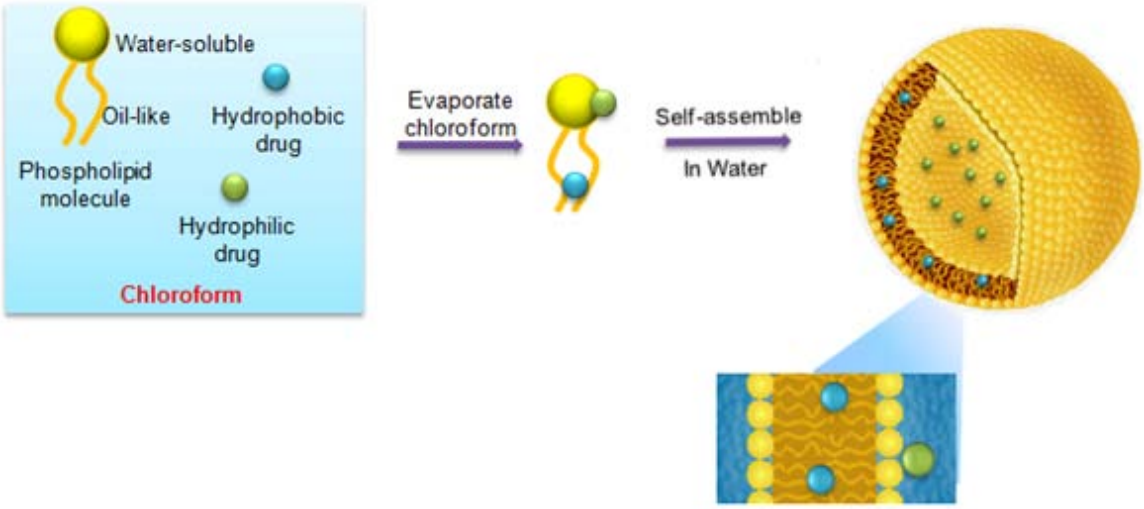

Figure 2.5 Schematic of drug-loaded liposome formation.

Liposomes are hollow spherical vesicles made from amphiphilic phospholipid molecules. Liposomes are biocompatible and can be used for encapsulation of both hydrophobic and hydrophilic drugs due to their hydrophilic core and hydrophobic shell properties. The most widely studied form of liposomes is lipid bilayer vesicles with the size ranging from 100 nm to 800 nm. Different preparation methods can produce liposomes with different sizes and characteristics. The most common and simple procedure for drug-loaded

liposome fabrication is the thin-film hydration method (Figure 2.5), in which the thin film of the mixture of lipids and drugs are hydrated with an aqueous solution.

Table 2.2 Sample of some liposome-based drugs for cancer chemotherapy.

Carrier*	Drug	Indication	Status/Name	Ref.
Non-PEG-modified	Doxorubicin	Breast, ovarian cancer	Approved/Myocet	[46, 47]
	Daunorubicin	Kaposi's Sarcoma	Approved/ Daunoxome	[48]
	Cytarabine	Leukemia Lymphoma	Phase III/Depocyt Approved/Depocyt	[49]
PEG-modified	Doxorubicin	Ovarian, breast cancers	Approved/Doxil, Caelyx	[50, 51]
	Doxorubicin	Stomach cancer	Phase I/ MCCDDP-465	[52]
	Irinotecan	Advanced solid tumors	Phase I/IHL-305	[53]
Thermally sensitive PEG-modified	Doxorubicin	Liver cancer	Phase III/ Thermodox	[54, 55]
FOL-PEG-modified	Doxorubicin	Solid tumors	*In vitro*	[56-58]
FOL/TMSP-PEG-modified	Docetaxel	Solid tumors	*In vitro*, *in vivo*	[59]
LHRH-PEG-modified	Paclitaxel	Non-small lung cancer	*In vitro*, *in vivo*	[60]
Anti-CD30-PEG-modified	Doxorubicin	Anaplastic large cell lymphoma	*In vitro*, *in vivo*	[61]
TH-PEG-modified	Paclitaxel	Acidified tumors	*In vitro*, *in vivo*	[62]
P18-4-PEG-modified	Doxorubicin	Breast cancer	*In vitro*	[63]

* FOL: folate, TMSP: tumor microenvironment-sensitive polypeptides, LHRH: luteinizing hormone-releasing hormone TH (AGYLLGHINLHHLAHL(Aib)HHIL-NH2)

The concept that liposomes could be used as drug delivery systems was established in 1971 by Gregoriadis [64]. Many types of anticancer drug-loaded liposomes have been developed and some of them are listed in Table 2.2. The initial drug-loaded liposomal

systems were developed based on non-modified liposomes. However, the short circulation time has been observed for these non-modified liposomal systems. Therefore, PEG was lately attached onto liposomes to increase their circulation time [65-67] and surface modification of liposomes with ligands was developed. Among them, many liposomal systems have been successfully developed for clinical use. Liposomes have been widely used for drug delivery in research and clinical trials due to their attractive properties such as biocompatible, able to encapsulate both hydrophilic and hydrophobic drugs, able to form highly homogeneous vesicles, able to modify the surface property. However, there are some limitations of using liposomal systems. The highly leakage of the lipid bilayers may lead to extravasation of toxic drugs in the healthy cells. Liposomes have low permeability to hydrophilic drugs but high permeability to hydrophobic drugs that leads to a problematic for the retention of highly hydrophobic drugs [68]. Other limitations are less sustained release property, fast oxidation of phospholipids and high production cost [42].

2.4.2 Polymer-drug conjugates

Polymer-drug conjugates are another common approach for small anticancer drug delivery, which manipulate small anticancer agents to improve their cell specificity. Typically, a polymer-drug conjugate typically has tripartite structure: a polymer, a linker and an active agent. Lately, much more elaborate systems with additional of cell-specific targeting ligands and/or intracellular trafficking moieties provide the ability to effectively target [60, 69] and penetrate the diseased cells (Figure 2.6).

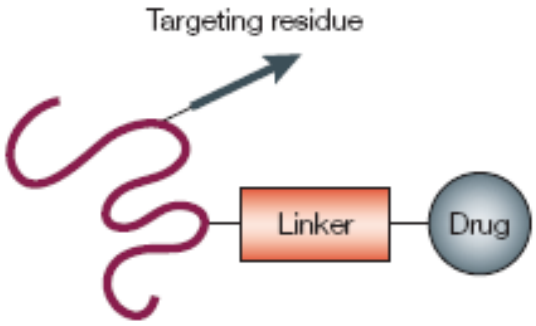

Figure 2.6 Schematic of drug delivery system using polymer-drug conjugate system [70].

Polymer-drug conjugates use specific water-soluble polymers as inert functional parts of conjugated systems to improve circulation time of the drugs and reduce their exposure to healthy cells. As shown in Table 2.3, various biocompatible polymers with a linear, random-coil structure have commonly been used to fabricate polymer-drug conjugates including PEG, hydroxypropylmethacrylamide (HPMA), poly(glutamic acid) (PGA), polyamidoamine (PAMAM). The most challenging part for designing an effective polymer-drug conjugate is the availability of a bio-responsive linker. The linker should be stable during transport of the system but able to release the drug at a designed rate at the targeted tumor. Peptide linkers have been popularized by the successful design of HPMA-GFLG-doxorubicin conjugates. This GFLG tetrapeptide linker is stable in the blood circulation but is cleaved in the cell by the liposomal thiol-dependent protease cathepsin B [70]. Other linkers such as cis-aconityl, hydrazone and acetal have also been used as an alternative for polymer-drug conjugates. In addition, the system can easily be precipitated in vivo due to the high and localized concentration of hydrophobic drug molecules bound along the polymer chain [71-73]. Therefore, drug-polymer conjugates must be designed with considerable low drug content to avoid precipitation. Moreover,

the system can easily accumulate in the glomeruli of kidneys and be quickly cleared due to their small size of 5-15 nm.

Table 2.3 Sample of polymer-drug conjugates.

Polymer*	Drug**	Indication	Status/Name	Ref.
PGA	Camptothecin	Advanced solid tumors	Phase I/ C TAM-2106	[74-76]
	Paclitaxel	Lung cancer	Phase III/ Xyotax	[77, 78]
		Advanced solid tumors	Phase I	[79]
PEG	Asparaginase	Leukemia	Approved/ Oncaspar	[80]
HPMA	DACH-Pt	Ovarian cancer	Phase II/AP5346	[81-84]
	Doxorubicin	Breast, lung, colorectal cancers	Phase II/PK1	[37, 85]
MSH-HPMA	Doxorubicin	Murine melanoma	*In vitro, in vivo*	[69]
LHRH-modified (PEG)	Paclitaxel	Non-small lung cancer	*In vitro, in vivo*	[60]
LHRH-modified (PAMAM)	Paclitaxel	Non-small lung cancer	*In vitro, in vivo*	[60]

* MSH: melanocyre-stimulating hormone
**DACH-Pt: 1,2-diaminocyclohexane-platium

2.4.3 Polymeric nanoparticles (NPs)

Polymeric nanoparticles (NPs) are spherical structures with various sizes ranging from 100 nm up to micron-size depended on the molecular weight of the polymers. Polymeric NPs can be used to delivery different types of anticancer drugs via physical interactions or chemical bonds (Figure 2.7) between drugs and polymers. The chemical bonds between drug and NP allow a delay in the release of drug until the nanoparticles reach the targeted delivery site. In addition, larger amount of drug can also be chemically loaded

into the NP. However, the alteration of drug activity after the conjugation is a drawback of the polymer-drug conjugated NPs for practical application.

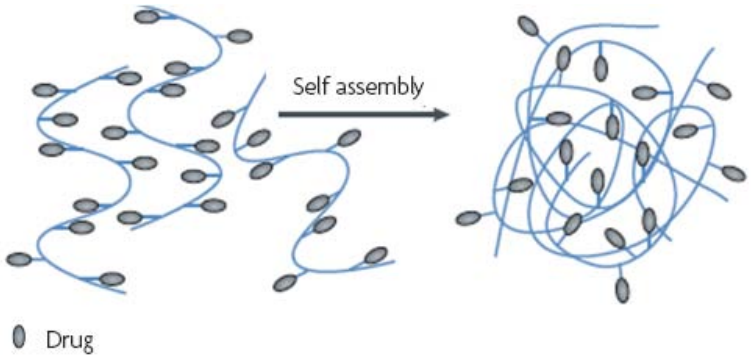

Figure 2.7 Schematic of polymer-drug conjugate nanoparticles [86].

As shown in Table 2.4, many polymers or copolymers have been used for fabricating carriers for drug delivery systems. In the early stage, most of studies are based biodegradability, biocompatibility [34, 87-89] polymers/copolymers including poly(D,L-lactide) (PLA) and poly(D,L-lactide-co-glycolide) (PLGA), PEG-PLGA, PEG-PCL, PEG-PEI. Subsequently, drug-loaded NPs have been further developed by attaching ligands on their surface to improve the treatment efficacy. However, only few systems have been approved for clinical trials such as abumin-based and cyclodextrin-PEG systems for delivery of paclitaxel and captothecin, respectively. The clinical application of this system has been limited due to the large particle size and highly possibility of aggregation.

Table 2.4 Nanoparticle-based drugs for cancer chemotherapy [31, 86].

Carrier*	Drug	Indication	Status/Name	Ref.
Abumin-based	Paclitaxel	Breast cancer	Approved/Abraxane	[90]
PLGA	Paclitaxel, etanidazole	Solid tumors	*In vitro*	[91, 92]
Nanoparticles	Docetaxel	Solid tumors	Phase I/Docetaxel-PNP	[31]
Cyclodextrin-PEG	Captothecin	Gastric cancer	Phase II/CRLX101	[93-95]
PEG-PLGA	Doxorubicin, paclitaxel	Solid tumors	*In vitro, in vivo*	[96, 97]
FOL-TPGS/TPGS-PLGA	Doxorubicin	Solid tumors	*In vitro*	[87]
FOL- TPGS-PLA	Paclitaxel	Solid tumors	*In vitro*	[98]
Trastuzumab-modified PLGA-MMT	Paclitaxel	Breast cancer	*In vitro*	[99]
TAT-PEG-PEI	Doxorubicin/ DNA	Solid tumors	*In vitro*	[100]
APT-PEG-PEI	Doxorubicin/ Bcl-xL shRNA	Prostate	*In vitro*	[101]
CGKRK peptide-PEG-PCL	Paclitaxel	Solid tumors	*In vitro, in vivo*	[102]
Anti-CD 133-PLGA	Paclitaxel	Breast Cancer	*In vitro, in vivo*	[103]

* TPGS: tocopheryl polyethylene glycol succinate, APT: anti-PSMA aptamer, PEI: poly(ethyleneimine)

2.4.4 Polymeric micelles

Polymeric micelles are typically formed by self assembly of amphiphilic polymers which have hydrophobic blocks and hydrophilic blocks. In the aqueous medium, micelles are formed with a hydrophobic core and a hydrophilic shell structures at the concentration above their critical micelle concentrations (CMC), through hydrophobic interactions between the hydrophobic segments of the polymer, as well as through solvation and steric repulsion among the hydrophilic segments of the polymer. Polymeric micelles have been using as anticancer drug carriers based on various interactions between the drugs and

core of micelles such as the hydrophobic, electrostatic, π-π interactions, hydrogen or covalent bondings.

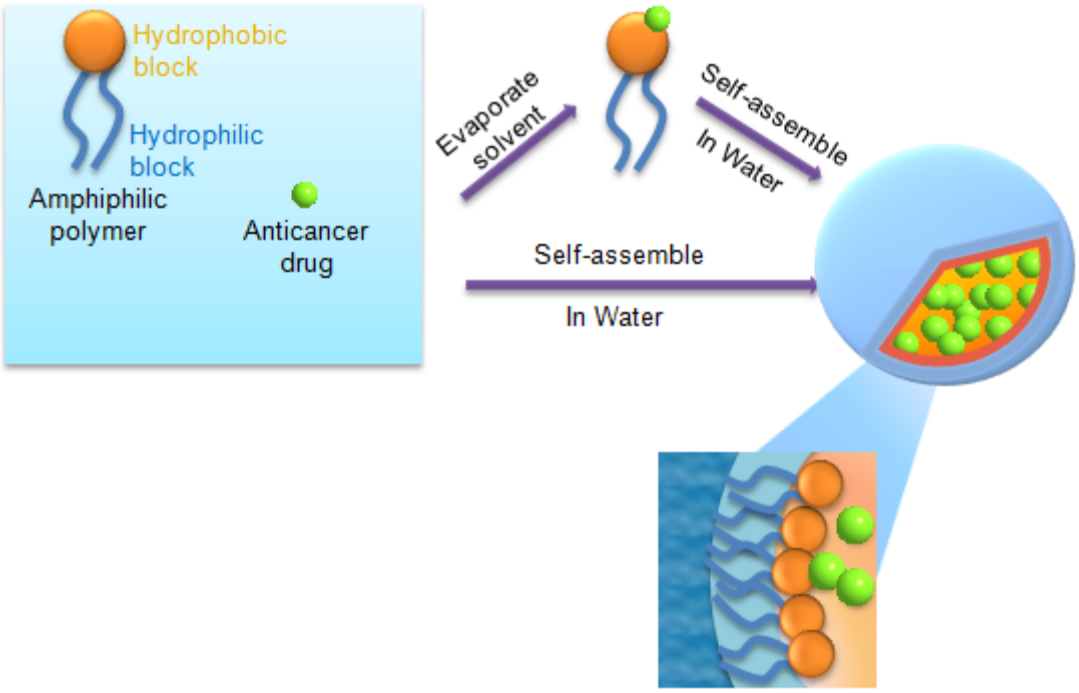

Figure 2.8 Schematic of preparation of physical drug-loaded polymeric micelles.

Drug-loaded micelles can be prepared by two methods as shown in Figure 2.8. In direct self-assembly method, the amphiphilic copolymer and the drug are directly solubilized in an aqueous medium at a concentration above its CMC. In contrast, in dialysis method, both copolymer and drug are firstly dissolved in an organic medium. Subsequently, the resulting drug-polymer solution is subjected to solvent exchange against aqueous phase via dialysis method to induce the micelle formation. The fabrication method is generally selected based on the building blocks of the micelle system and the drug properties. The more water soluble amphiphilic copolymers and drugs are generally fabricated into micelles via the former direct dissolution method. On the other hand, the highly

hydrophobic drugs and poor water soluble copolymers with strong hydrophobic tails are usually fabricated into micellar forms through the dialysis method.

For cancer therapeutic applications, the micelle vehicle should have low toxicity, low immunologic response, as well as low CMC to ensure stable particulate-delivery system under huge extent of dilution by blood upon intravenous injection to the host organism. In micellar drug delivery systems, the hydrophobic core of micelles can act as a reservoir for hydrophobic drugs, while the hydrophilic shell protects the micelle from the macrophage recognition and determines its circulation time. Polyethylene glycol (PEG) has been proven as a material that can increase the circulation time of particles and provide better protection to particles from liver uptake and plasma protein adsorption [104]. Therefore, PEG is the most popular used corona-forming polymer currently with a molecular range from 2 to 15 kDa (Table 2.5). Core-forming blocks can consist of various polymer blocks such as poly(D,L-lactide-co-glycolide) (PLGA), poly(D,L-lactide) (PLA), poly(glutamic acid) (PGA), poly(asparate) (PAsp), polyaspartate modified with 4-phenyl-butanol (PAPB), poly(carbonate-co-lactide) (P(CB-co-LA)), phosphatidylethanolamine (PE), poly(l-lactide-co-2-methyl-2-carboxyl-propylene carbonate) (P(LA-co-MCC)), poly (L-cystine bisamine-g-sulfadiazine) (PCBS), poly(ε-caprolactone) (PCL), acid-functionalized polycarbonate (PAC), urea-functionalized polycarbonate (PUC). The selection of core forming blocks is based on the nature structure and functional property of the encapsulated drugs. Polymeric micelles have commonly been used for delivering hydrophobic or amphiphilic drugs, they may also be used to encapsulate several hydrophilic drugs by using polymers that exhibit specific

interactions with the drugs such as formation of complexation [105-108], or electrostatic [109]. Typically, the amphiphilic copolymers with hydrophilic-lipophilic balance (HLB) values between 5 and 19 are used to form micelles for drug delivery. When the HBL value gets closer to 0 (hydrophobic extreme), the CMC value is reduced. The micelle with lower CMC value is more desirable for drug delivery system because the stability of the system upon dilution by the blood is increased. However, copolymers with low HBL values may lead to the less hydrophilic micelles which cause the fast aggregation and clearance from the bloodstream. Therefore, many researches are still on going to further optimize the more suitable polymeric micelles for drug delivery system.

Table 2.5 Drug-loaded polymeric micellar formulations.

Carrier*	Drug	Indication	Status/Name	Ref.
PEG-PLGA	Doxorubicin	Solid tumors	*In vitro*	[110]
PEG-PLA	Paclitaxel	Breast, lung and ovarian cancers	Approved/ Generxol-PM	[111-113]
PEG-PGA	DACHPt	Orthotopic scirrhous gastric	*In vitro, in vivo*	[107, 108]
	Cisplatin	Advanced solid tumors	Phase I/ NCDDP-6004	[106, 114]
	SN-38	Breast cancer	Phase II/ NK012	[115, 116]
PEG-PAsp	Doxorubicin	Pancreatic and colorectal cancers	Phase II/ NK911	[117]
	CDDP	Solid tumors	*In vitro*	[118]
PEG-PCL	Doxorubicin, paclitaxel, cyclopamine	Colon cancer, ovarian cancer	*In vitro, in vivo*	[119, 120]
PEG-PAPB	Paclitaxel	Stomach cancer	Phase II/ NK105	[121-123]
P(MDS-co-CES)	Paclitaxel, herceptin	Breast cancer	*In vitro*	[124]
Pluronic L61, F127	Doxorubicin	Gastric cancer	Phase III/ SP1049C	[125, 126]

PEG-PAC/PEG-PUC	Doxorubicin	Solid tumors	*In vitro, in vivo*	[127]
PEG-P(CB-co-LA)/PEG-PLA	Bicalutamide	Prostate cancer	*In vitro*	[128]
pH-sensitive PEG-PDPA	Chlorin e6	Lung cancer	*In vitro*	[129]
pH-sensitive PAE-g-ADPC	Doxorubicin	Solid tumors	*In vitro*	[130]
Anti-VEGF- PEG-PAsp	Adriamycin	Liver tumor	*In vitro, in vivo*	[131]
FOL-modified (PEG-PLGA)	Doxorubicin	Solid tumors	*In vitro*	[132]
FOL-modified (PEG-PAE)	Doxorubicin	Solid tumors	*In vitro*	[133]
FOL-modified (PEOz-PCL)	Doxorubicin	Solid tumors	*In vitro, in vivo*	[134]
ACUPA-modified (PEG-PLA or PEG-PLGA)	Docetaxel	Advanced solid tumors	Phase I/BIND-014	[135]
A10-modified (PEG-PLA)	Doxorubicin	prostate cancer	*In vitro, in vivo*	[136]
TAT-modified (PEG-PE)	Paclitaxel	Solid tumors	*In vitro, in vivo*	[137]
TAT-modified (PEG-Cholesterol)	Ciprofloxacin	Brain infection	*In vitro, in vivo*	[138, 139]
TAT-modified (PEG-PLA/PEG-P(LA-co-MCC)	Daunorubicin	Solid tumors	*In vitro*	[140]
TAT-modified (PEG-PLA/PCBS-PEG)	Doxorubicin	Acidic solid tumors	*In vitro*	[141]

* PAE: poly(β-amino ester), anti-VEGF: anti-vascular endothelial growth factor, PEOz: poly (2-ethyl-2-oxazoline)

Currently, polymeric micelles are popular pharmaceutical carriers for the delivery of anticancer drugs due to their advantages over other systems [142]. They are small size with a narrow distribution that is considered ideal for stable and long term circulation in the blood stream because it evades the RES uptake. Moreover, while remaining stable in the blood over a long time period, the carriers are small enough to pass through small blood vessel pores of less than 400 nm [143]. From this point of view, polymeric micelles are an effective delivery system in term of the enhanced permeability and retention (EPR) effect and overcoming the RES system [9]. The second advantage is the high static and dynamic structural stability [144, 145]. Static stability is described by a CMC. Dynamic

stability is described by the low dissociation rates of micelles. The high structural stability of polymeric micelles provides sustainable delivery of drug *in vivo* because the shape and structure of the micelles can be maintained upon injection into the patient's body. The third advantage is the high solubility of micelles in aqueous media. Due to the encapsulation of anticancer drugs in the core of polymeric micelles, the precipitation of drug *in vivo* can be prevented by utilizing a hydrophilic outer shell layer that works as a barrier against the inter-micellar aggregation. The fourth advantage is that the system can be modified easily to change the size, surface property and also the interaction with drugs.

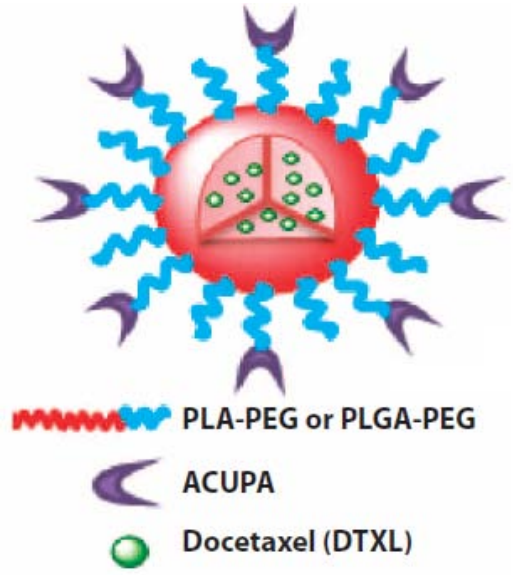

Figure 2.9 Schematic of BIND-014, a docetaxel (DTXL)-loaded micelle system with small-molecule (ACUPA) targeting ligands.

As the application of polymeric micelle system in cancer drug therapy becomes very appealing owing to its suitable characteristics as drug carrier, some drug-load micellar systems have been reached to clinical phases or even been approved for clinical use as shown in Table 2.5. Generxol-PM is a paclitaxel-loaded micellar system that has been

approved for the treatments of breast, lung and ovarian cancer [111, 112]. Other drugs-loaded micellar systems have been approved for clinical trials such as the delivery of doxorubicin [117, 125, 126], cisplatin [106, 114], SN-38 [115, 116]. Specially, BIND-014 is the first active targeted drug-loaded nano-system that has been approved for phase I human clinical trial [135]. BIND-014 is a targeted micellar system using amphiphilic polymers poly(D,L-lactide)-poly(ethylenglycol) (PLA-PEG) or poly(D,L-lactide-co-glycolide)-PEG with small-molecule (ACUPA) targeting ligands to physically encapsulate docetaxel (DTXL) (Figure 2.9) for the treatment of advanced solid tumors.

2.5 Overview of current drug delivery strategies

Traditional cancer treatments often kill healthy cells and cause toxicity to the patient. Therefore, it would be desirable to develop chemotherapeutics that can either passively or actively target cancerous cells. Passive targeting exploits the characteristic feature of tumor biology that allows carriers to accumulate in the tumor by the enhanced permeability and retention (EPR) effect. Active approaches achieve this by conjugating carriers containing chemotherapeutics with molecules that bind to overexpressed antigens or receptors on the target cells (Figure 2.10).

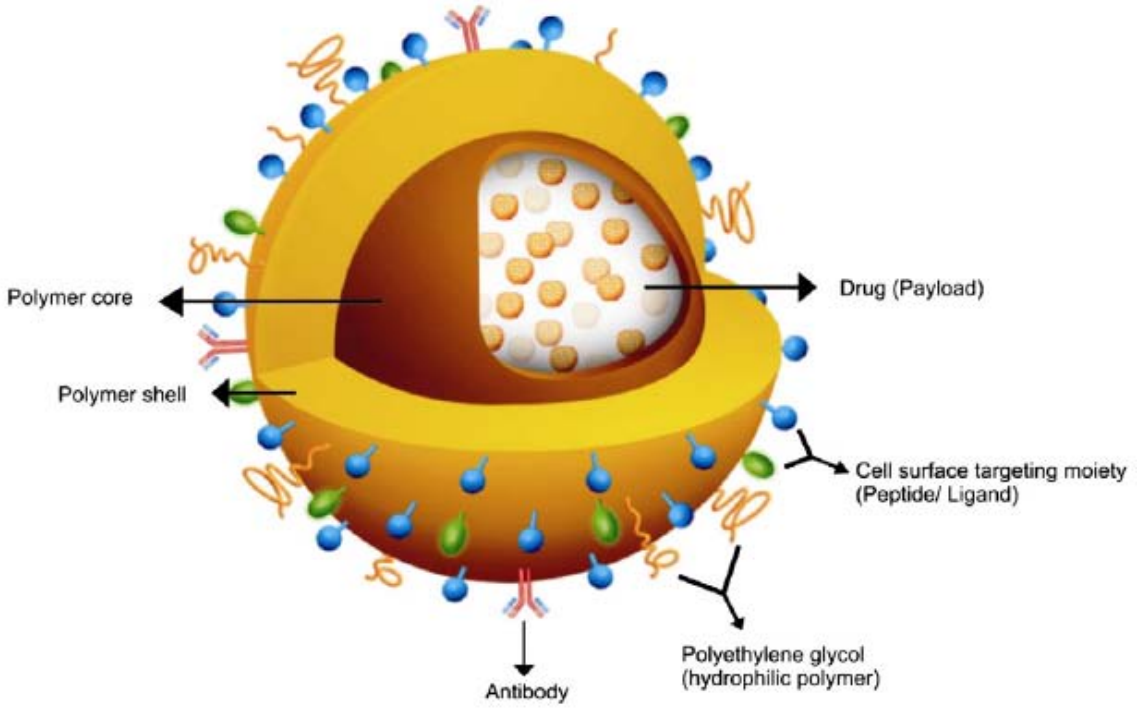

Figure 2.10 Schematic of multifunctional polymeric carriers for active drug delivery [24].

2.5.1 Passive delivery

General features of tumors include leaky blood vessels and poor lymphatic drainage. Whereas free drugs may diffuse nonspecifically, a drug carrier can escape into the tumor tissues via the leaky vessels by the EPR effect (Fig. 2.11). The increased permeability of the blood vessels in tumors is characteristic of rapid and defective angiogenesis (formation of new blood vessels from existing ones). Furthermore, the dysfunctional lymphatic drainage in tumors retains the accumulated drug carriers and allows them to release drugs into the vicinity of the tumor cells. Although passive targeting approaches form the basis of clinical therapy, they suffer from several limitations. Ubiquitously targeting cells within a tumor is not always feasible because some drugs cannot diffuse efficiently and the random nature of the approach makes it difficult to control the process.

This lack of control may induce multiple-drug resistance (MDR). MDR occurs because transporter proteins that expel drugs from cells are over-expressed on the surface of cancer cells. The passive strategy is further limited because certain tumors do not exhibit the EPR effect, and the permeability of vessels may not be the same throughout a single tumor. The same phenomenon has been observed from the cancer treatment using Doxil in clinical. The treatment results show that Doxil fails to penetrate deeply into the tumor that results in the lesser efficacy compared to the traditional DOX [8].

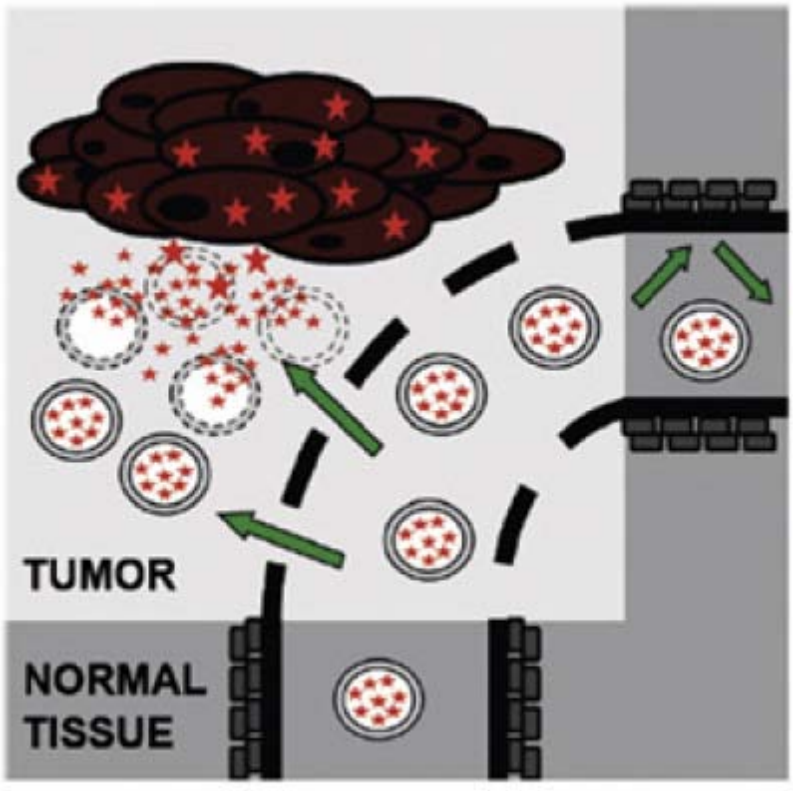

Figure 2.11 Schematic of a passive targeted drug delivery system [31].

2.5.2 Active delivery by targeting to cancer cells

To overcome the limitations of passive delivery, the drug-loaded carriers should be modified with molecules that bind to over-expressed antigens or receptor on the cancer

cells. This selective binding can be achieved by attaching targeting agents, such as ligands, to the surface of the carrier. Due to the high interaction between the ligands and receptors on cancer cell surface and the over-expressed on the receptors on cancer cells but lack of that on healthy cells, the drug-loaded carriers actively bind to cancer cells through ligand–receptor interaction while bypassing the healthy cells. The bound carriers are internalized, and the drug is released inside the cell (Figure 2.12).

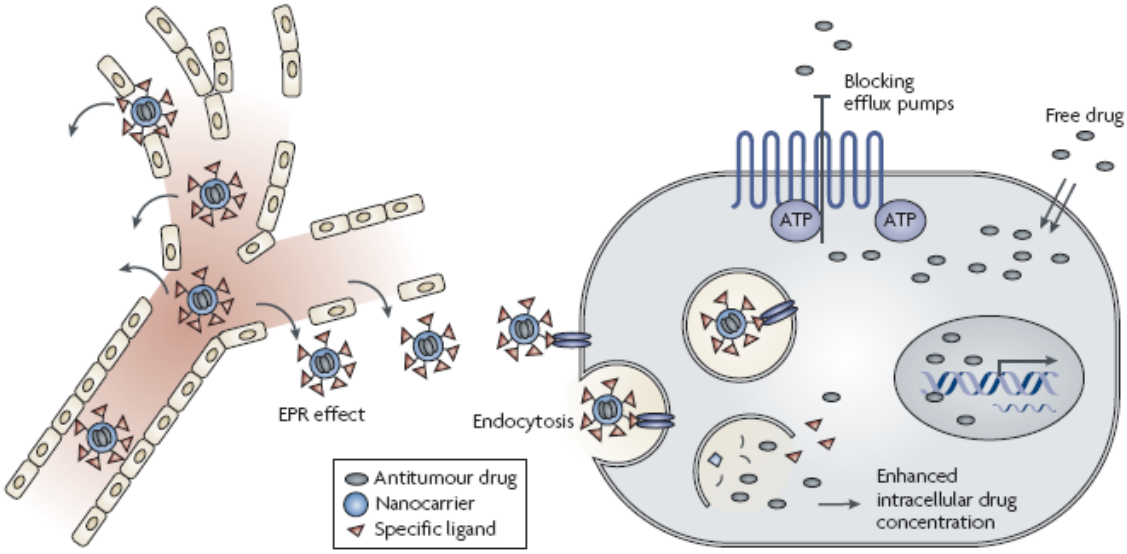

Figure 2.12 Active drug targeting to cancer cells due to the high binding affinity between the targeting moiety on the drug-carrier surface and the over-expressed receptors on the tumor cell membrane [86].

Cancer cell targeting ligands are classified as protein (mAb, Fab, $F(ab')_2$, scFv), aptamers, vitamins (folate, biotin), peptides and other ligands (transferrin, hyaluronan). One of the common ligands for cancer cell targeting is folate that required by all eukaryotic cells for 1-carbon metabolism and *de novo* nucleotide synthesis. Folate receptor (FR) expression has been detected at very high levels in >90% of ovarian and

other gynecological cancers, and at high to moderate levels in brain, lung, and breast carcinomas [146-148]. The fact that FRs bind to folate-conjugated carriers with high affinity (10^{-9} M) and that the carriers are subsequently transported nondestructively into the target cells only adds to the utility of this strategy for tumor-specific drug [149].

2.5.3 Active delivery by targeting to endothelial cells

Receptors expressed on the apical surfaces of epithelial cells often constitute good targets, since these receptors in normal epithelia are inaccessible to parenterally administered drugs. The drug-loaded endothelial cell targeted carriers have been designed by modification the carrier surface with ligands that can target to the endothelial over-expressed receptors (Figure 2.13). Antibody fragment L19 [150, 151] and derivaties of oligoopeptides RGD [152, 153] and NGR [154] have been used as ligands for carrier modification to target endothelial cells.

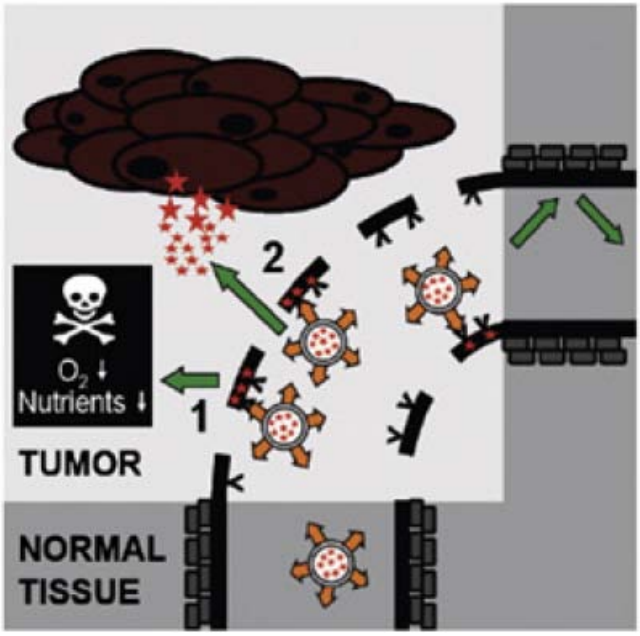

Figure 2.13 Active drug targeting to receptors over-expressed on endothelial cells [31].

2.5.4 Cell-penetrating peptides

Cell-penetrating peptides (CPPs) correspond to the number of known natural and synthetic short peptides of less than 30 amino acids with cell-penetrating capabilities. Many short peptides have been identified as CPPs based on their ability of transporting diverse types of carriers. Table shows some frequently used CPPs for the transport of various carriers. Among them, TAT peptide, the HIV1-derived trans-activator of transcription peptide, is one of the most intensively studied CPPs that was firstly investigated by Green [155] and Frankel in 1988 [156]. The increase cellular uptake of different TAT sequences has been demonstrated by researchers as shown in Table 2.6. Different TAT sequences such as YGRKKRRQRRR, GRKKRRQRRR, RKKRRQRRR, GRKKRRQRRPPQ, GGYGRKKRRQRRR have been proven as cell-penetrating moieties which can enhance the penetrating of the TAT-modified carriers into the cells.

Table 2.6 Representative CPPs and their applications.

CPPs	Sequences	Carrier types	Ref.
TAT_{47-57}	YGRKKRRQRRR	Micelle, liposome, nanoparticle, plasmid, polymeric liposome	[139, 157-165]
TAT_{48-57}	GRKKRRQRRR	Nanoparticle	[166]
TAT_{49-57}	RKKRRQRRR	Protein, nanoparticles	[167, 168]
TAT_{48-60}	GRKKRRQRRPPQ	siRNA, protein, peptide, liposome, nanoparticle	[169-172]
TAT	GCGGGYGRKKRRQRRR	Micelle, nanoparticle	[141, 173, 174]
TAT	GGYGRKKRRQRRR	Micelle, nanoparticle	[175]
Penetratin	RQIKIWFQNRRMKWKK	Peptide, siRNA, liposome	[176]
Transportan	GWTLNSAGYLLGKINLKALAALAKKIL	Protein	[177]
MPG	GALFLGFLGAAGSTMGAWSQPKKKRKV	Plasmid, siRNA	[178]
Pep-1	KETWWETWWTEWSQPKKKRKV	Protein, peptide	[179]
MAP	KLALKLALKALKAALKLA	Protein	[180]
SAP	VRLPPPVRLPPPVRLPPP	Protein, peptide	[181]
SynB	RGGRLSYSRRRFSTSTGR	Doxorubicin	[182]

In drug delivery field, CPPs have been proven effective at increasing the treatment efficacy of therapeutics by improving cellular uptake with lower toxicity and more controlled administration than other delivery vectors [183-185]. CPPs have been conjugated to a variety of therapeutics including small molecules [182, 186-190], proteins [191-194], antibodies [195], nucleic acids [196-198], liposomes [158, 199, 200], micelles [137, 157, 201, 202] or nanoparticles [159, 203-205] to trigger the transportation of therapeutics across the cell membrane into the cytoplasm of cells.

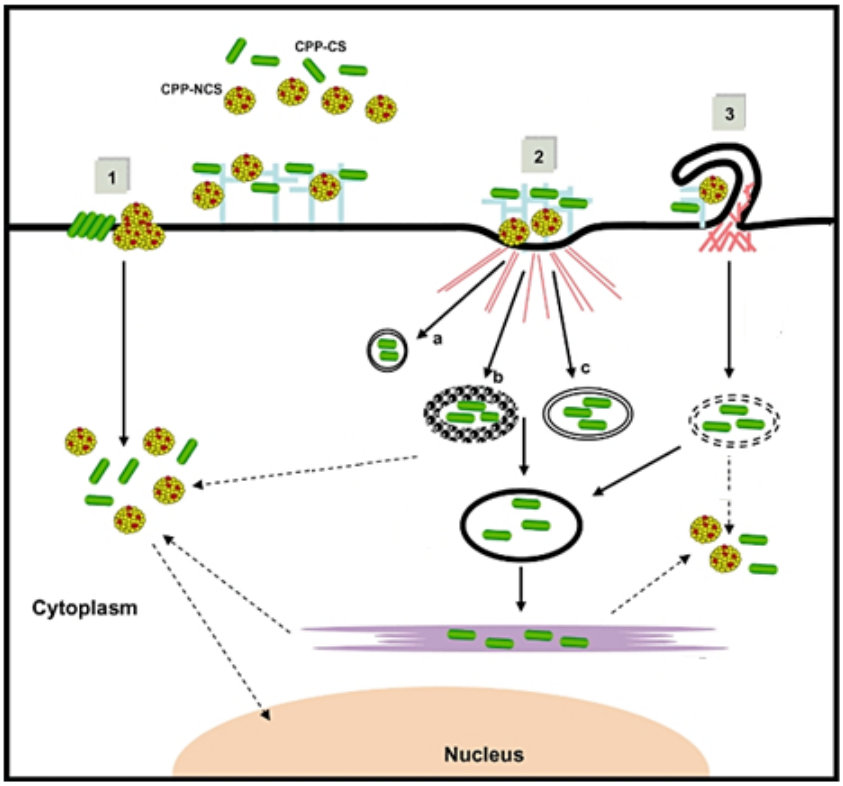

Figure 2.14 Model of cellular uptake and intracellular trafficking of CPPs. CPP-carriers may enter the cell via (1) membrane fusion, (2) endocytosis pathway, and (3) macropinocytosis [206].

Although cellular internalization of CPPs has been observed in various cell types, their mechanism of activity has not yet completely elucidated. It is proposed that CPP-conjugated small-sized carrier cross cells via (1) membrane fusion or (2) endocytosis pathway (caveolin-dependent, clathrin-dependent, clathrin- and caveolin-independent) [206-208], while CPP-conjugated large-sized carrier enter cells via (3) macropinocytosis [194, 206, 209] as shown in Figure. It seems that there might be multiple mechanisms in cellular uptake of CPP-conjugated carriers depending on the nature of CPPs, the size and nature of carriers, cell membrane composition, physiological state of the cells [176, 210, 211].

2.6 Combination chemotherapy

2.6.1 Overview of combination chemotherapy

Single agent therapy has seen limited success in cancer treatment due to the toxicity at high drug dosage, the heterogeneity of cancer cells and the drug resistance [212-215]. Recently, a variety of different types of combination therapy, which involves the administration of different classes of chemotherapeutics to a patient, has been used for cancer treatments to maximize cancer therapeutic efficacy while minimizing toxicity. Many studies have demonstrated that the combination chemotherapy can exhibit better cancer treatment efficacy while having lower MDR effect in various types of cancer diseases such as breast cancer [216-218], lung cancer [219], ovarian adenocarcinoma [214], synovial sarcoma, osteosarcoma and uterine leiomyosarcoma [215]. Some combinations have also been shown clinically to treat cancer disease more effectively in comparison to the administration of a single agent as shown in Table 2.7.

Table 2.7 Synergistic combinations in clinic [220].

REFERENCE	DRUG 1	DRUG 2	DRUG 3
Langer, *el al.* (1999) Drugs 58 Suppl. 3:71-75	Cisplatin or Vindesine	+ UFT (Tegafur/ uracil)	
FDA[a] (Colon or Rectal Cancer)	Leucovorin	+ 5-FU	
FDA (Colon or Rectal Cancer)	Irinotecan	+ Leucovorin	+ 5-FU
FDA (Breast Cancer)	Herceptin	+ Paclitaxel	
FDA (Breast Cancer)	Xeloda	+ Docetaxel	
FDA (Ovarian and Lung Cancer)	Paclitaxel	+ Cisplatin	
FDA (Lung Cancer)	Etoposide	+ Other FDA-approved Chemotherapeutic agents	
FDA (Lung Cancer)	Gemcitabine	+ Cisplatin	
FDA (Prostate)	Novantrone (mitoxantrone hydrochloride)	+ Corticosteroids	
FDA (Acute Nonlymphocytic Leukemia)	Novantrone	+ Other FDA-approved drugs	
FDA (Acute Nonlymphocytic Leukemia/Acute Lymphocytic Leukemia)	Daunorubicin (DNR, Cerubidine)	+ Other FDA-approved drugs	
FDA (Chronic Myelogenous Leukemia)	Busulfex (Busulfan; 1,4-butanediol, dimethanesulfonate; BU, Myleran)	+ Cyclophosphamide (Cytoxan)	

[a]FDA: United States Food and Drug Administration

2.6.2 Principle of drug selection in the combination

The effects of combinations of drugs are enhanced when the combined therapy provides a synergistic effect. To obtain a synergistic effect, the drugs in the combination treatment generally has to be chosen following the principles such as (i) using drugs with non-overlapping toxicities so that each drug in the combination can be administered at near maximal dose, (ii) combining drugs with different mechanisms of action so that multiple sites in biochemical pathways can be attacked thus resulting in synergy, and (iii) combining drugs that exhibit synergistic effect against cancer cells, or additive antitumor activity with a favorable toxicity profile.

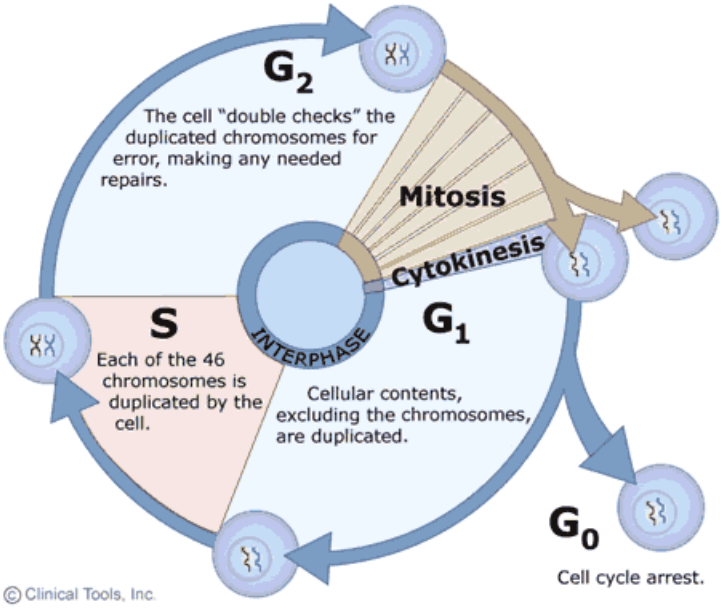

Figure 2.15 Cell cycle phases [221].

Based on the above principles, drugs in a combination should firstly exhibit different pharmacological effects. Because most of anticancer drugs are cell cycle specific, the cell cycle of drugs in a combination is another rational target to enhance the treatment efficacy. As shown in Figure 2.15, a single parent cell divides into two identical daughter cells through a cell cycle that includes several phases including G1, S, G2, and M. G_1 (Gap 1) is a growth phase in which proteins and enzymes that are required in S phase are formed. Subsequently, the cell enters the S (Synthesis) phase. During this phase, the DNA duplication occurs, that is the most basic function of the cell cycle. After S phase, the cell enters the G2 phase, where repair might occur along with preparation for mitosis in M (Mitosis) phase. In M phase, the nuclear envelope breaks down, microtubules attach to the chromosome's kinetochores aligning them at the mitotic spindle's equator. After M phase, the cell enters G_1or G_0 (quiescent phase).

2.6.3 Some commonly used anticancer drugs and their combinations

Many types of anticancer drugs which have distinct mechanisms of action have been investigated and clinically used. For the purpose of this thesis, the discussion is focused on the mechanisms of action of four anticancer drugs (Figure 2.16) and their combinations (doxorubicin+paclitaxel, paclitaxel+tamoxifen, and doxorubicin+cisplatin).

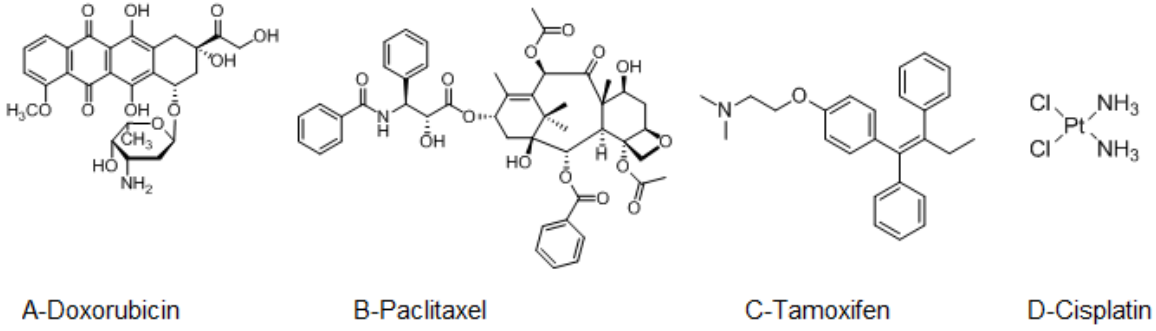

Figure 2.16 Molecular structures of (A) doxorubicin, (B) paclitaxel, (C) tamoxifen, and (D) cisplatin.

Doxorubicin (DOX) is one of the most potent and widely cytotoxic chemotherapeutic agents with a significant and use-limiting-side-effect profile. DOX is an anthracycline antibiotic that works by inhibiting the synthesis of nucleic acids within cancer cells and exhibits the most effective in treating the cancer cells in the S phase. It is a very powerful chemo-drug for treatment of some leukemias, hodgkin's lymphoma, as well as cancers of the bladder, breast, stomach, lung, ovaries, thyroid, soft tissue sarcoma, multiple myeloma, etc. However, DOX also has a number of undesirable side effects such as cardiotoxicity and myelosuppression which leads to a very narrow therapeutic index.

Paclitaxel (PTX) is an effective mimotic inhibitor anticancer agent that can block cell cycle in G_2 and M phase. PTX, a microtubule-stabilizing agent, promotes polymerization

of tubululin causing cell death by disrupting the dynamics necessary for cell division. It has neoplastic activity especially against primary epithelial ovarian carcinoma, breast, colon, and non-small cell lung cancers. PTX therapeutic efficacy is limited by its poor aqueous solubility. In addition, systemic administration of PTX is also associated with several side effects such as dyspnea, hypotention, nephrotoxicity and neurotoxicity.

Tamoxifen (TAM) is the most commonly used therapeutic agent for the treatment of estrogen receptor-possitive breast cancer. It is a hormonal drug that acts as an anti-estrogen by binding to the estrogen receptor but do not activate it. Because of this competitive antagonism, TAM interferes with the body's ability to make estrogen by blocking the activity of aromatase, an enzyme needed for the final steps of estrogen production. TAM is effective in blocking cell cycle progression on G0, G1 and early S phase. Besides the promising success rates of TAM in cancer treatment, it also has estrogenic effects in the uterus and other side effects including endometrial cancer, fatty liver, pulmonary emboli, venous thrombosis, reduced cognition and ocular side effects.

Cisplatin (CDDP) is an alkylating agent that has activity in many different cancer diseases such as testicular, ovarian, lung, bladder, testicular, head and neck cancers. CDDP inhibits tumor growth by binding with DNA to form adducts and intrastrand cross-links that change the conformation of the DNA and inhibit DNA replication. Although CDDP functions as a non-cell cycle specific, cancer cells appear to be maximally sensitive to CDDP in G_1 phase. CDDP causes some severe side effects

including nausea, vomiting, bone marrow effects, significant renal dysfunction, and acoustic nerve dysfunction.

The two drugs in (DOX+PTX), (PTX+TAM) or (DOX+CDDP) combinations have different mechanisms of actions and non-overlapping toxicities. Therefore, these combinations may exhibit synergistic effect in cancer therapy. Because the effect of the combination strongly influenced by the combination ratios, combinations at different fixed drug ratios are evaluated to define the optimum ratio(s) which exhibit(s) synergistic effect.

2.6.4 Determination of combined chemotherapeutic effect

Evaluation of drug interactions in combinations is conducted in vitro by a series of concentrations (Figure 2.17A) to obtain dose response curves (Figure 2.17B) for the drugs and combinations. After that, the drug interactions of combinations are assessed as shown in Figure 2.17C. Briefly, individual drugs are firstly screened separately in vitro assay(s) to determine their individual activities. Then, pairs of drugs at different fixed ratios are combined and assayed in the same condition. Cell growth or cell viability are measured using a variety of cytotoxicity assays such as 3-(4,5-dimethylthiazol-2-yl)-2,5-diphenyltetrazolium bromide (MTT) assay [222], trypan blue [223], glutamate pyruvate transaminase (GPT) assay, lactate dehydrogenase (LDH) assay [224], propidium iodide staining [225], clonogenic assays [226], mitochondrial membrane potential (MMP) assay [227], sodium 3'-[1-(phenylaminocarbonyl)-3,4-tetrazolium)-bis-(4-methoxy-6-nitro) benzene sulphonic acid hydrate (XTT), 3-(4,5-dimethylthiazol-2-yl)-5-(3-

carboxymethoxyphenyl)-2-(4-sulphophenyl)-2H-tetrazolium (MST) [228]. MTT assay is preferred for *in vitro* cytotoxicity study because it is very robust and is metabolised by most cell types. However, it is recommended to apply for than one assay to confirm the results of individual assays when detailed information is required [228].

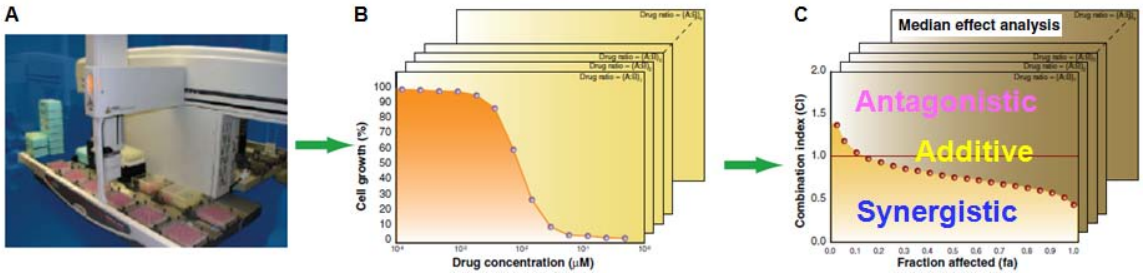

Figure 2.17 In vitro evaluation of synergistic drug interactions [229].

Combination effects over concentration ranges of combined ratios may be determined using various available mathematical algorithms such as Isobologram methods [230, 231], the fractional product method, Chou and Talalay median-effect method [232, 233]. Chou-Talalay median-effect method has been widely used for determination of combination effects because it can provide similar accuracy compared to other methods while requires lesser number of measurements. The analysis utilizes the dose-effect equation:

$$log(f_a/f_u) = mlog(D) - mlog \qquad (2-1)$$

where f_a and f_u are the fraction affected and unaffected by the dose respectively, Dose is the dose of the drug used, and $Dose_m$ is the median-effect dose signifying the potency. This equation is further manipulated to calculate the combination index (CI) of the combined two drugs (eq. 2-2) based on additive effect of the two drug-effect equation from Loewe additivity model:

$$CI = \frac{(Dose)_1}{(Dose_x)_1} + \frac{(Dose)_2}{(Dose_x)_2} \qquad (2-2)$$

where $(Dose)_1$ and $(Dose)_2$ were the dose of drug 1 and drug 2 in the combination that kill x% cells, $(Dose_x)_1$ and $(Dose_x)_2$ were the dose of drug 1 and drug 2 in single drug treatment to kill x% cells.

The interaction of the two drugs can be classified as synergistic (CI < 1), additive (CI = 1) or antagonistic (CI > 1) (Figure 2.20C) based on the fraction affected or cell viability data [219].

CHAPTER 3. Surface modification of polymeric micelle particles for enhancement of cancer targeting and penetrating ability

3.1 Introduction

The use of polymeric micelles as drug carriers started in the 1980s by Bader et al. [234, 235], and these class of carriers started to be known to improve drug delivery efficiency in the 1990s [236, 237]. From 1990s until recent years, micelles have further investigated to explore more about their biological and medicinal uses in cancer treatment [128, 139, 238]. Several polymeric micelle carriers have been evaluated in clinical trials and they have been found to be a potential type of drug carrier system [122, 239-242]. The unique features that have made polymeric micelles attractive are small size, biodegradability and high flexibility for structural and chemical modification [243].

Early generation of polymeric micelles simply entered tumors by passive targeting and may not deliver sufficiently high concentration of anticancer drugs inside the cancer cells [110]. Therefore, polymeric micelles with surface modification targeting cancer cells specifically and being able to across the plasma membrane of cells efficiently may offer new opportunities in the area of cancer therapy. However, efficient drug transportation through the plasma membrane still remains a major hurdle for drug delivery [244]. Improving the transport process across the plasma membrane significantly reduces the amount of administered drug, and the side effects on healthy tissues.

A family of positively charged short peptides, known as cell-penetrating peptides (CPPs), was identified in mid-1990s [245]. CPPs are considering as promising candidates for drug delivery since they are capable of transporting attached macromolecules from extracellular space through the cell membrane into cytoplasm in both *in vitro* and *in vivo* studies [138, 159, 172, 246]. One of the CPPs receiving great attention is TAT peptide, a cationic peptide derived from the human immunodeficiency virus type 1 (HIV-1) [247]. Many studies have used TAT to transport intracellular cargoes, such as DNA [248], quantum dots, polymers [249], micelles [138, 141], nanoparticles [159] and liposomes [250]. Moreover, the TAT peptide has been shown to exhibit no toxicity to many cells, such as to Hela and Jurkat cells with the concentration of up to 20-30 μM [251] and to lymphocytes up to 300 μM [252].

Although highly efficient for *in vitro* cellular uptake, *in vivo* application of CPPs is much more complicated. The main reason is the lack of cell specificity, thus limiting the clinical application of CPP-mediated delivery systems. Dowdy et al. showed that after intraperitoneal injection, CPP were found in the lung, liver, kidney, brain and other tissues [172]. To achieve high efficiency of tumor-specific drug delivery, it is important to modify the delivery carriers with a ligand that is able to target to specific cancer cells of interest. Folate (FOL) is a targeting ligand having high binding affinity to folate receptors overexpressed in ovarian, breast, brain, lung, colorectal cancer cells [253-255] and has widely been used to modify many delivery carriers such as nanoparticles [87], liposomes [256], micelles [257-260].

In this study, to enhance efficient delivery of anticancer drug into cancer cells, we have developed a novel hydrophobic drug delivery system based on polymeric micelles with multifunctional surface properties as shown in Figure 3.1.

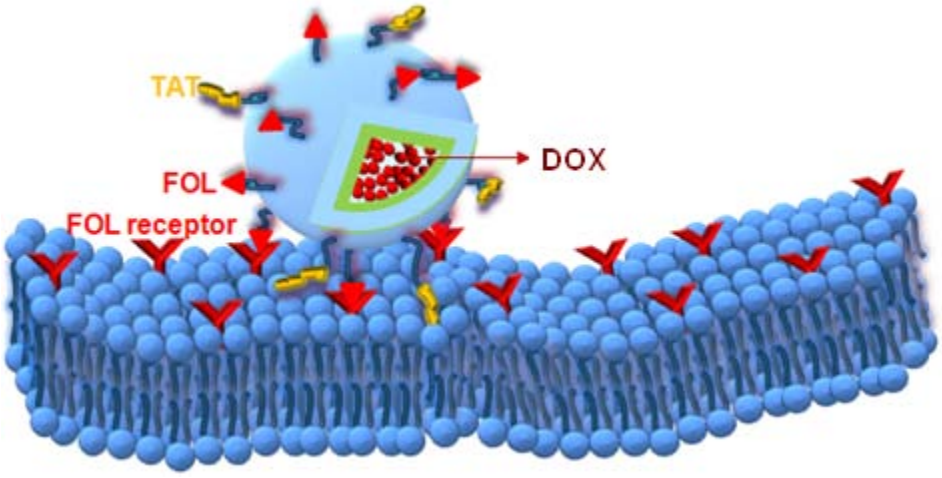

Figure 3.1 Schematic of the drug-loaded multi-functionalized polymeric micelle that is investigated in this study.

Mixed polymeric micelles based on PLGA-PEG, PLGA-PEG-FOL and PLGA-PEG-TAT copolymers were fabricated to encapsulate DOX (hydrophobic form), a model drug in this study. Micellar properties such as the critical micelle concentration (CMC), size, zeta potential, drug loading content and *in vitro* release were investigated. Furthermore, cytotoxicity study of DOX-loaded polymeric micelles was performed using human oral cavity carcinoma (KB) cell line. Finally, the cellular uptake efficiency of different micelles was evaluated using laser scanning confocal microscopy.

3.2 Experimental section

3.2.1 Materials

Poly(ethylene glycol) bis(amine) (PEG-diamine, Mw:10,000), poly(ethylene glycol) 2-aminoethyl ether acetic acid (NH_2-PEG-COOH, Mw: 10,000) were purchased from Laysan Bio Inc (USA). 75:25 poly(D, L-lactide-co-glycolide) with carboxylic end group (PLGA, Mw: 5,600) was acquired from Lakeshore Biomaterials (USA). TAT peptide of the sequence NH_2-Tyr(tBu)-Gly-Arg(Pbf)-Lys(Boc)-Lys(Boc)-Arg(Pnf)-Arg(Pbf)-Gln(Trt)-Arg(Pbf)-Arg(Pbf)-Arg(Pbf) (NH_2-YGRKKRRQRRR) was custom-synthesized by GL Biochem (Shanghai) Ltd (China). Poly(ethylene glycol)-amine (PEG-amine, Mw: 5,000), N-hydroxysuccinimide (NHS), dicyclohexylcarbodiimide (DCC), folic acid, pyridine, dichloromethane (DCM), N,N-dimethylformamide (DMF), dimethyl sulfoxide (DMSO) and triethylamine (TEA), trifluoroacetic acid (TFA), triiso-propysilane (TIS), coumarin 6 (C6), 3-[4,5-dimethylthiazolyl-2]-2,5-diphenyl tetrazolium bromide (MTT), ninhydrin kit were all purchased from Sigma-Aldrich (USA). Doxorubicin (DOX) was obtained from Boryung (Korea). Methanol, acetonitrile (ACN), tetrahydrofuran (THF), chloroform, diethyl ether were purchased from Tedia (USA). Folate-free RPMI 1640 medium, fetal bovine serum (FBS), Trypsin-EDTA and penicillin-streptomycin were obtained from Invitrogen (USA). KB human oral cavity carcinoma cell line was purchased from ATCC (USA). Reagent graded water was obtained from the Milli-Q Plus System (Millipore Corporation, USA). All chemicals were used directly without further purification.

3.2.2 Synthesis of PLGA-PEG

PLGA-PEG block co-polymer was synthesized by the previously reported method with a slight modification [257]. Briefly, PLGA dissolved in DCM was activated by DCC and NHS at room temperature under N_2 atmosphere for 24 h. The resultant solution was filtered and precipitated by dropping into ice-cold diethyl ether, followed by completely drying under vacuum for 2 days. The activated PLGA and PEG-amine (molar ratio of activated PLGA:PEG-amine = 1:1.2) dissolved in DCM were allowed to react at room temperature under N_2 atmosphere for 3 h. The resultant solution was precipitated by dropping into ice-cold diethyl ether. The precipitated product, PLGA-PEG was dissolved in DMSO and dialyzed against de-ionized (DI) water for 2 days (MWCO: 10,000), and was further centrifuged to remove impurity and obtain PLGA-PEG. The product was freeze-dried in a freeze drier for 2 days.

3.2.3 Synthesis of PLGA-PEG-FOL

The synthesis of PLGA-PEG-FOL followed a 3-step reaction [257]– PLGA activation (as mentioned in the previous section), FOL capping to form PEG-FOL, and conjugation of PLGA with PEG-FOL to form PLGA-PEG-FOL. PEG-FOL was first synthesized by reacting PEG-diamine (Mw: 10,000) with folic acid and DCC/NHS (molar ratio of PEG-diamine:folic acid:DCC:NHS = 1:1:2:2) in DMSO in the presence of pyridine. The reaction was carried out for 10 h in the dark at room temperature under N_2 atmosphere. The mixture was then diluted with DI water and centrifuged to remove the insoluble by-product dicyclohexylurea (DCU). The supernatant was further filtered to obtain clear yellow solution. The solution was dialyzed against DI water for 2 days (MWCO: 1000) to

remove DMSO and unreacted folic acid in the mixture and freeze-dried. The trace amount of unreacted PEG-diamine was then removed by batch adsorption with cellulose phosphate cation exchange resin using 5 mM phosphate buffer pH 7.0 as start buffer. PEG-FOL was further purified by a DEAE sephadex anion exchange column with 20 mM Tris-HCl pH 8.0 as start buffer to remove FOL-PEG-FOL side product. The reaction of activated PLGA and PEG-FOL (molar ratio of activated PLGA:PEG-FOL = 1:1.2) was carried out for 8 h in DMSO at room temperature under N_2 atmosphere. The product was precipitated twice in ice-cold diethyl ether, dissolved in DMSO for dialysis against DI water for 2 days (MWCO: 10,000), centrifuged to remove unconjugated PLGA, and then freeze-dried.

3.2.4 Synthesis of PLGA-PEG-TAT

NH_2-PEG-COOH with Mw of 10,000 Da was used to fabricate PLGA-PEG-TAT copolymer. PLGA was firstly conjugated to NH_2-PEG-COOH by the reaction between the carboxylic group of PLGA and the amine group of NH_2-PEG-COOH which is similar with PLGA-PEG conjugation described in the previous session. Subsequently, the protected-TAT peptide with the sequence of NH_2-YGRKKRRQRRR was conjugated to PLGA-PEG through the carboxylic group on its PEG [138, 139]. Briefly, DCC, NHS dissolved in DCM was added to the solution of PLGA-PEG-COOH in DCM to activate the carboxylic group of PLGA-PEG-COOH under room temperature for 6 h. Upon completion, the activated polymer was then precipitated with ice-cold diethyl ether, and centrifuged to recover the activated polymer. The product was further vacuum-dried overnight. The coupling reaction of protected-TAT and activated PLGA-PEG-COOH to

form PLGA-PEG-TAT was carried out for 24 h in DCM. The product was purified by being precipitated in ice-cold diethyl ether and dried. The conjugated TAT was deprotected by mixing the TAT-conjugated copolymer to the cocktail containing 95% TFA, 2.5% TIS, and 5% DI water for 3 h. PLGA-PEG-TAT was precipitated in ice-cold diethyl ether and centrifuged to recover the polymer as pellet. The polymer was vacuum-dried and further purified by dialyzing against DI water (MWCO: 3,000 Da) for 1 day. The final product was freeze-dried for subsequent use.

3.2.5 Characterization of polymers

The amount of free amine group in the unconjugated PEG (PEG-amine or PEG-diamine) after coupling reactions was quantified by Ninhyidrin assay. Ninhydrin is a chemical that reacts with free amines of PEG to produce purple color salt. The amount of the resultant purple color salt can be detected with a UV-vis spectrophotometry at 570 nm.

^{1}H NMR spectrum of the samples was recorded on a Bruker AMX 500 spectrometer using deuterated chloroform ($CDCl_3$) and deuterated dimethyl sulfoxide (DMSO-d_6) as solvents at 25°C.

Molecular weight of the copolymers was measured using an Aligent high performance liquid chromatography - gel permeation chromatography (HPLC-GPC) system equipped with a differential refractive index (RI) detector and PLgel 5 µm mixed-D column (7.5 x 300 mm). THF was used as eluent at a flow rate of 1 mL/min at 25ºC. The injection volume was 20 µl. A series of narrow polystyrene standards were used for calibration.

3.2.6 Critical micelle concentration (CMC)

Fluorescence spectroscopy was used to estimate the critical micelle concentration (CMC) of PLGA-PEG, PLGA-PEG-FOL, PLGA-PEG-TAT copolymers in PBS using pyrene as a hydrophobic fluorescent probe [261]. Briefly, a series of solutions containing 0.0025 – 25 mg/L copolymers and 0.6 μM pyrene were prepared and allowed to equilibrate at room temperature overnight under gentle shaking. The excitation spectra were recorded from 300 to 360 nm with an emission wavelength at 390 nm [262]. The intensity ratios of $I_{337.5}/I_{334.5}$ were plotted against the logarithm of polymer concentration. The CMC value was estimated as the point of the intersection of the best fit lines at low and high concentration respectively.

3.2.7 Preparation and characterization of doxorubicin loaded polymeric micelles

DOX-loaded micelles with different weight percentage of 3 polymers (i.e., PLGA-PEG, PLGA-PEG-FOL and PLGA-PEG-TAT) were prepared using dialysis method as previously described with slight modification [257]. First, DOX.HCl was neutralized with twice the number of mole of TEA in DMSO overnight to obtain the DOX free base in hydrophobic form [263]. The mixtures of polymers were dissolved in DMSO at a total concentration of 10mg/ml. The DOX solution was added into the polymer solution and mixed by vortex for 10min. The mixture was transferred into dialysis bag (MWCO: 3,000 Da) for dialyzing against DI water for 2 days to produce micelles and remove untrapped DOX and TEA. The resultant micelles are represented as the weight percentage of the polymer contained the functional moiety used in preparing the micelles. For example,

TAT(10)/FOL(20)-modified micelles implies the micelles were prepared from 10 wt% PLGA-PEG-TAT:20 wt% PLGA-PEG-FOL:70 wt% PLGA-PEG.

The hydrodynamic size and zeta potential of polymeric micelles were measured at 25°C by Nano Sizer (Malvern Instruments, UK). Aqueous micelle solutions were prepared using deionized water. The concentration of polymeric micelles was kept at 1 mg/ml. The micelle solutions were filtered through a 0.80 μm cellulose membrane filter before measurements. The average values were calculated from at least 3 measurements performed on each samples. To determine DOX loading level and encapsulation efficiency, 1 mg of DOX-loaded micelles was dissolved in 1 ml DMSO. The DOX concentration was estimated with UV-vis spectrophotometry at 480 nm. The DOX content was determined using the calibration curve of DOX in DMSO range from 0 to 50 μg/ml.

3.2.8 *In vitro* release of doxorubicin (DOX)

DOX-loaded micelle solutions (2 mg in 1 ml of PBS, pH 7.4) were transferred to dialysis tube (MWCO: 2,000 Da) and dialyzed against 3 ml PBS in a tube at 37°C with shaking at 100 rev/min. To measure the release of DOX at different time intervals, PBS solution in the tube was all withdrawn and replaced with 3 ml fresh PBS. The content of DOX in PBS was determined using microplate reader (Tecan – Infinite M200, Austria). Briefly, PBS solution was transferred to 96-well plate and detected by microplate reader with excitation wavelength at 480 nm and emission wavelength at 570 nm. The release amount

of DOX was determined using the calibration curve of DOX in PBS range from 0 to 10 ppm. The drug release studies were performed in triplicate for each of the samples.

3.2.9 Preparation of Coumarin 6-loaded micelles

Coumarin 6 (C6)-loaded micelles were prepared by a similar dialysis method used for DOX- loaded micelles. Briefly, 1.5 mg of C6 and 30 mg of polymers were dissolved in 3 ml of DMSO. This solution was then transferred into the dialysis bag (MWCO: 3,000 Da) for dialyzing against DI water for 2 days to produce micelles and removed untrapped C6. The micelles were lyophilized to solid powder form.

3.2.10 *In vitro* cellular uptake

The cell target and cell penetration tests of micelles with and without TAT/FOL were carried out in KB cells by labeling the micelles with C6. The cells were cultured in 12 mm round glass coverslips placed in 24-well plates for 1 day. Cells were then treated with 30 µM C6-loaded micelles for 3 h. Since TAT peptide was reported to penetrate cell membrane within 4 min [264], the chosen incubation times were sufficient to demonstrate the TAT activity. Subsequently, cells were washed 3 times with cold PBS, fixed with 4% cold paraformaldehyde for 30 min at room temperature, and washed with PBS again. The fixed cells on were observed under confocal microscope (Nikon C1, Japan) at excitation wavelength of 480 nm and emission wavelength of 590 nm.

3.2.11 *In vitro* cytotoxicity of DOX-loaded micelles

The ability of DOX-loaded micelles to inhibit cell proliferation was evaluated using human KB carcinoma cell line with MTT viability assay. Cells cultured in free folic RPMI media supplemented with 10% FBS and 1% penicillin-streptomycin at 37°C in humidified environment of 5% CO_2 were seeded onto 96-well plates at a seeding density of 5000 cells/well and incubated for 48 h to permit cell attachment. The cells were then treated with DOX-loaded micelles at different concentrations for 3 days. After 3 days of incubation, the cells were washed once with PBS, and grown for another 48 h. The growth medium was then replaced with free serum medium containing 0.5 mg/mL MTT and incubated for 4 h. MTT containing medium was next discarded and replaced with 150 μl DMSO to dissolve the formazan crystals for 15 min under shaking. The samples were then analyzed with a microplate reader (Tecan – Infinite M200, Austria) using a test wavelength of 570 nm and a reference wavelength of 630 nm. The data were presented as mean and standard deviation of 6 replicates.

3.3 Results and discussion

3.3.1 Characterization of PLGA-PEG

PLGA-PEG was synthesized by the reaction between carboxylic group of PLGA (Mw: 5,600 Da) and primary amine group of PEG (Mw: 5000 Da). Therefore, the coupling reaction could be confirmed by the disappearance of the primary amine group of PEG-amine reactant in the resultant product. Ninhydrin assay which is able to detect the presence of amine group was carried out to determine the amount of unconjugated PEG in the final PLGA-PEG product [265]. Ninhydrin results suggest that the coupling

reaction occurred and PLGA-PEG was produced with the presence of 15.6 ± 1.7 % of unconjugated PEG in the product.

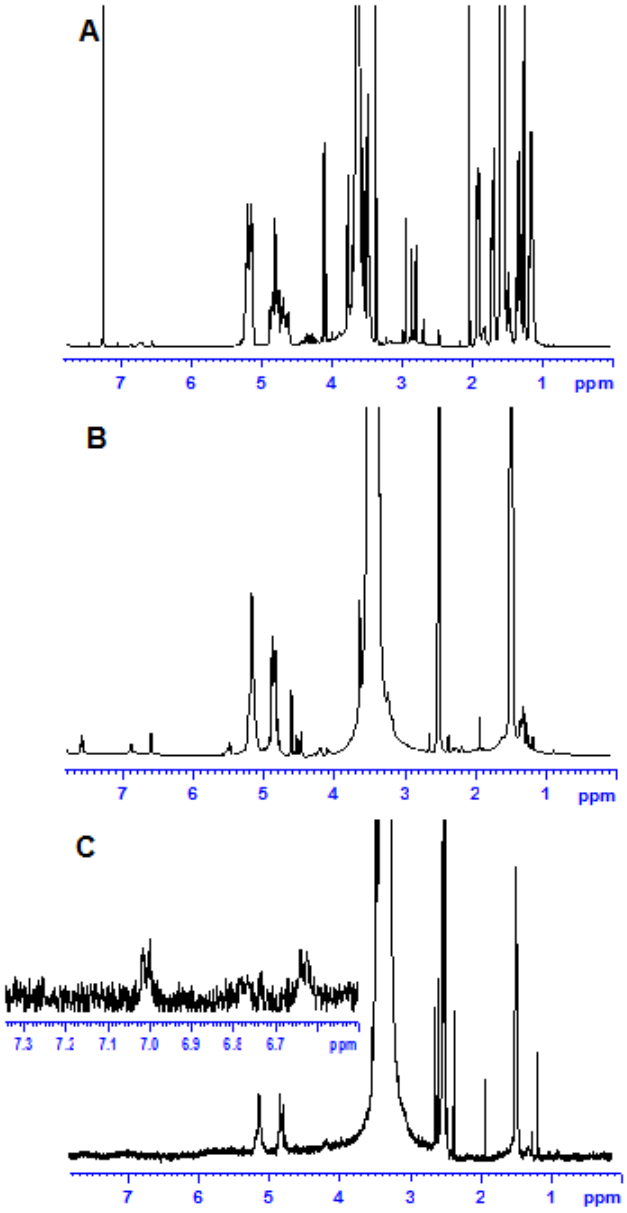

Figure 3.2 ^{1}H NMR spectra of (A) PLGA-PEG, (B) PLGA-PEG-FOL, and (CDDP) PLGA-PEG-TAT.

In addition, ^{1}H NMR analysis shows that PLGA-PEG was successfully synthesized. From Figure 3.2A, the multiple peaks at δ3.5-3.7 are from the proton of CH_2 groups in PEG.

The lactic proton and glycolic protons of PLGA are indicated by the presence of the peaks at δ5.2 and δ4.8, respectively [266]. The molecular weight of the final product PLGA-PEG was characterized by GPC. The GPC results further indicate that PLGA-PEG polymer was successfully prepared.

3.3.2 Characterization of PLGA-PEG-FOL

PLGA-PEG-FOL polymer was characterized using GPC, ^{1}H NMR, ninhydrin and UV spectroscopy. Similar to PLGA-PEG synthesis, ninhydrin tests indicate that the purity of PLGA-PEG-FOL is approximately 84.9± 0.6 %. Figure 3.2B shows the peaks at δ3.5-3.7, δ5.2 and δ4.8 which are assigned to PEG and PLGA as mentioned in the previous session. In addition, the presence of the new peaks at δ6.6 and δ7.6, which belong to the protons on the benzene ring of FOL, indicates that PLGA-PEG-FOL was successfully synthesized [257]. Compared to Figure 3.2A, the PEG peak in the Figure 3.2B is more intensive because larger PEG polymer (Mw: 10,000 Da) was used for PLGA-PEG-FOL fabrication. GPC result further verifies that PLGA-PEG-FOL was prepared with a low amount of impurity. Furthermore, UV spectroscopy measuring the amount of FOL also confirms 82.7± 1.0 % purity of PLGA-PEG-FOL product.

3.3.3 Characterization of PLGA-PEG-TAT

In this study, the short sequence of TAT peptide was used since it was previously showed to increase cellular internalization of carriers more efficiently as compared to longer TAT sequences [267]. Figure 3.2C shows the ^{1}H NMR spectrum of PLGA-PEG-TAT. The new peaks at δ6.6 and at δ7.0 present to the protons from the benzene ring in tyrosine of

TAT peptide [138]. By comparison the intensity of the peaks attributed to PLGA and TAT, the yield of TAT coupling is estimated at around 40%.

3.3.4 Critical micelle concentration (CMC)

The copolymers consisting of hydrophobic and hydrophilic blocks can self-assemble to form micelles in aqueous solution. The formation of micelles with PLGA-PEG, PLGA-PEG-FOL and PLGA-PEG-TAT was evidenced by the existence of CMC measured using fluorescence spectroscopy with pyrene as the fluorescence probe. As shown in Figure 3.3, the gradual shift of the peak in the excitation spectra of pyrene from 334.5 to 337.5 is observed, indicating the change in the vibration structure of the pyrene emission. At low polymer concentration, the intensity ratio of $I_{337.5}/I_{334.5}$ does not change much. However, at high polymer concentration (above CMC value), the intensity ratio changes sharply, which indicates the presence of pyrene in the hydrophobic core of micelles. The CMC of non-modified micelles (100% PLGA-PEG), FOL(10)-micelles (10 wt% PLGA-PEG-FOL:90 wt% PLGA-PEG), TAT(10)-micelles (10 wt% PLGA-PEG-TAT:90 wt% PLGA-PEG), and TAT(10)/FOL(10)-micelles (10 wt% PLGA-PEG-TAT:10 wt% PLGA-PEG-FOL:80 wt% PLGA-PEG) micelles are 3.61 mg/L, 3.68 mg/L, 4.34 mg/L and 5.50 mg/L respectively.

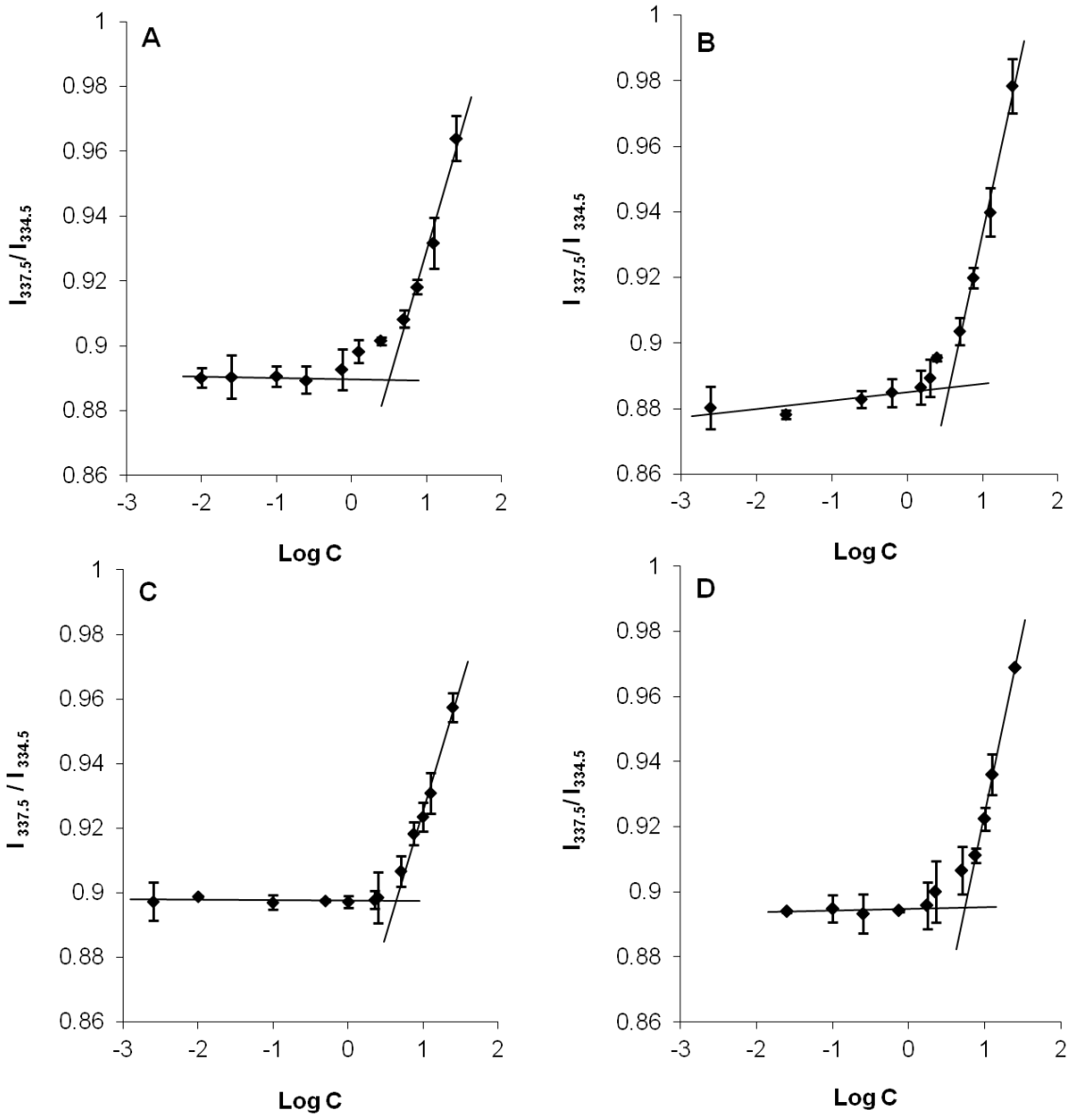

Figure 3.3 Plot of $I_{337.5}/I_{334.5}$ ratio as a function of polymer concentration (Log C) in PBS. (A) PLGA-PEG, (B) 10 PLGA-PEG-FOL: 90 PLGA-PEG, (CDDP) 10 PLGA-PEG-TAT: 90 PLGA-PEG, and (DOX) 10 PLGA-PEG-TAT: 10 PLGA-PEG-FOL: 80 PLGA-PEG.

Among all the micelles, the CMC of micelles with FOL and TAT functional groups are slightly higher than that of the non-modified micelles. A possible reason is that the molecular weight of PEG used in PLGA-PEG-FOL and PLGA-PEG-TAT is larger than that used in PLGA-PEG which reduces the hydrophobicity of the polymers. As a result,

larger amount of polymers are needed to form the micelles. Moreover, TAT(10)-micelles have higher CMC values than FOL(10)-micelles. This is because of the strong interaction of TAT with water molecules [138] hence even more PLGA molecules are needed to form the core of TAT-modified micelles. As mentioned above, the composition of TAT(10)/FOL(10)-micelles contains both PLGA-PEG-FOL and PLGA-PEG-TAT with 10 wt% of each polymer; therefore, their CMC is higher than FOL(10)-micelles and TAT(10)-micelles.

3.3.5 Particle size, zeta potential

Table 3.1 Characterization of DOX- loaded polymeric micelles.

Micelles	DLC (%)	EE (%)	Size (nm)	Polydispersitive indext (PdI)	Zeta potential (mV)
Non-modified micelles	1.91	47.8	63.74	0.184	-13.30
FOL(10)-micelles	2.03	50.8	94.61	0.219	-12.25
TAT(10)-micelles	2.10	52.5	81.07	0.235	-13.00
TAT(10)/FOL(10)-micelles	1.95	48.8	106.30	0.251	-9.48

The size of drug delivery carriers is important since it influences drug efficacy and pharmacokinetics. Hobbs et al. [268] showed that liposomes with diameters from 100 nm – 200 nm were more efficient in diffusing along the vessel of tumors than larger liposomes. Moreover, it was proven that the uptake of the reticuloendothelial system (RES) is size dependent, the smaller size of carriers would result in the lesser uptake; therefore, the clearance would be reduced [269]. The size of all micelles in this study is less than 200 nm, which indicates the suitability for drug delivery (Table 3.1). Compared

to previously TAT-micelle system based on TAT-PEG-cholesterol with the size at around 200 nm, our reported TAT/FOL-modified micelles with smaller size are more suitable for drug delivery by reducing the RES uptake. In addition, the zeta potential of particles also plays an important role in RES uptake. It was proven that the RES uptake of particles cannot be avoided if their zeta potential values are above -5 mV [269]. The zeta potential values of the micelles used in this study are lower than -5 mV (Table 3.1), which indicate that the micelles can escape from the RES uptake.

3.3.6 *In vitro* drug release and drug loading

Drug loading content (DLC) and encapsulation efficiency (EE) in different micelle formulations (Table 3.1) shows no significant difference in the amount of DOX-loaded among non-modified micelles, FOL(10)-micelles, TAT(10)-micelles and TAT(10)/FOL(10)-micelles. DOX was successfully incorporated into the core of micelles by physical interaction with drug loading content of approximately 2%. Similarly, the DOX release profiles from all four micelles shown in Figure 3.4 are almost the same with less than 10%, 15% release within the first 6 h and 24 h respectively. Then the drug is slowly released and maintains more than 60% of the drug in the micelles after 12 days incubation with pH 7.4 PBS.

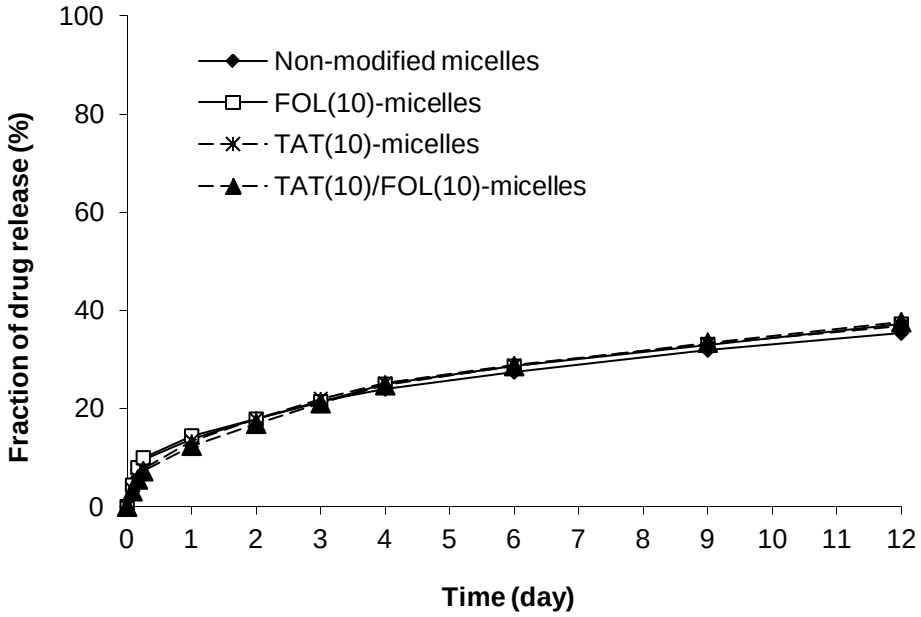

Figure 3.4 *In vitro* release profiles of DOX from different kinds of micelles. The experiments were conducted in triplicate in PBS (pH 7.4) at 37ºC. The standard deviation of these drug release curves is not shown to make the figure to be seen easily. The standard deviation is quite small (less than 10%).

Compared to previously reported DOX- loaded polymeric micelle systems prepared from other amphiphilic materials, such as poly(N-isopropylacrylamide-co-N,N-dimethylacrylamide-co-2-aminoethyl methacrylate)-poly(10-undecenoic acid) (2.5% DLC and 40% drug release within the first 24 h [270]), the PLGA-PEG system used here exhibits a more sustainable DOX release rate and reasonable DLC.

3.3.7 Cytotoxicity of DOX- loaded micelles

As proven in previous studies, functional moieties should be located above the carrier surface for the unhindered interaction between the moieties with the cells [137]. Therefore, a higher molecular weight of PEG was used for fabrication of PLGA-PEG-FOL and PLGA-PEG-TAT polymers compared to PLGA-PEG. To quantitatively evaluate the cell cytotoxicity of the micelles, the KB cells were utilized as an *in vitro*

model. To assess the changes in proliferation, the cells were incubated with DOX- loaded micelles for 72 h and examined using the MTT assay. The toxicity of all blank micelles without loaded drug to KB cells was measured at a tested concentration of 2.0 mg/mL for 72 h. The polymer concentration used in the blank micelle tests was higher than the concentration of polymers in all cytotoxicity tests with the presence of DOX. Blank micelle tests indicate that micelles at concentration of 2.0 mg/mL were practically non-toxic to KB cells.

3.3.7.1 Effect of PLGA-PEG-FOL concentration on FOL-modified micelles

The targeting ability of FOL-modified micelles relies on the specific binding between FOL and FOL receptors. Hence the amount of FOL on the surface of micelles can affect the targeting ability of micelles. It was reported that few FOL molecules on the micellar surface reduced the binding ability, however, too many FOL molecules on the surface also decreased targeting ability and affect normal cells [257]. Therefore, the cytotoxicity effect of DOX-loaded FOL-micelles with various FOL concentrations has been investigated. Four micelle systems with 0-30 wt% PLGA-PEG-FOL in the polymer carriers are selected for the demonstration and named as non-modified micelles, FOL(10)-micelles, FOL(20)-micelles and FOL(30)-micelles. The number in the bracket indicates the weight percentage of PLGA-PEG-FOL in the blend of PLGA-PEG and PLGA-PEG-FOL used in preparing micelles.

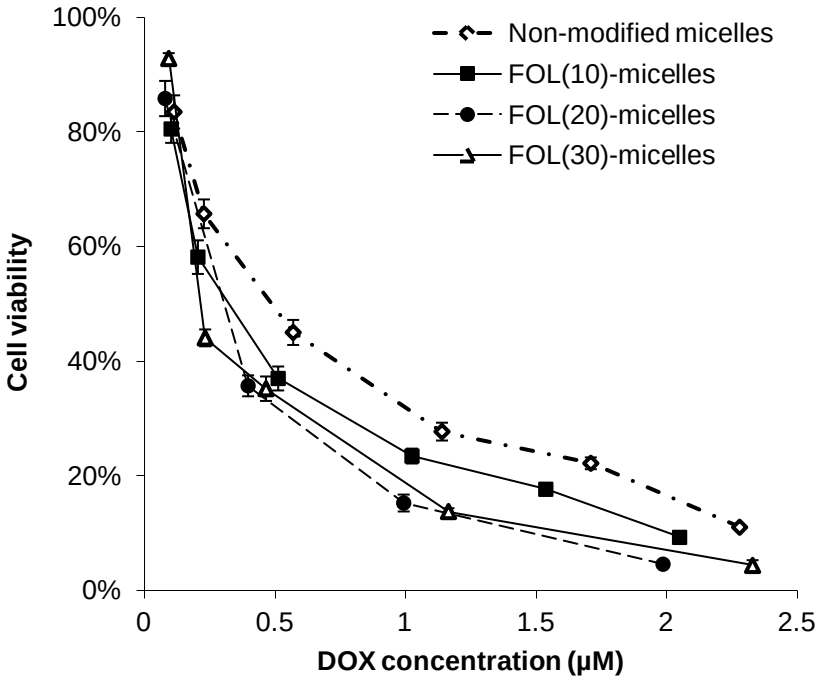

Figure 3.5 Effect of FOL concentration of the FOL-micelles on the viability of KB cells after being treated with 4 types of DOX- loaded micelles: non-modified micelles, FOL(10)-micelles, FOL(20)-micelles, and FOL(30)-micelles for 3 days.

The cell viability of KB cells after being treated under different DOX concentration using FOL(0-30)-micelles is shown in Figure 3.5. The cell viability first decreases when increasing FOL concentration up to 20% because the interaction between micelles and cells is stronger with higher popular of FOL on the micelle surface. On the other hand, micelles with higher density of FOL ligand on a surface interact with larger amount of FOL receptors on the cell membrane that may also leads to lower micelles internalization rate. Increasing FOL concentration in each micelle leads to the faster delivery of FOL into cancer cells. Hence, FOL receptor recycling system is down-regulated faster because of the faster satisfaction of the FOL requirement of cancer cells. Therefore, further increase of FOL content to 30% cannot help to increase the efficiency of the micelles in this study which is in agreement with our previous report [257]. As shown in Table 3.2,

the lowest IC_{50} (0.273 μM) is from FOL(20)-micelles. However, this optimal FOL concentration (20%) is lower than our previous PLGA-PEG-FOL studies (40-65%) [257]. In our previous study, the PEG with the same molecular weight was used for the synthesis of both PLGA-PEG and PLGA-PEG-FOL. Therefore, more amount of FOL in the micelles could be needed in order to get the maximum targeting compared to this study in which higher molecular weight of PEG was used in PLGA-PEG-FOL synthesis.

Table 3.2 IC_{50} values of DOX incorporated micelles with various surface modifications after incubation with KB cells for 3 days.

Micelles	IC_{50} (μM)
Non-modified micelles*	0.529
FOL(10)-micelles*	0.326
FOL(20)-micelles	0.273
FOL(30)-micelles	0.328
TAT(10)-micelles*	0.293
TAT(10)/FOL(10)-micelles*	0.171
TAT(10)/FOL(20)-micelles	0.147

*DOX-loaded micelle systems with different surface modifications (See Section 3.3.7.3).

3.3.7.2 Effect of FOL concentration on TAT/FOL-modified micelles

TAT peptide is a non-selective peptide thus it is able to penetrate into both cancer and normal cells. Besides, its high positive charge may change the surface charge of the system to a more positive charged one which increases the RES uptake. Hence, low

amount of TAT should be used in order to obtain micelles with minimal non-selective penetration and RES uptake. It was proven that micelle systems with 2 mol% TAT were good for the homo distribution of micelles and less precipitated than the micelles with higher than 2 mol% TAT by more than 2 times [173]. Although some recent studies used 100% TAT-conjugated polymers to form carriers [138, 139, 173], 10 wt% PLGA-PEG-TAT polymer was used in this project to obtain micelles with approximately 2.5 mol% TAT. The advantages of using such a low amount of TAT are to reduce the RES uptake by maintaining a negative charged system and minimizing non-selective penetration.

The previous section shows that the most efficient FOL-micellar system is FOL(20)-micelles. However, the addition of TAT moiety may change the optimal concentration of FOL in the micelles. Therefore, DOX- loaded TAT/FOL micelles with the blending of 10 wt% PLGA-PEG-TAT and 0-20 wt% of PLGA-PEG-FOL, or TAT(10)/FOL(0-20)-micelles, were investigated. From Table 3.2, the IC_{50} values of DOX- loaded TAT/FOL micelles decrease as the amount of FOL on the surface increases (0.293 µM, 0.171 µM and 0.147 µM for TAT(10)-micelles, TAT(10)/FOL(10)-micelles and TAT(10)/FOL(20)-micelles respectively. While a significant decrease in the IC_{50} of TAT(10)/FOL(10)-micelles compared to TAT(10)-micelles is observed, only a decrease is shown when increasing the FOL from 10% to 20%. Moreover, the anticancer efficacy of TAT(10)/FOL(20)-micelles is similar or even lower than TAT(10)/FOL(10)-micelles at high treatment concentrations (Figure 3.6). This phenomenon is similar with the FOL effect as described in the previous section (3.3.7.1). It may due to the high density of FOL molecules on the micellar surface that interfere the activity of TAT molecules to the

cancer cells. Therefore, TAT(10)/FOL(10)-micelles would be sufficient to enhance cancer treatment against KB cells, with low IC_{50} of 0,171 µM, which is nearly two times lower than the micelles with single functional moiety.

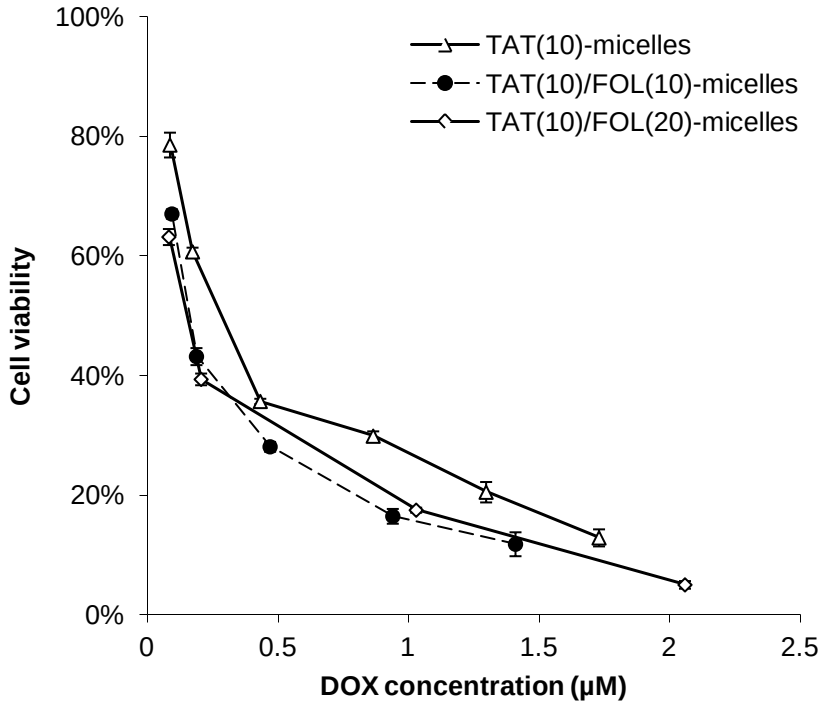

Figure 3.6 Effect of FOL concentration of the TAT(10)/FOL-micelles on the viability of KB cells after being treated for 3 days using 3 types of DOX-loaded micelles: TAT(10)-micelles, TAT(10)/FOL(10)-micelles, and TAT(10)/FOL(20)-micelles.

3.3.7.3 Effect of different functional moieties on the cancer treatment efficacy of micelles

Combining the data set in Section 3.3.7.1 and this section allows us to compare the effect of TAT and FOL functional moieties on the anticancer efficacy of DOX-loaded micelles. Table 3.2 shows that the IC_{50} of non-modified micelles are approximately 1.6, 1.8 and 3 times higher than FOL(10)-micelles, TAT(10)-micelles and TAT(10)/FOL(10)-micelles respectively. This suggests that multi-functional micelle system is a better system since it can overcome the limitation of mono-functional system.

This TAT(10)/FOL(10) system shows higher efficiency than the previous system [137] using TAT- micelles based on TAT- PEG-phosphatidylethanolamine, which only showed less than 2 times enhancement compared to the non-modified micelles. As reported for a TAT- pH sensitive micelle system, the TAT- micelles showed from around 0.3 to less than 1.8 times enhancement at pH conditions ranging 6-7 compared to the non-modified micelles [271]. The results indicate that this multi-functionalized micelle system, TAT(10)/FOL(10)-micelles, is potentially useful for drug delivery applications.

3.3.8 Cellular uptake

Figure 3.7 shows the confocal images of KB cells incubated with C6-loaded micelles. As can be seen, TAT/FOL-modified micelles entered the cells more efficiently than micelles without or with only FOL or TAT. The stronger fluorescence intensity in Figure 3.7B and 3.7C compared to that of Figure 3.7A indicates that 10% PLGA-PEG-FOL or 10% PLGA-PEG-TAT in the micelle formulation could enhance the cellular uptake ability of micelles. Together with the FOL targeting group, the TAT/FOL-modified micelles exhibit enhanced cellular uptake of the drug (Figure 3.7D). The result indicates that the TAT/FOL-micelle system can be potentially applied as an efficient carrier for drug delivery.

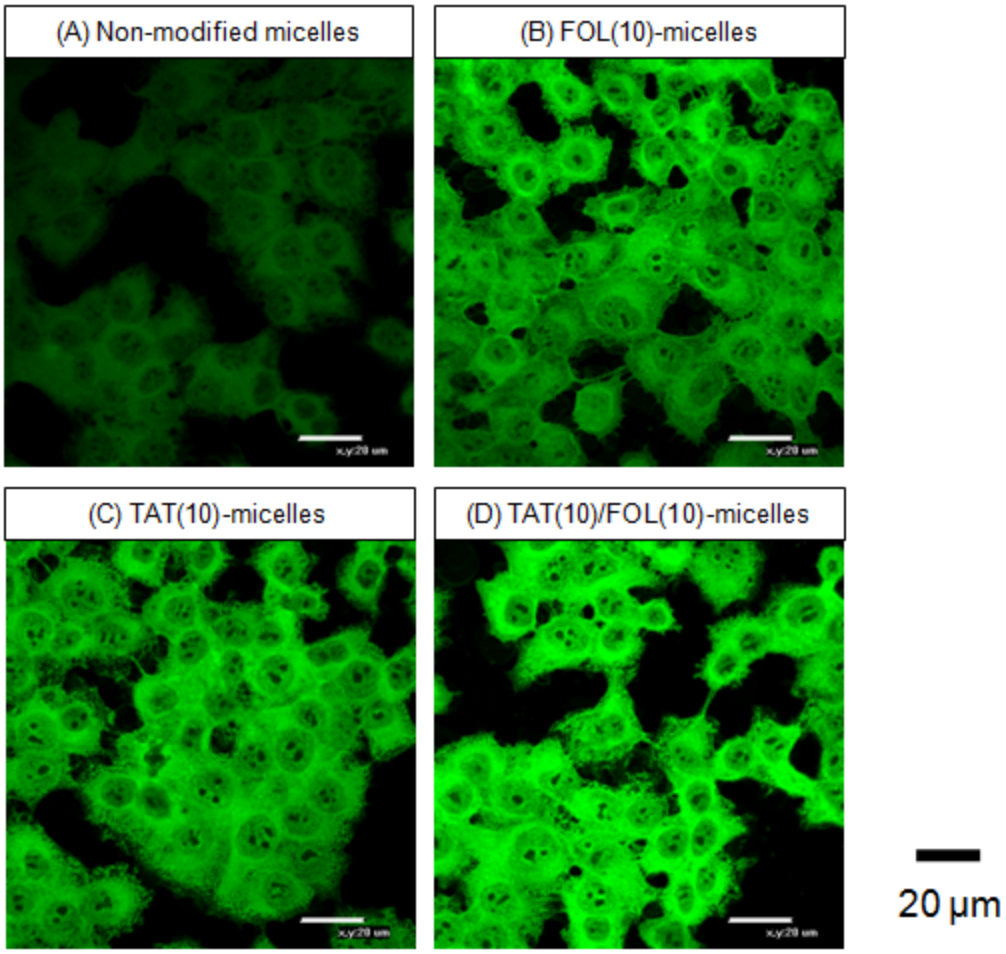

Figure 3.7 Confocal images of KB cells treated with fluorescence (C6) labeled (A) non-modified micelles, (B) FOL(10)-micelles, (C) TAT(10)-micelles, and (D) TAT(10)/FOL(10)-micelles.

3.4 Conclusions

In this study, PLGA-PEG, PLGA-PEG-FOL and PLGA-PEG-TAT copolymers were successfully synthesized. Four micelles with different ratio of PLGA-PEG, PLGA-PEG-FOL and PLGA-PEG-TAT copolymers were fabricated with low CMC. All micelles had small size for drug delivery. Micelles with both TAT and FOL modification were able to enter KB cells more efficiently. Due to enhancement in cellular uptake, TAT/FOL-modified micelles achieved higher cytotoxicity compared to non-modified micelles,

FOL-modified micelles, or TAT-modified micelles. Such TAT/FOL modified micelles represent a promising drug carrier system for drug delivery. To further develop the multi-functionalized micellar drug delivery system invested in this chapter, the following two chapters (Chapter 4 and 5) describes the methods for investigation of synergistic combination delivery using TAT/FOL-functionalized micelles. By controlling the ratio of released drugs at synergistic regime, synergistic treatment efficacy can be obtained.

CHAPTER 4. Synergistic co-delivery of doxorubicin and paclitaxel using multi-functionalized micelles for cancer treatment

4.1 Introduction

Single agent therapy has seen limited success in cancer treatment due to the toxicity at high drug dosage, the heterogeneity of cancer cells and the drug resistance [212-215]. Therefore, combination therapy has been preferred in different cancer treatment due to its lower toxicity at the required effect. In addition, synergistic combinations could promote the response rate compared to single drugs and result in the higher therapeutic effect.

With different activities to cancer cells, the pairing of chemotherapeutic agents (DOX and PTX) for combination treatment can have higher and synergistic therapeutic effect. DOX works by binding to DNA and inhibiting nucleic acid synthesis while PTX promotes microtubule assembly from tubulin dimers and stabilizes microtubules by preventing depolymerization [12]. Due to the different mechanism of DOX and PTX on cancer cells, several studies have been conducted to study the value of the combination of DOX and PTX in cancer treatment. Firstly, this drug combination has shown enhanced response rate and patient survival rate in breast cancer treatment [213]. In addition, these two drugs do not exhibit cross-resistance in metastatic breast cancer treatment [213].

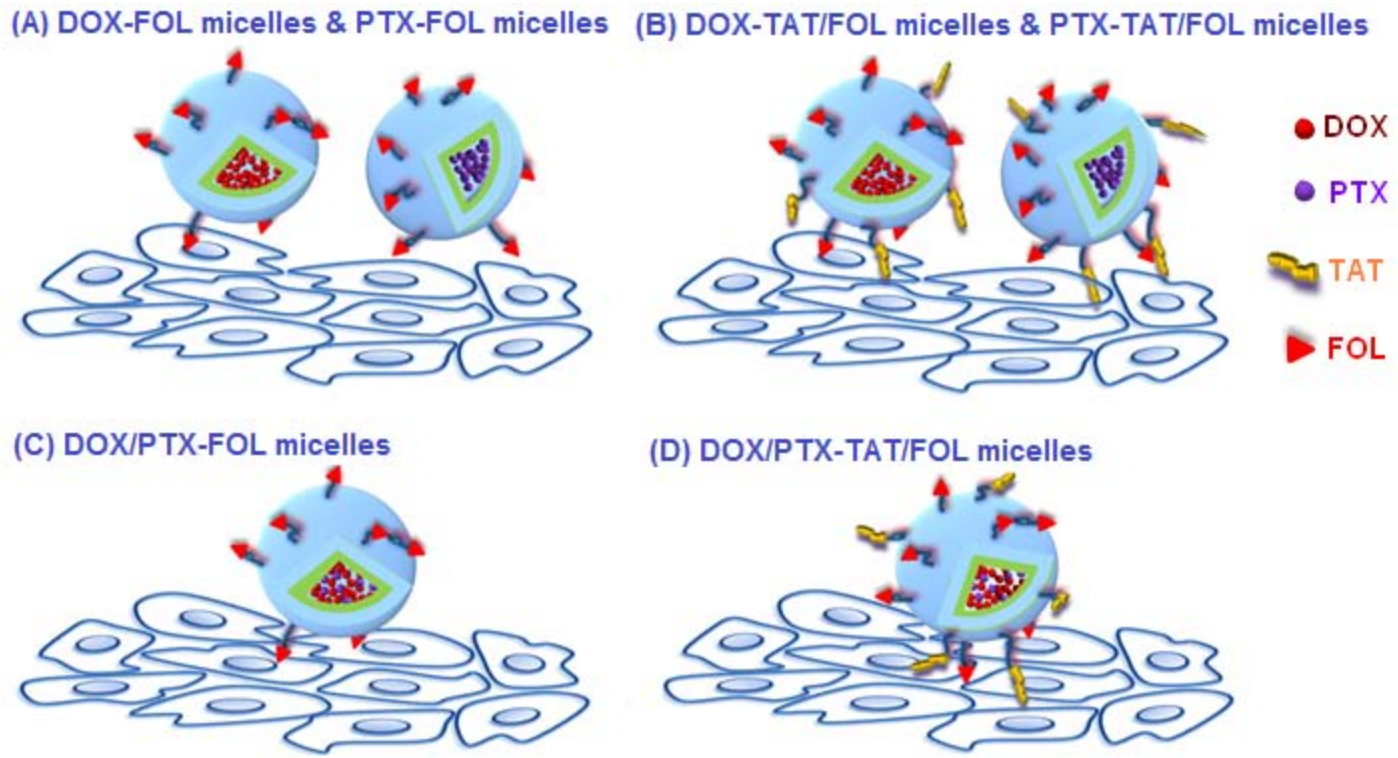

Figure 4.1 Strategies to delivery of DOX and PTX at synergistic ratio to the cancer cells via micellar systems: (A) DOX and PTX encapsulated separately into FOL modified micelles (DOX-FOL micelles & PTX-FOL micelles) were co-delivered into cancer cells; (B) co-delivery of DOX- TAT/FOL micelles & PTX-TAT/FOL micelles with the utilization of TAT to enhance the treatment efficacy; (CP) and (D) dual drugs, DOX and PTX, were simultaneously encapsulated into the FOL modified micelles or TAT/FOL micelles to form DOX/PTX-FOL micelles and DOX/PTX-TAT/FOL micelles respectively.

In this chapter, a novel drug delivery system based on polymeric micelles with multifunctional surface properties has been developed for the combination of two anticancer drugs DOX and PTX. The effects of different free drug combinations on the mouth epidermal carcinoma KB cells was first investigated, and the combination that exhibits good synergy over a wide treatment concentration range has been chosen as the guide composition for subsequent drug-encapsulating studies. Secondly, co-delivery of two single drug-loaded micelles using FOL modified system (DOX-FOL micelles & PTX-FOL micelles) in Figure 4.1A and TAT/FOL modified system (DOX-TAT/FOL micelles & PTX-TAT/FOL micelles) in Figure 4.1B were then investigated. Finally, dual drugs-encapsulated micelles with FOL modification (Figure 4.1C) and TAT/FOL modification (Figure 4.1D) were evaluated.

4.2 Experimental section

4.2.1 Materials

Three self-synthesized block copolymers (PLGA-PEG, PLGA-PEG-FOL and PLGA-PEG-TAT) in Chapter 3 were used in this study as carrier materials. Dimethyl sulfoxide (DMSO) and triethylamine (TEA), 3-[4,5-dimethylthiazolyl-2]-2,5-diphenyl tetrazolium bromide (MTT), tween 80 and paclitaxel (PTX) were all purchased from Sigma-Aldrich (USA). Doxorubicin (DOX) was obtained from Boryung (Korea). Methanol, acetonitrile (ACN), tetrahydrofuran (THF), chloroform, diethyl ether were purchased from Tedia (USA). Folate-free RPMI 1640 medium, fetal bovine serum (FBS), Trypsin-EDTA and penicillin-streptomycin were obtained from Invitrogen (USA). Human oral cavity carcinoma KB cell line was purchased from ATCC (USA). Reagent graded de-ionized

(DI) water was obtained from the Milli-Q Plus System (Millipore, USA). All chemicals were used directly without further purification.

4.2.2 Preparation and characterization of doxorubicin (DOX) and paclitaxel (PTX) loaded polymeric micelles

4.2.2.1 Preparation of micelles

D-loaded micelles were prepared using dialysis method as previously described with slight modification [257]. First, DOX.HCl was neutralized with twice the number of mole of TEA in DMSO overnight to obtain the DOX free base (hydrophobic form) [263]. The mixtures of PLGA-PEG, PLGA-PEG-FOL, PLGA-PEG-TAT at various weight ratios were dissolved in DMSO at a total concentration of 10 mg/ml. The DOX solution was added into the polymer solution and mixed by vortex for 10 min. The mixture was transferred into dialysis bag (MWCO: 3,000 Da) for dialyzing against DI water for 2 days to produce micelles and remove untrapped DOX and TEA.

PTX-loaded micelles were prepared by three steps: (1) dissolving of PTX and mixture of three polymers as mentioned above into DCM, (2) evaporating DCM to form a thin film matrix and (3) forming micelles by adding water into the film under stirring. Further purification by dialyzing against DI water was carried to remove un-encapsulated drug.

Combination DOX/PTX-loaded micelles were produced using the thin film evaporation method as described in the above paragraph for PTX-loaded micelle preparation.

However, DOX.HCl was first neutralized with TEA in a very low amount of DMSO before being adding into the DCM solution of PTX and polymers.

4.2.2.2 Characterization of DOX- and PTX-loaded polymeric micelles

The hydrodynamic size and zeta potential of polymeric micelles were measured at 25°C by NanoSizer (Malvern Instruments, UK). Aqueous micelle solutions were prepared using deionized water. The concentration of polymeric micelles was kept at 1 mg/ml. The micelle solutions were filtered through a 0.80 μm cellulose membrane filter before measurements. The average values were calculated from at least 3 measurements performed on each samples.

The drug loading content (DLC) and encapsulation efficiency (EE) of DOX in micelles was estimated with a UV-vis spectrophotometry at 480 nm by dissolving 1 mg of DOX-loaded micelles in 1 ml DMSO. The DOX content was determined using the calibration curve of DOX in DMSO range 0 - 50 μg/ml.

The amount of PTX in micelles was analyzed using a high performance liquid chromatography (HPLC, Agilent 1200, USA) equipped with a ZORBAX 300SB-C18 column. The micelles were dissolved in DCM to destroy the micellar structure and dissociate PTX from the polymers. The samples were then flowed through the column with a solution of ACN/water (50/50, v/v) as a mobile phase. The PTX was detected with a UV detector at 265 nm wavelength. A calibration of PTX was established at low

concentration from 0.5 to 50 µM/mL for the quantitative calculation of PTX concentration.

4.2.3 *In vitro* release study

DOX-loaded micelle solutions (2 mg in 1 ml of PBS, pH 7.4) were transferred to dialysis tube (MWCO: 2,000 Da) and dialyzed against 3 ml PBS in a tube at 37°C with shaking at 100 rev/min. To measure the release of DOX at different time intervals, PBS solution in the tube was all withdrawn and replaced with 3 ml fresh PBS. The withdrawn solutions were transferred to 96-well plate and analyzed by a microplate reader (Tecan – Infinite M200, Austria) with excitation wavelength at 480 nm and emission wavelength at 570 nm to determine the amount of DOX in that solutions. The absolute amount of DOX was determined using the calibration curve of DOX in PBS range from 0 to 10 ppm. The drug release studies were performed in triplicate for each of the samples.

The method for investigation of PTX release was similar with the above method used for DOX-loaded micelles. However, the addition of 0.05 w/v% of Tween 80 into the PBS solution was applied in this study due to the less solubility of PTX in the pure PBS. The released PTX in the PBS solutions was extracted into the organic phase for HPLC analysis by adding equal volume of DCM into the PBS solutions. The solutions were further mixed for 24 h before discarding the PBS for the completion of PTX extraction into DCM. The amount of PTX was determined using the method as used for the determination of the loading amount of PTX in micelles.

4.2.4 *In vitro* cytotoxicity study

The ability of various treatments to inhibit cell proliferation was evaluated using human carcinoma KB cell line with MTT viability assay. Cells cultured in free folic RPMI media supplemented with 10% FBS and 1% penicillin-streptomycin at 37°C in humidified environment of 5% CO_2 were seeded onto 96-well plates at a seeding density of 10,000 cells/well and incubated for 2 days to permit cell attachment. The cells were then treated with free drugs or micelles at different concentrations for 2 days. Afterwards, the cell viability was analyzed by MTT assay as described clearly in Chapter 3.

4.2.6 Determination of combination effects

Effects of the DOX and PTX combination were analyzed by a Calcusyn software (Biosoft, USA) derived from the Chou and Talalay's principle [232, 233] as described in Chapter 2. CI values of free drug combinations (DOX/PTX) were determined using equation 2-2, with $(Dose_x)_1$ and $(Dose_x)_2$ being the concentration of free DOX and free PTX in single treatments that kill x % KB cells, $(Dose)_1$ and $(Dose)_2$ being the concentration of free DOX and free PTX in the combination. CI values of DOX/PTX combinations in micellar forms were determined with $(Dose_x)_1$ and $(Dose_x)_2$ being the DOX-loaded micelles and PTX-loaded micelles in single micellar treatments that kill x % KB cells, $(Dose)_1$ and $(Dose)_2$ being the concentration of DOX and PTX in the micellar combination.

4.3 Results and discussion

4.3.1 *In vitro* cytotoxicity interaction between free doxorubicin (DOX) and free paclitaxel (PTX)

This study has been designed to investigate the synergistic drug combination based on DOX and PTX for cancer treatment using KB cell line for all experiments. The changes in the cytotoxicity effect of combined DOX/PTX were investigated at different ratios to find out the synergistic DOX/PTX ratio for KB cell treatment. The combinations of free DOX and free PTX are presented as DOX/PTX_x/y while x/y is the molar ratio of DOX/PTX in the combination.

Table 4.1 IC_{50} of different treatment compositions of free drugs, DOX and P, to KB cells after 2 days incubation.

Treatment compositions	IC_{50} (μM)
DOX	1.564
DOX/PTX_1/0.1	0.866/0.0866
DOX/PTX_1/0.2	0.185/0.037
DOX/PTX_1/1	0.135/0.135
DOX/PTX_0.2/1	0.0893/0.447
DOX/PTX_0.1/1	0.057/0.570
PTX	0.459

Figure 4.2 shows the response of KB cells treated with different combinations at various concentrations. Figure 4.2A shows the KB cell viability after being treated with DOX/PTX combinations as the function of DOX concentration. Lower cell viability is

observed when a higher ratio of DOX/PTX is used for all DOX-based combinations (DOX/PTX_1/0.1, 1/0.2, 1/1). Moreover, the IC_{50} values of DOX in DOX-based combinations are 2-10 times lower than that of free DOX treatment (Table 4.1). However, minimal change in cell viability (Figure 4.2B) and IC_{50} values of PTX (Table 4.1) are observed when a low amount of DOX is added into the PTX-based combinations at ratios of DOX/PTX_0.2/1 and DOX/PTX_0.1/1.

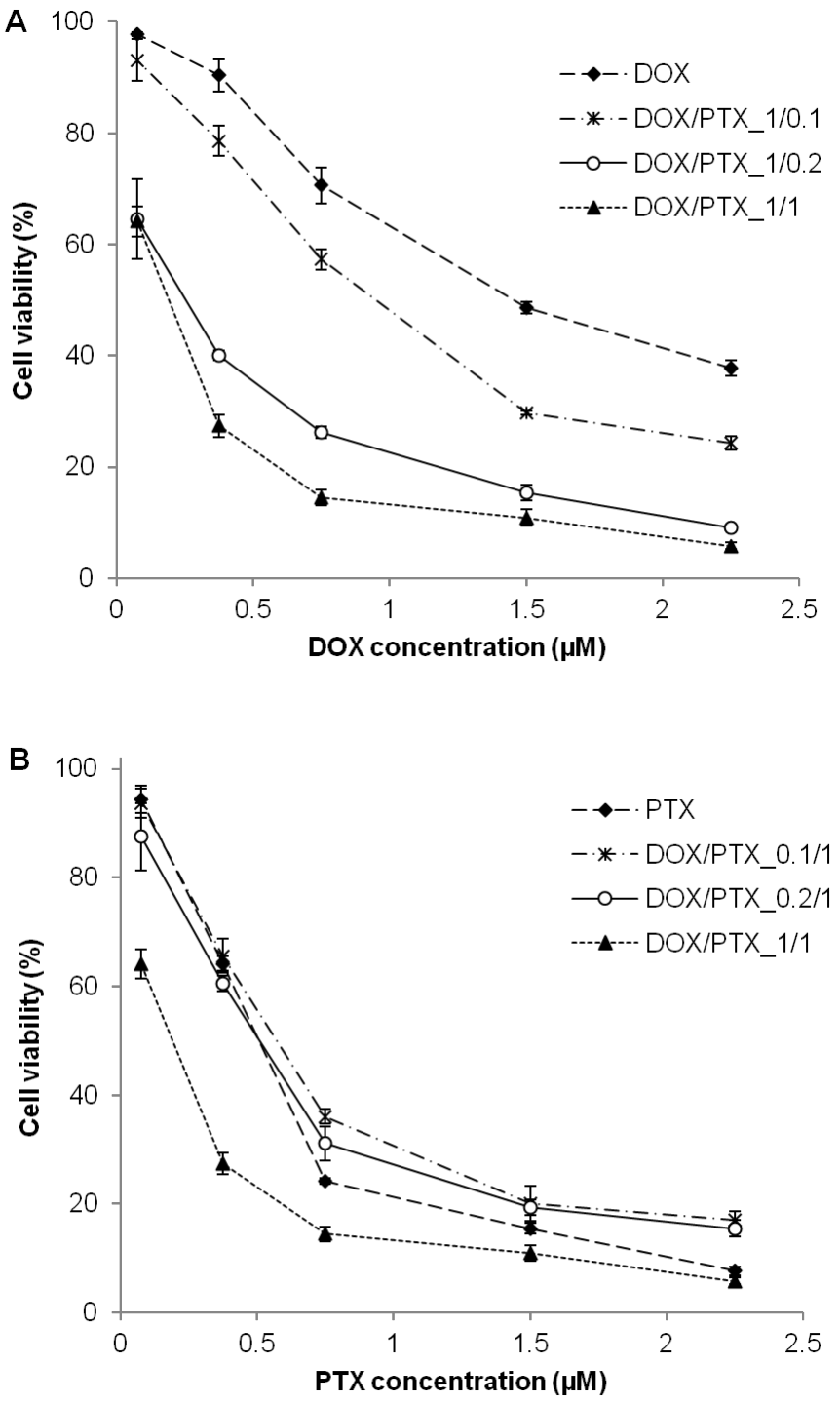

Figure 4.2 Cytotoxicity of DOX and PTX combinations at (A) higher ratio of DOX and (B) higher ratio of PTX against KB cells for 2 days treatment.

These results suggest that (1) the DOX-based combinations is better than PTX-based combinations, (2) the DOX-based combinations may exhibit a synergistic effect and (3) PTX-based combinations with low amount of DOX may not exhibit any synergistic effect for the KB cell treatment. However, the good synergistic combination may not be able to determine from the data as shown in Figure 4.2 or Table 4.1. Therefore, further analysis needs to be carried on these cytotoxicity results to obtain the more quantitative data using Calcusyn software.

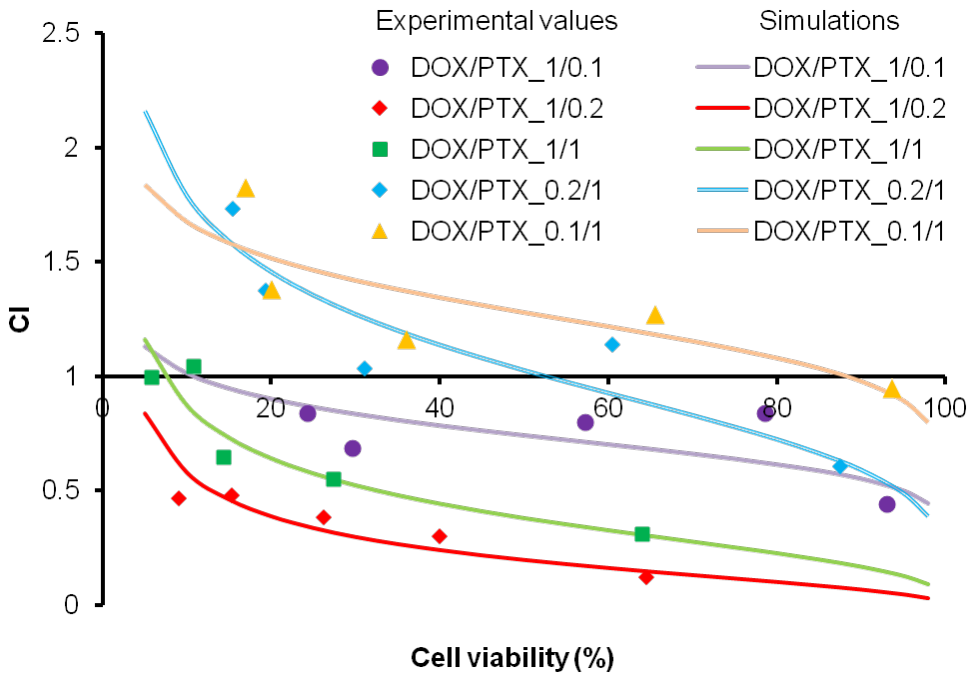

Figure 4.3 Plot of the combination index (CI) as the function of cell viability for KB cells treated with free DOX and free PTX combinations.

The effect of DOX/PTX combinations can be presented more clearly by CI values in Figure 4.3 with cell viability as the dependent value. The CI values of all combinations at fixed ratios of DOX/PTX of 1/0.1, 1/0.2, 1/1, 0.2/1 and 0.1/1 as a function of the cell viability from 5% to 98% was simulated and presented in Figure 4.3 as the similar method shown in previous studies [219, 272]. A decrease in PTX in the DOX-based

combinations from DOX/PTX_1/1 to DOX/PTX_1/0.2 could reduce the CI values of the combination. However, further reducing PTX, to the ratio of DOX/PTX_1/0.1, does not further reduce the CI value. For the PTX-based combinations, the CI values increase with the decrease in the amount of added DOX as compared the CI values among DOX/PTX_1/1, DOX/PTX_0.2/1 and DOX/PTX_0.1/1. Higher antagonistic interaction (CI > 1) of DOX and PTX is observed in the PTX-based combinations (DOX/PTX_0.2/1 and DOX/PTX_0.1/1). However, higher synergistic interaction (CI < 1) is observed in the DOX-based combinations. The DOX/PTX_1/0.2 combination shows the lowest CI values with below 1 for all treatment concentrations that result in 5 - 98% cell viability. Therefore, DOX/PTX_1/0.2 combination is chosen as the optimal synergistic composition for the following drug-encapsulated studies.

4.3.2 Size and zeta potential characterization of drug-loaded polymeric micelles

The size of drug delivery carriers is important since it influences drug efficacy and pharmacokinetics. Hobbs et al. [273] showed that liposomes with diameters from 100 nm – 200 nm are more efficient in diffusing along the vessel of tumors than larger liposomes. Moreover, it was proven that the uptake of the reticuloendothelial system (RES) is size dependent. Smaller size carriers would have the lesser uptake, and consequently lower clearance [274]. All micelles in this study are 130 nm or less in hydrodynamic size (Table 4.2). The size of TAT/FOL-modified micelles in this study is at 106 nm, which is smaller compared to previously TAT-modified micelle system based on TAT-PEG-cholesterol with the size at around 200 nm [138]. Hence, our reported TAT/FOL-modified micelles are more suitable for drug delivery. In addition, the zeta potential of particles also plays

an important role in RES uptake. It was proven that the RES uptake of particles cannot be avoided if their zeta potential values are above -5 mV [274]. From Table 4.2, the highest zeta potential value among the micelles in this study is less than -9 mV, making them a potential multi-targeting candidate to evade RES uptake.

Table 4.2 Characterization of polymeric micelles.

Micelles	DLC (%)	EE (%)	Size (nm)	Zeta potential (mV)
DOX-micelles	1.91	47.8	63.7	-13.3
DOX-FOL micelles	2.03	50.8	94.6	-12.3
DOX-TAT/FOL micelles	1.95	48.8	106.3	-9.5
PTX- micelles	1.17	54.6	105.2	-15.1
PTX-FOL micelles	1.20	56.1	113.8	-14.0
PTX-TAT/FOL micelles	1.12	52.3	132.8	-10.6
DOX/PTX(1/0/25)-FOL micelles	1.40	39.4 (DOX) 62.3 (PTX)	119.6	-12.2
DOX/PTX(1/0.25)-TAT/FOL micelles	1.44	41.6 (DOX) 59.1 (PTX)	123.2	- 9.3

4.3.3 *In vitro* drug release and drug loading of singe drug-loaded micelles

Drug loading content (DLC) in different single drug-loaded micelle formulations is tabulated in Table 4.2 DOX has been successfully incorporated into the core of micelles by physical interaction with no significant difference in the amount of loaded DOX among the DOX-, DOX-FOL, and DOX-TAT/FOL micelles at the DLC of approximately 2%.

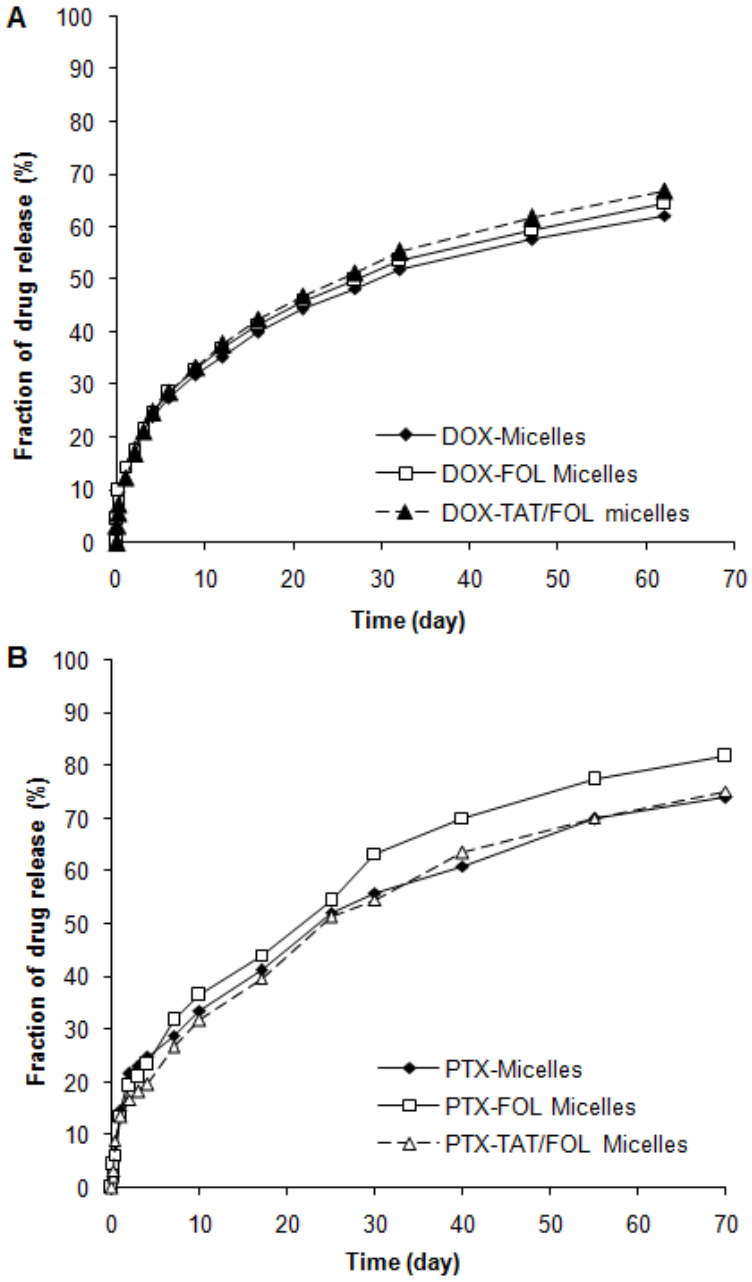

Figure 4.4 *In vitro* release profiles of (A) DOX from DOX- micelles, DOX- FOL micelles and DOX- TAT/FOL micelles; and (B) PTX from PTX-micelles, PTX-FOL micelles and PTX-TAT/FOL micelles. The experiments were conducted in triplicate in PBS (pH 7.4) at 37ºC. The standard deviation of these drug release curves is not shown to make the figure to be seen easily. The standard deviation is less than 15%.

Similarly, PTX is also incorporated into the three micelle systems (PTX, PTX-FOL, PTX-TAT/FOL) with the same amount of drug content of approximate 1%. The reason of lower PTX amount in the micelles compared to DOX is to maintain the small size of PTX-loaded micelles. Due to the larger size of PTX molecule and the different in the preparation method, PTX-loaded micelles tend to have larger size compared to DOX-loaded micelles when having the same DLC. The DOX and PTX release profiles from all micelles shown in Figure 4.4 are almost the same with less than 10%, 15% release within the first 6 h and 24 h respectively. Then the drugs are released slowly released after that. The amount of DOX and Pare maintained more than 30% in the micelles after 60 days incubation with pH 7.4 PBS.

4.3.4 *In vitro* drug release and drug loading of dual drug-loaded micelles

As investigated in the previous section (Section 4.3.1), the combination of DOX and PTX exhibits good synergistic effect to KB cells at the molar ratio of DOX/PTX at approximately 1/0.2. In addition, it is observed that DOX- loaded micelles and PTX-loaded micelles have similar drug release rate (Figure 4.4). Therefore, the co-encapsulated micelles (DOX/PTX-FOL micelles and DOX/PTX-TAT/FOL micelles) were prepared from the initial molar ratio of DOX to PTX at 1/0.2.

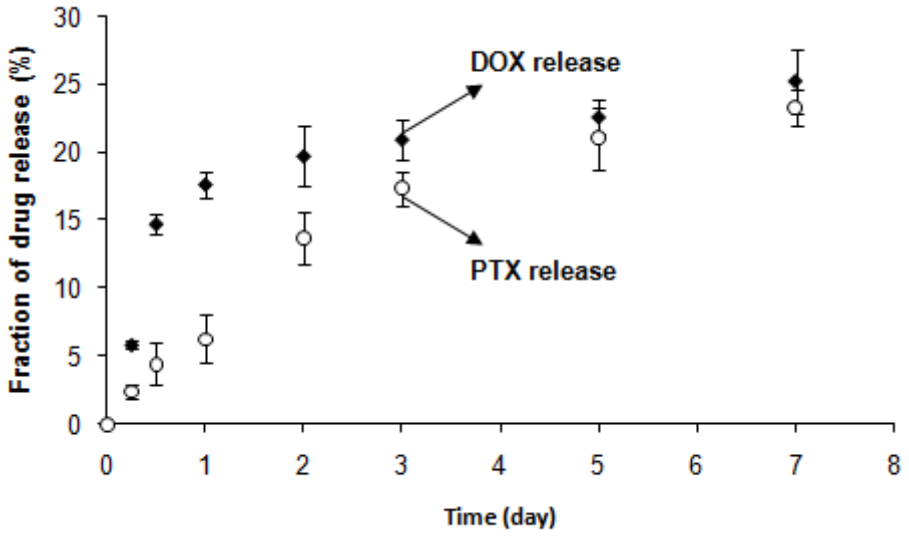

Figure 4.5 *In vitro* release profiles of DOX/PTX(1/0.25)-loaded micelles conducted in triplicate in PBS (pH 7.4) at 37ºC.

The co-encapsulated micelles would ideally have 1 parts of DOX/0.2 part of PTX and release the drugs at the DOX/PTX ratio of 1/0.2. However, the DLC and drug release rate of DOX and PTX in the co-encapsulated micelles do not result as expected (Table 4.2 and Figure 4.5). DLC of DOX and PTX in the co-encapsulated micelles is approximately 1/0.25. This means the encapsulation efficiency of PTX is slightly higher than that of DOX. This may be due to the higher hydrophobicity of PTX compared to D, which results in the stronger interaction of PTX to the core of micelles. While the same release rates are observed for single drug-loaded micelles, the slower release rate of PTX in the DOX/PTX (1/0.25)-loaded micelles is shown in Figure 4.5. It may be due to the much lower encapsulation amount of PTX compared to its of DOX in the DOX/PTX (1/0.25)-loaded micelles. It can be concluded that the PTX amount compared to DOX amount in the DOX/PTX-loaded micelles was 20-30% higher than the designed value. However, the

release rate of PTX was slower than DOX. Therefore, the final amount of DOX/PTX could be still considered in the designed ratio.

4.3.5 Cytotoxicity enhancement of drug-loaded micelles with the addition of TAT on the micelle surface

DOX or PTX encapsulated micelles with different surface modifications have demonstrated enhanced targeting property and cancer treatment effect [259, 275] including our previous study with the use of FOL micelles [257]. To further enhance the treatment efficiency, the effect of TAT peptide on the performance of drug-loaded micelles would be discussed in this study. TAT peptide is a non-selective peptide able to penetrate into both cancer and normal cells. Hence, a low amount of TAT should be used in order to obtain micelles with minimal non-selective penetration. It has been shown that micelle systems with 2 mol% TAT exhibit a homogeneous distribution of micelles and less precipitation compared with the micelles with 4 mol% or more TAT [173]. Although recent studies used 100% TAT-conjugated polymers to form carriers [138, 139, 173], this study aims to demonstrate the possibility of enhancing the treatment efficiency by incorporating a very low amount of TAT into drug carriers. Drug-loaded TAT/FOL micelles were prepared from 10 wt% PLGA-PEG-TAT polymer to obtain micelles with about 2.5 mol% PLGA-PEG-TAT.

The toxicity of all blank micelles was tested at a high concentration of 2.0 mg/mL. With less than 5 % of KB cell proliferation was affected, blank micelles could be practically non-toxic to KB cells at a high tested concentration of 2.0 mg/mL. Figure 4.6 shows that

the cell viability of KB reduces at higher micelle concentration. It can be seen that TAT/FOL-modified micelles are the most efficient in cancer treatment than the unmodified or FOL-modified micelles. As presented in Table 4.3, the IC_{50} of DOX-micelles and PTX-micelles are at 3.873 µM and 0.79 µM respectively. And these values are reduced to 1.084 µM and 0.246 µM for DOX- TAT/FOL and PTX-TAT/FOL micelles. In short, the required dosage to kill 50% KB cells of the drug loaded-TAT/FOL micelles is approximately one third of that of the drug loaded-micelles. This result suggests that the presence of FOL and TAT on the micelles can promote the effectiveness of the drug-loaded micelles.

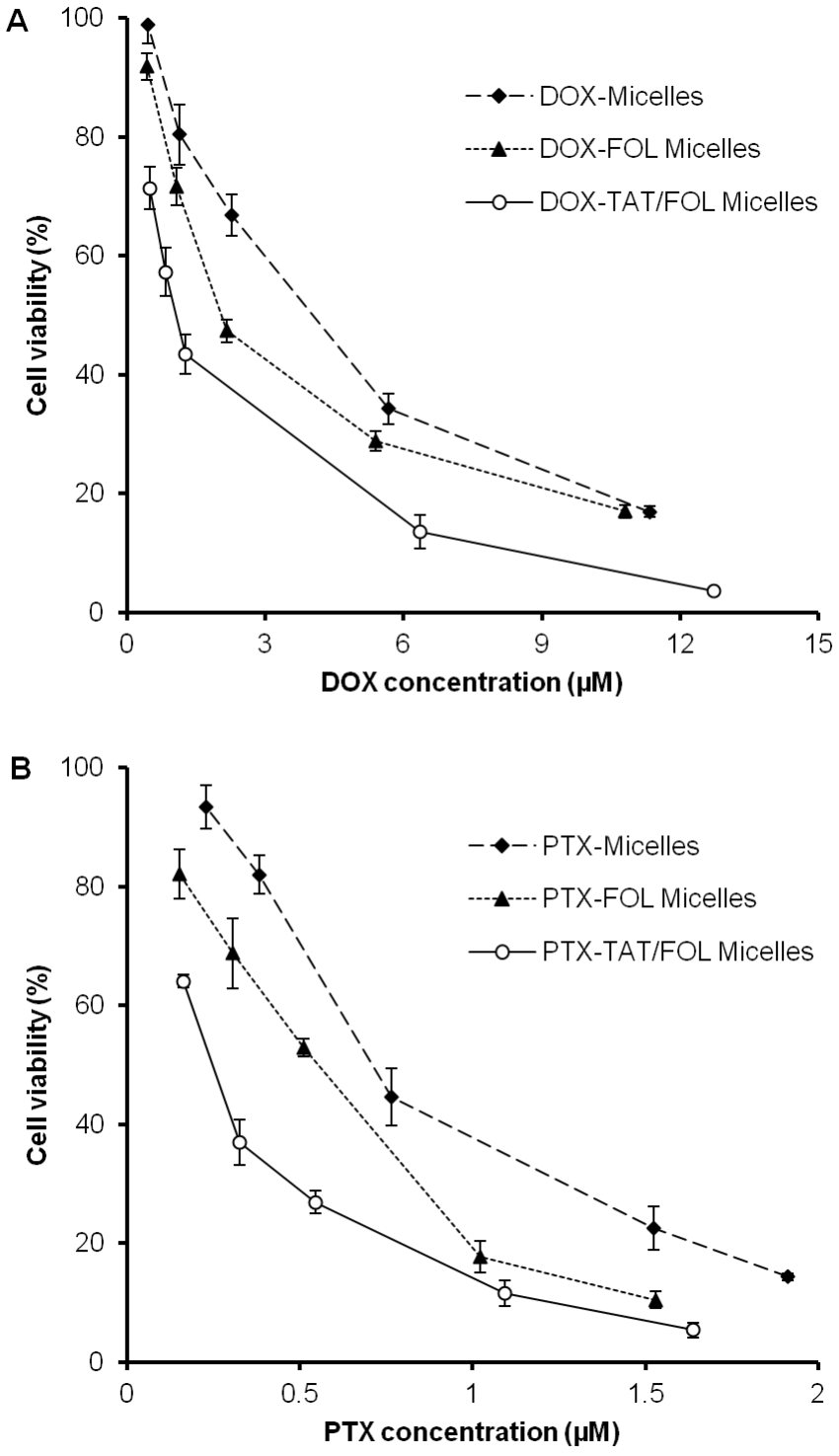

Figure 4.6 Effect of FOL and TAT/FOL modifications on the cytotoxicity of drugs-loaded micelles to KB cell treatment as investigated using (A) DOX- loaded micelles and (B) PTX-loaded micelles.

The current TAT/FOL system shows higher efficiency than the previous system [137] using TAT-modified micelles based on TAT-PEG-phosphatidylethanolamine, which only shows less than 2 times enhancement compared to the non-modified micelles. As for a reported TAT-modified pH-sensitive micelle system, the TAT-modified micelles show ~0.3 to 1.8 times enhancement at pH conditions ranging 6-7 compared to the non-modified micelles [271].

Table 4.3 Effect of micellar surface modifications to the cancer treatment efficiency.

Micelles	IC_{50} (μM)
DOX-micelles	3.873
DOX-FOL micelles	2.556
DOX-TAT/FOL micelles	1.084
PTX- micelles	0.790
PTX-FOL micelles	0.446
PTX-TAT/FOL micelles	0.246

The cytotoxicity effect of single drug encapsulated micelles has been characterized in this work as parameters to determine the CI values of co-delivery of DOX- FOL micelles & PTX-FOL micelles, co-delivery of DOX- TAT/FOL micelles & PTX-TAT/FOL micelles, DOX/PTX-FOL micelles and DOX/PTX-TAT/FOL micelles in the subsequent studies.

4.3.6 Synergistic effect of the co-delivery of DOX- loaded micelles and PTX-loaded micelles

Co-delivery of two single drug-loaded micelles (Figure 4.1A and 4.1B) can potentially be a more flexible method to obtain the synergistic treatment compared with the dual drugs-loaded micelles (Figure 4.1C and 4.1D). Because the combined ratios in the co-delivery of two single drug-loaded micelle system can be easily varied for specific treatment. In this study, two systems with FOL modification (DOX-FOL micelles & PTX-FOL micelles) and TAT/FOL modification (DOX-TAT/FOL micelles & PTX-TAT/FOL micelles) at molar ratio of DOX/PTX of 1/0.2 have been used to demonstrate the possibility of using the two single drug-loaded micelles to co-deliver DOX and PTX at synergistic effect and the enhancement of the TAT/FOL modification compared to FOL alone. The co-delivery of two single drug loaded micelles was noted as DOX micelles & PTX micelles_x/y at molar ratio of DOX/PTX at x/y.

Table 4.4 IC_{50} of different micellar treatments: (1) co-delivery of two singe drug loaded micelles at the ratio of DOX/PTX at 1/0.2, and (2) dual drugs-loaded micelles at the ratio of DOX/PTX at 1/0.25.

	Treatment	IC_{50} (μM)
Co-delivery systems	DOX-FOL micelles & PTX-FOL micelles_1/0.2	0.469/0.094
	DOX-TAT/FOL micelles & PTX-TAT/FOL micelles_1/0.2	0.219/0.044
Dual drugs-loaded systems	DOX/PTX(1/0.25)-FOL micelles	0.416/0.104
	DOX/PTX(1/0.25)-TAT/FOL micelles	0.172/0.043

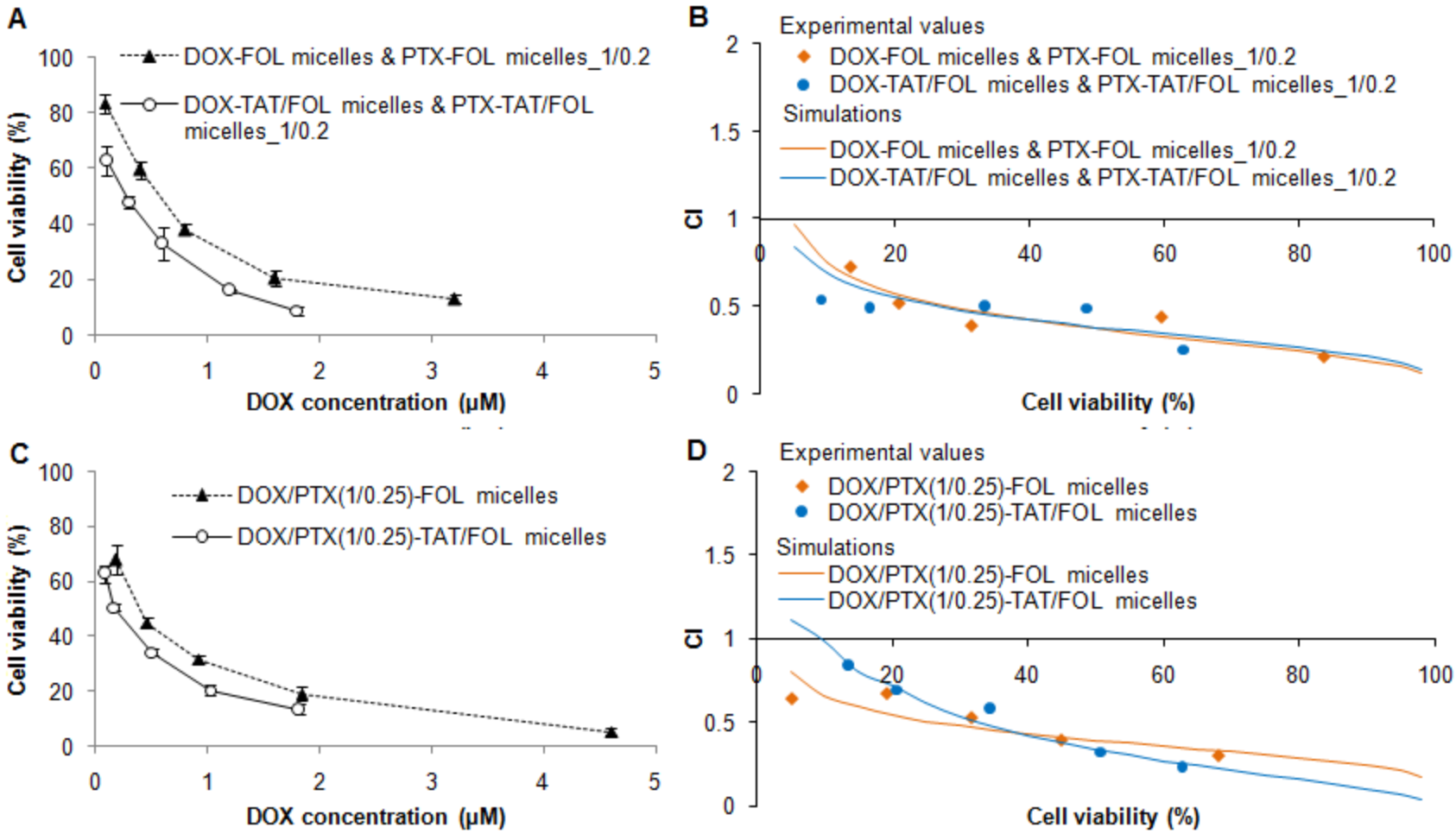

Figure 4.7 Cytotoxicity dose response of KB cells with various DOX and TAM delivery strategies: (A) the co-delivery of two single drug-loaded micelles (Fig. 1A & 1B) at DOX/PTX ratio of 1/0.2, and (C) the dual drugs-encapsulated micelles at the encapsulated DOX/PTX ratio of 1/0.25. Synergistic effects of (B) the co-delivery of DOX- loaded micelles & PTX-loaded micelles treatments and (D) the dual DOX/PTX-loaded micelles were presented as the CI values as the function of cell viability.

The higher cancer treatment efficacy of the system with TAT/FOL modification compared to FOL alone is shown as the lower required treatment dose at the same treatment effect (Figure 4.7A). The required dose to kill 50% KB cells of the DOX-TAT/FOL micelles & PTX-TAT/FOL micelles_1/0.2 system is more than 2 times lower than that of DOX-FOL micelles & PTX-FOL micelles_1/0.2 system (Table 4.4). Figure 4.7B presents the CI values of different combinations as the function of cell viability. Obviously, both co-delivery of single drug-loaded micelle systems show the synergistic effect with all CI values < 1 for the wide range of treatment concentrations which is the same phenomenon as observed in the DOX and PTX combination (Section 4.3.1).

4.3.7 Synergistic effect of dual drugs-loaded micelles and the surface modifications

DOX/PTX-FOL micelles and DOX/PTX-TAT/FOL micelles at the synergistic combination of DOX/PTX (approximately 1/0.25) have been studied to investigate the effects of dual DOX/PTX encapsulation as well as surface modification in KB cell treatment (Figure 4.1C and 4.1D). As shown in Figure 4.7C, dual DOX/PTX micelles with TAT/FOL modification show higher cancer treatment efficiency than FOL-modified micelles. The IC_{50} values of DOX/PTX (1/0.25)-FOL micelles and DOX/PTX (1/0.25)-TAT/FOL micelles are 0.416/0.104, 0.172/0.043 respectively as tabulated in Table 4. Based on the IC_{50} values, the addition of TAT enhances the activity of the DOX/PTX (1/0.25)-FOL micelles to approximate 2.4 times. This observation is in consistent to the data of TAT/FOL vs. FOL only modification in single drug-loaded micelle delivery (Section 4.3.5) and co-delivery of two single drug-loaded micelles (Section 4.3.6).

The synergistic effects of the DOX/PTX-FOL micelles and DOX/PTX-TAT/FOL micelles are calculated following the analysis of the cytotoxicity curves of the single drug treatments (i.e., DOX-FOL micelles, DOX-TAT/FOL micelles, PTX-FOL micelles and PTX-TAT/FOL micelles) in Figure 4.6 and the cytotoxicity curves of the combination treatments in Figure 4.7C. The CI values which are computed and presented in Figure 4.7D show the synergistic effect of the two dual drugs-loaded micelle systems. In this study, *in vitro* cytotoxicity results show that the co-delivery of two single drug-loaded micelles and the dual drugs-loaded micelles exhibit the same synergistic effect to KB cells. However, the effect of the two methods may be different *in vivo* application as the micelles are circulated in the body's blood vessel before being delivered to the targeted tumors. The co-delivery of two single drug-loaded micelles may leads to the change in the designed drug ratio at the targeted tumors. However, the delivery of dual drugs-loaded micelles has higher possibility in maintaining the initial drug ratio at the targeted tumors because the two drugs are encapsulated at the synergistic ratio into the same carrier. Therefore, the dual-drug loaded micelle system with FOL and TAT modifications is a better method for cancer treatment.

4.4 Conclusions

Synergistic effects of DOX and PTX at several fixed-ratios have been investigated for mouth epidermal carcinoma treatment (KB cells). The result suggests that DOX-based combination at molar ratio of DOX/PTX at 1/0.2 may be the optimal ratio for KB cell treatment. To reduce the side-effects and control the release, the drugs have been encapsulated into micelles. DOX and PTX are encapsulated into micelles and delivered

by two methods which are (1) co-delivery of two single drug-loaded micelles or (2) dual drugs-loaded micelles. The two methods show the same synergistic effect but they contain their own advantage and limitation. For the co-delivery of two single drug-loaded micelles, the combination ratio could be easily varied for specific treatment with the limitation of maintaining the designed ratio *in vivo* treatment. The dual drugs-loaded micelles have higher possibility in maintaining the initial drug ratio for *in vivo* application which could overcome the limitation of the co-delivery of two single drug-loaded micelles. However, the variation of drug ratios of the two drugs in the dual drugs-loaded micelles would require further optimization for specific applications. Moreover, the addition of a low amount of TAT (about 2.5%) onto the micelles has been shown the enhancement in the cancer treatment by about 2 times.

This chapter has investigated the optimal synergistic drug ratio in the combination of two chemodrugs (DOX and PTX) and co-delivered this synergistic combination using TAT/FOL micelles. In the next chapter, the combination of a hormonal agent (TAM) and a chemodrug (PTX) is investigated for breast cancer treatment. The work in the following chapter addresses objective 3 in chapter 1.

CHAPTER 5. Dual-functionalized micellar system for synergistic delivery of hormone therapeutic and chemotherapeutic agents for breast cancer treatment

5.1 Introduction

Breast cancer is the leading cancer in women global with an estimate of 226 thousands new cases in the United States in 2012, which is approximate 29 % among women cancers. The two leading treatments for breast cancer patients are chemotherapy and hormone therapy. Chemotherapy uses cytotoxic drugs to kill cancer cells all over the patient's body. There are different types of chemotherapy drugs for breast cancer therapy, such as: (1) anthracyclines (doxorubicin, epirubicin) that deform DNA structure of cancer cells, (2) taxanes (paclitaxel, docetaxel) that prevent cancer cells from dividing, or (3) alkylating agents (cyclophosphamide) that target DNA of cancer cells. Hormone therapy is specifically used for breast cancer patients with hormone receptor-positive tumors. Various types of hormone therapy classes are: (1) selective estrogen–receptor modulators (tamoxifen, raloxifene, toremifene) that block estrogen receptors in breast cancer cells and starve them, (2) aromatase inhibitors (exemestane, anastrozole, megestrol, letrozole) that suppress production of estrogen in adrenal glands, or other hormonal therapies (goserelin acetate, fulvestrant) treat breast cancers that are dependent on estrogen for survival.

Besides the traditional single drug therapy, the therapy with the combination of two or more anticancer drugs has been widely applied to treat cancer diseases due to its

advantages compared to single agent therapy which has been limited due to the toxicity of the high drug dosage, the heterogeneity of cancer cells and the drug resistance [212-215]. Therefore, combination therapy has been more preferable thanks to its wide application for different cancer patients and perhaps its lower toxicity at the required effect. In addition, synergistic combinations could promote the response rate compared to single drugs, resulting in the better cancer cell treatment effect.

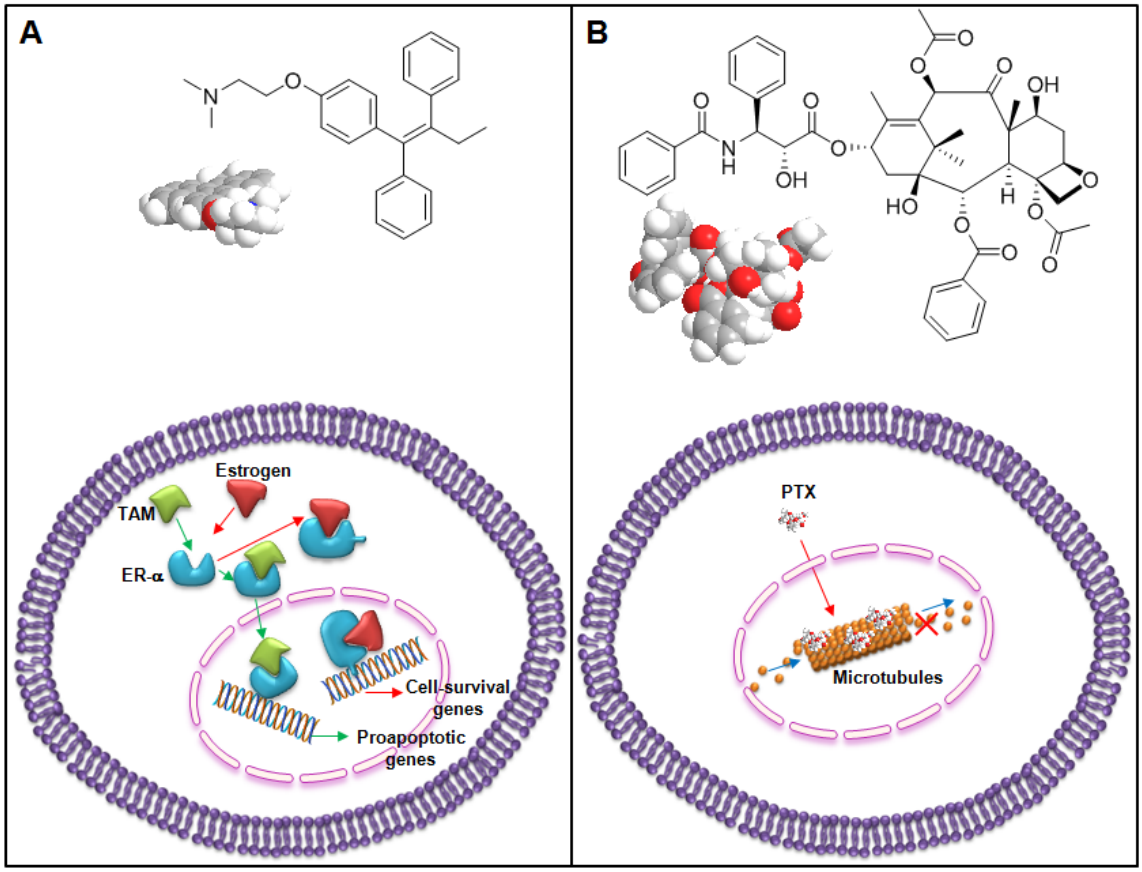

Figure 5.1 Molecular structures of two anticancer drugs and their pharmacodynamics in cancer cells: (A) tamoxifen (TAM) and (B) paxlitaxel (PTX).

This chapter demonstrates new drug delivery approaches for breast cancer treatment based on the synergistic effect of drug combinations and the higher treatment efficacy of

carrier modifications. A common chemotherapy drug – paclitaxel (PTX) and a first widely used hormone therapy drug – tamoxifen (TAM) were used as combined treatments in this study. PTX promotes microtubule assembly from tubulin dimmers, stabilizes microtubules by preventing depolymerization [12] as shown in Figure 5.1A. While TAM prevents the effects of estrogen to breast cancer cells [11] as insulated in Figure 5.1B. Therefore, a pair of TAM and PTX would be promising synergistic combinations for breast cancer treatment with higher efficacy than the treatment with TAM or PTX alone. Prior to the encapsulation, the effects of different combinations of the two drugs were investigated to find out the synergistic ratio as a guide composition for subsequent drug-encapsulating studies. Mixed polymeric micelles based on PLGA-PEG, PLGA-PEG-FOL and PLGA-PEG-TAT copolymers were employed as carriers for TAM and PTX delivery. The resultant drug-loaded micelles have hundreds nanometer size and exhibit targeting moiety (FOL) and cell penetrating peptide (TAT) on the surfaces. Therefore, they selectively accumulate into cancer cells with high binding affinity by active delivery that overcomes the limitations of free drugs (PTX and TAM) delivery (Figure 5.2).

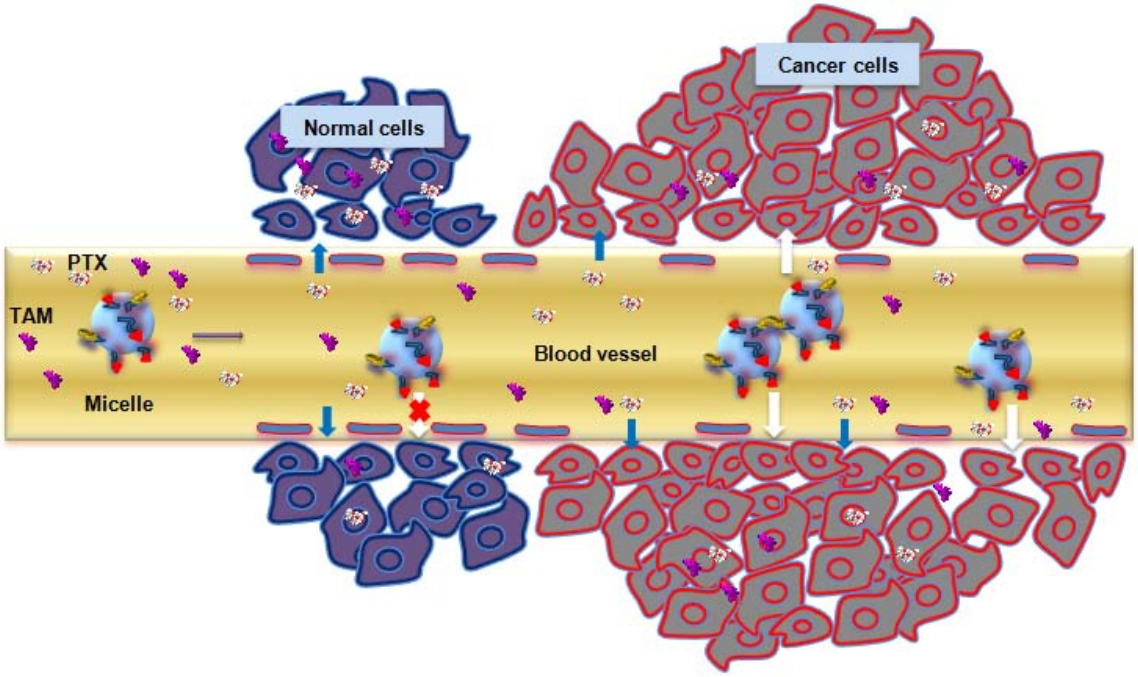

Figure 5.2 The free drugs (TAM and PTX), which have small molecular weight and is normally cleared rapidly from the blood, accumulate in both normal cells and cancer cells. While the micelles modified by a targeting moiety (FOL, in red) and a cell penetrating peptide (TAT, in yellow) at hundreds nanometer size accumulate largely in the cancer cells.

The combined TAM and PTX treatments using micelles as carriers were studied with two methods. The first method was carried out by co-delivery of two single drug-loaded micelles (Figure 5.3A). The second method demonstrated the effect of dual drugs-loaded micelles (Figure 5.3B).

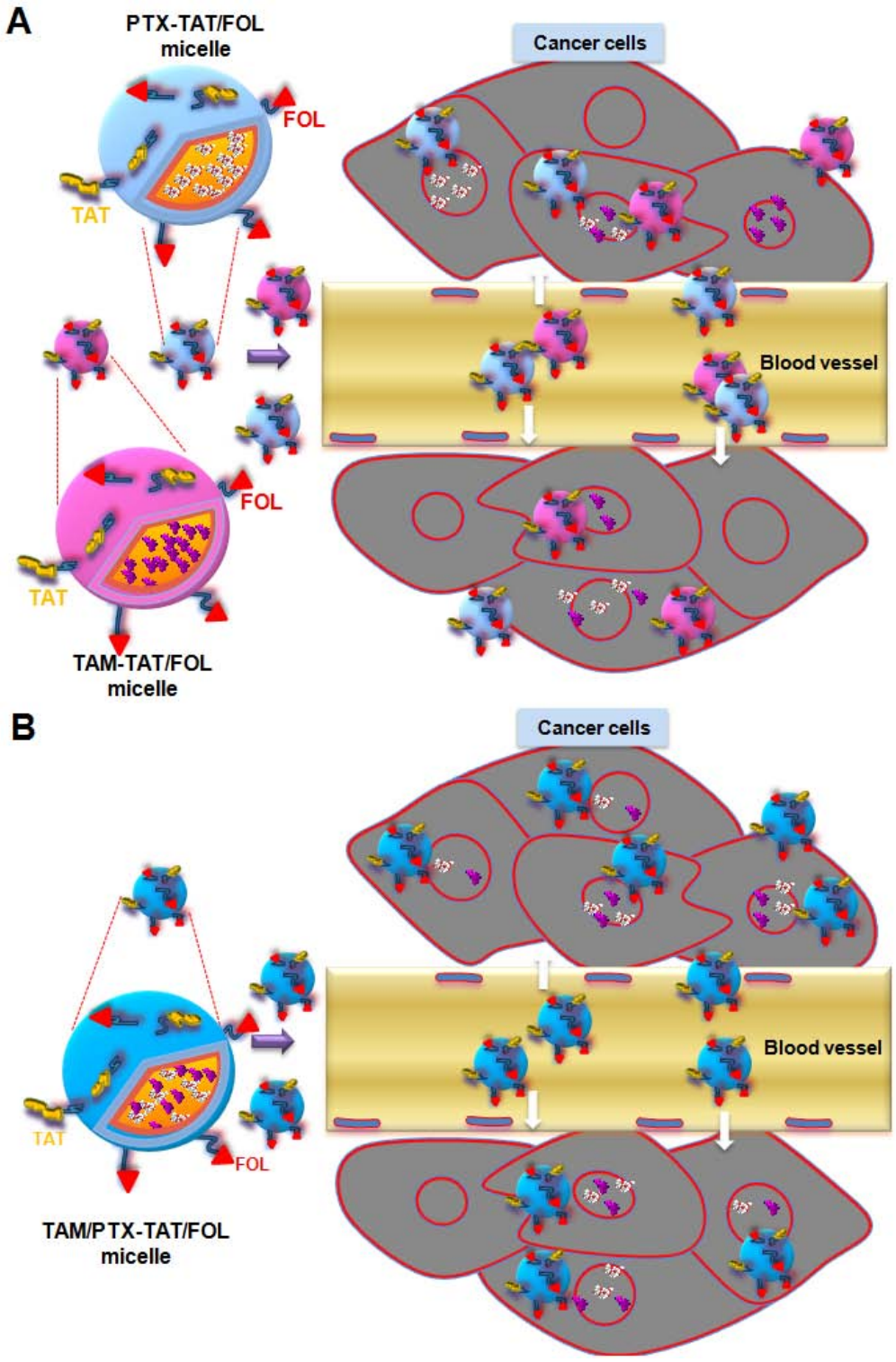

Figure 5.3 Cancer treatment by a synergistic combination of tamoxifen (TAM) and paclitaxel (PTX) utilized the drug delivery technology. Two treatment approaches: (A) co-delivery two drug-loaded micelles, TAM- TAT/FOL micelles & PTX-TAT/FOL micelles and (B) dual drugs-loaded micelles, TAM/PTX-TAT/FOL micelles.

5.2 Experimental section

5.2.1 Materials

Three block copolymers poly(D,L-lactide-co-glycolide)-poly(ethylene glycol) (PLGA-PEG), poly(D,L-lactide-co-glycolide)-poly(ethylene glycol)-folate (PLGA-PEG-FOL) and poly(D,L-lactide-co-glycolide)-poly(ethylene glycol)-TAT (PLGA-PEG-TAT) were synthesized for micellar fabrication as presented in Chapter 3. Tween 80, 3-[4,5-dimethylthiazolyl-2]-2,5-diphenyl tetrazolium bromide (MTT), tamoxifen (TAM) and paclitaxel (PTX) were all purchased from Sigma-Aldrich (USA). Methanol, dichloromethane (DCM), acetonitrile (ACN), tetrahydrofuran (THF), chloroform, diethyl ether were purchased from Tedia (USA). Triethylamine (TEA) was acquired from Alfa Aesar. Folate-free RPMI 1640 medium, fetal bovine serum (FBS), Trypsin-EDTA and penicillin-streptomycin were obtained from Invitrogen (USA). Estrogen receptor-positive human breast cancer cell line (MCF-7) was purchased from ATCC (USA). All chemicals were used directly without further purification.

5.2.2 Preparation and characterization of PTX and TAM loaded polymeric micelles

Drug-loaded micelles were prepared by three steps: (1) dissolving of hydrophobic drugs (i.e., PTX and/or TAM) and mixture of three polymers as mentioned above in DCM, (2) evaporating DCM to form a thin film matrix and (3) forming micelles by adding water into the film under stirring. Further purification by dialyzing against de-ionized (DI) water was carried to remove un-encapsulated drug.

The hydrodynamic size and zeta potential of polymeric micelles were measured at 25°C by dynamic light scattering (DLS) (NanoSizer, Malvern Instruments, UK). Aqueous micelle solutions were prepared using deionized water. The concentration of polymeric micelles was kept at 1 mg/ml. The micelle solutions were filtered through a 0.80 μm cellulose membrane filter before measurements. The average values were calculated from at least 3 measurements performed on each samples.

The amount of TAM and PTX in micelles was analyzed using a high performance liquid chromatography (HPLC, Agilent 1200, USA) equipped with a ZORBAX 300SB-C18 column. The micelles were dissolved in DCM to destroy the micellar structure and dissociate the drugs from the polymers. Subsequently, DCM solvent was evaporated completely before the mobile phase solutions were added into the samples. The PTX-loaded samples were then flowed through the column with a solution of acetonitrile/water (50/50, v/v) as a mobile phase, and TEA/water/methanol (1/11/89, vol%) was used as the mobile phase for TAM-loaded sample elution. The TAM and PTX were detected with a UV detector at 227 nm and 265 nm wavelengths respectively. Standard curves of TAM and PTX were established at concentration form 0 to 50 μM/mL for the quantitative calculation of these drugs.

5.2.3 *In vitro* release study

Micelle solutions with concentration of 2 mg in 1 ml of PBS with the addition of 0.05 w/v% Tween 80 were transferred to dialysis tube (MWCO: 2,000 Da) and dialyzed against 3 ml 0.05 w/v% of Tween 80 in PBS in a tube at 37°C with shaking at 100

rev/min. Drug release at different time intervals was measured by quantitatively analyzing of the released drugs in the dialysis solution. The released drugs in the dialysis solutions were firstly extracted into the organic phase for HPLC analysis by adding equal volume of DCM into the aqueous solutions. The solutions were further mixed for 24 h before discarding the aqueous solution for the completion of drugs extraction into the organic phase. TAM and PTX were quantitatively determined by HPLC as used for the determination of the loading amount of TAM and PTX in micelles as described in the previous section.

5.2.4 *In vitro* cellular uptake

The cell target and cell penetration tests of micelles with and without TAT/FOL were carried out in MCF-7 cells by labeling the micelles with C6. The cells were cultured in 12 mm round glass coverslips placed in 24-well plates for 1 day. Cells were then treated with 30 μM C6-loaded micelles for 3 h. Subsequently, the cells were washed 3 times with cold PBS, fixed with 4% cold paraformaldehyde for 30 min at room temperature, and washed with PBS again. The fixed cells on coverslips were observed under confocal microscope (Nikon C1, Japan) at excitation wavelength of 480 nm and emission wavelength of 590 nm.

5.2.4 *In vitro* cytotoxicity study

The inhibiting ability of free drugs and drug-loaded micelles to breast cancer tumor proliferation was evaluated using MCF-7 cells with MTT viability assay. Cells cultured in free folic RPMI media supplemented with 10% FBS and 1% penicillin-streptomycin at

37°C in humidified environment of 5% CO_2 were seeded onto 96-well plates at a seeding density of 10,000 cells/well and incubated for 2 days to permit cell attachment. The cells were then treated with free drugs or drug-loaded micelles at different concentrations. After 3 days of incubation with drug solutions, the cell viability was measured by MTT assay as described in Chapter 3.

5.2.5 Median-effect analysis

Effects of the combined drug treatment compared to single drug treatments were analyzed by a Calcusyn software (Biosoft, USA) derived from the Chou and Talalay's principle [232, 233] to provide quantitative information on the interaction of the combined drugs. The combination index (CI) of the combined two drugs was determined based on the described equation in Chapter 2 (eq. 2-2).

5.3 Results and discussion

5.3.1 *In vitro* cytotoxicity interaction between free tamoxifen (TAM) and free paclitaxel (PTX)

Given that each type of anticancer drugs has a different working mechanism, the strategy of combining two drugs together is to capitalize on the synergistic efficacy enhancement arisen from executing both mechanisms simultaneously. However, different dose combinations can results in additive, antagonistic or synergistic treatment effects. Therefore, the molar ratios of TAM to PTX were first studied at 1/0, 1/0.5, 1/1, 0.5/1, 0.35/1, 0.2/1 respectively. As shown in Figure 5.4A, the increase in PTX ratio of the combined TAM/PTX treatments leads to the lower cell viability at the same TAM

concentration. This indicates that increasing PTX of the TAM/PTX ratio from 1/0 to 1/1 can result in the higher treatment efficacy. Similar effect can be observed when increasing TAM of the TAM/PTX ratios (Figure 5.4B). When increasing the TAM/PTX ratios from 0/1 to 0.2/1 and 0.35/1, the cell viability stays unchanged. Further increment to 0.5/1 results in the decrease in cell viability. This indicates that the combined TAM/PTX treatments at ratios of 0.2/1 and 0.35/1 have antagonistic effect while TAM/PTX_0.5/1 may give synergistic effect. The higher IC_{50} values of TAM/PTX_0.2/1 and TAM/PTX_0.35/1 (Table 5.1) further demonstrate the antagonistic effect of these ratios. Other combined ratios may exhibit synergistic effect, as the IC_{50} values of these ratios are equal or lower than that of free TAM or free PTX.

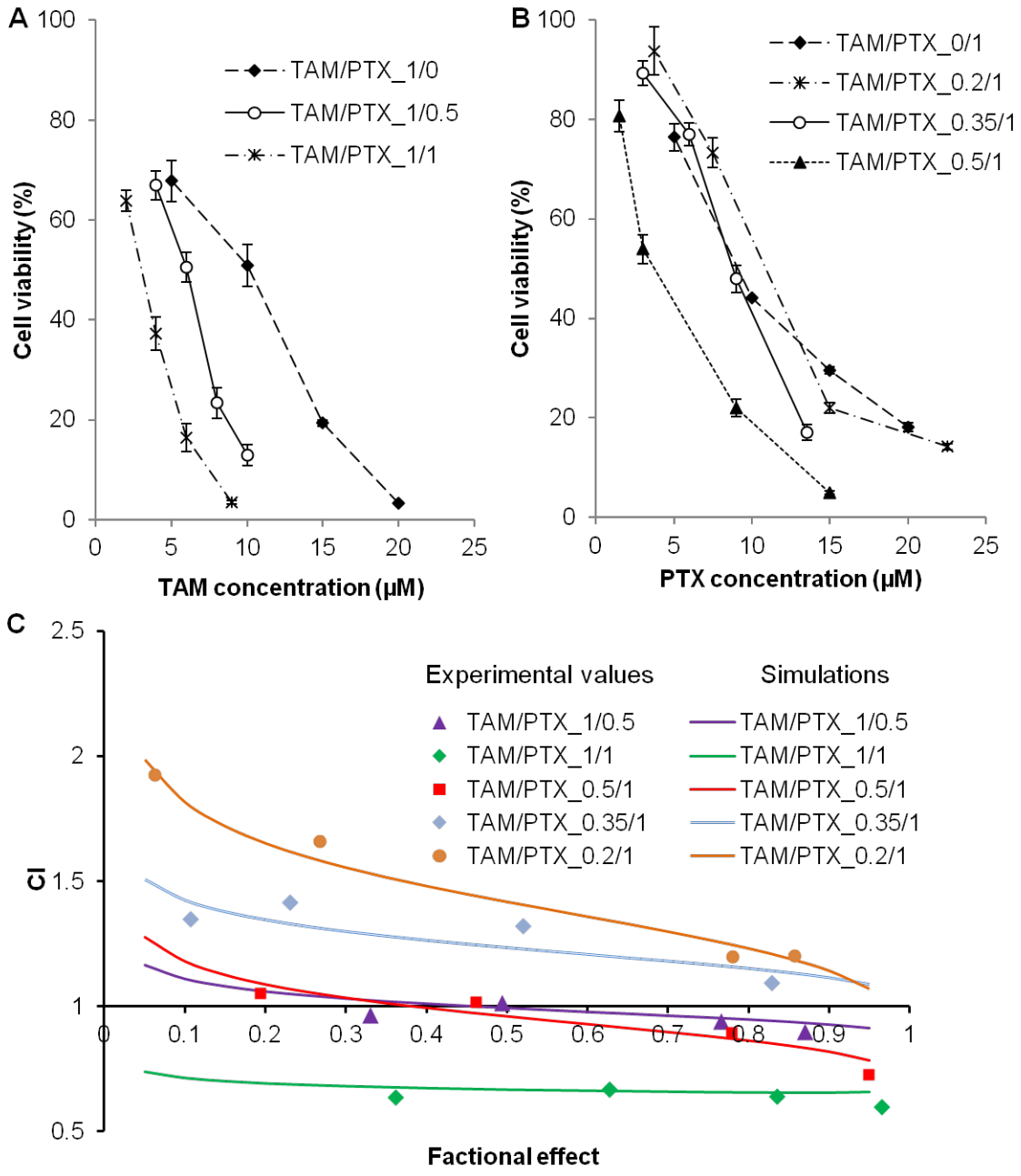

Figure 5.4 *In vitro* cytotoxicity study of combinations of free TAM and free PTX on MCF-7 cells: (A) MCF-7 viability vs. TAM concentration as increasing PTX in the combined TAM/PTX from 0 - 50% and (B) MCF-7 viability vs. PTX concentration as increasing TAM in the combined TAM/PTX from 0 - 33%. The combined treatment effects were presented as the combination index (CI) of different combined ratios versus factional effect of the drugs to the cells.

The Calcusyn software derived from median-effect principle was employed to provide more quantitative information on the effect of the combined treatments. The effects of the combinations are presented as the CI values as the function of factional effect of the treatment to the cells. This is the common method to present the effect of the combined treatments as reported by previous studies [11, 219]. It can be seen from Figure 5.4C that the TAM/PTX_1/1 treatment gives the synergistic effect over the whole range of concentrations. TAM/PTX_1/0.5 and TAM/PTX_0.5/1 treatments result in the synergistic effect at low concentrations while antagonistic at high treatment concentrations. Lower the TAM/PTX ratio (TAM/PTX_0.35/1 and TAM/PTX_0.2/1) leads to the antagonistic effect for all treatment concentration. Therefore, TAM/PTX_1/1 combination was used as the optimal synergistic composition for drug-encapsulated studies.

Table 5.1 IC_{50} of different treatment compositions of free TAM and free PTX to MCF-7 cells.

Treatment compositions	IC_{50} (μM)
TAM/PTX_1/0 (free TAM)	7.74
TAM/PTX_1/0.5	5.40/2.70
TAM/PTX_1/1	2.80/2.80
TAM/PTX_0.5/1	2.76/5.52
TAM/PTX_0.35/1	2.80/8.00
TAM/PTX_0.2/1	2.10/10.50
TAM/PTX_0/1 (free PTX)	9.16

5.3.2 Characterization of drug-loaded polymeric micelles

Physical properties of the drug-loaded micelles were analyzed by a DLS to obtain their hydrodynamics size and surface zeta potential which are important factors for the stability, prolong circulation, and efficacy of the drug delivery carriers [273, 274] . All drug-loaded micelles used in this study was found to have less than 200 nm in size and negative zeta potential (Table 5.2) that are suitable for drug delivery as indicated by previous studies [273].

Table 5.2 Characterization of single drug-loaded micelles and dual drugs-loaded micelles with TAT/FOL modification.

Micelles	DLC (%)	EE (%)	Size (nm)	Zeta potential (mV)
TAM-TAT/FOL micelles	1.21	56.5	161.8	-3.5
PTX-TAT/FOL micelles	1.12	52.3	132.8	-10.6
TAM/PTX(0.6/1)-TAT/FOL micelles	1.64	63.2 (TAM) 45.4 (PTX)	173.2	-4.7

The drug loading content (DLC) of the single-drug loaded micelles are approximately 1.2% (Table 5.2). Although the DLC of the two single drug loaded micelles (TAM-TAT/FOL micelles and PTX-TAT/FOL micelles) are almost equal, the release rate of TAM from TAM-TAT/FOL micelles is faster than the release rate of PTX from PTX-TAT/FOL micelles (Figure 5.5A). The faster release rate of TAM compared to PTX from the micelles may due to (i) the higher diffusivity of TAM through the micellar shell caused by the its smaller size compared to that of PTX and (ii) the faster dissociation of

TAM from the hydrophobic core of micelles caused by the less hydrophobic nature of TAM compared to PTX.

Based on the *in vitro* cytotoxicity study of the TAM/PTX ratios, the synergistic effect was observed at the treatment of TAM/PTX_1/1. Therefore, co-delivery of two single drug-loaded micelles was carried at the molar ratio of released TAM/released PTX at approximately 1/1 to obtain the synergistic effect of the combination. Figure 5.5A shows that the % release of TAM/PTX from the micelles is approximately 1.7/1. In addition, the DLC of the two single drug loaded micellar systems are similar. Co-delivery of two single drug-loaded micelles (TAM-TAT/FOL micelles & PTX-TAT/FOL micelles) was studied at the molar ratio of approximately 0.6/1 (presented as TAM-TAT/FOL micelles & PTX-TAT/FOL_0.6/1) to obtain the molar ratio of released TAM/ released PTX at 1/1. Similarly, the dual drugs-loaded micelles (TAM/PTX-TAT/FOL micelles) were prepared so that the dual drugs-loaded micelles could be formed at the TAM/PTX ratio of approximately 0.6/1 (presented as TAM/PTX(0.6/1)-TAT/FOL micelles). From the release profile of TAM/PTX(0.6/1)-TAT/FOL micelles in Figure 5.5B, the percentage release of TAM (calculated as (molar of released TAM/molar of loaded TAM)*100%) from the micelles is higher than that of PTX. This observation is in agreement with the release rate of single drug loaded micelles (Figure 5.5A). Combining the percentage release of TAM and PTX with the loading contents of TAM and PTX in the dual micellar system, the molar release of TAM to PTX is nearly 1 as shown in Figure 5.5B. This is the synergistic TAM/PTX ratio for the MCF-7 cells as determined in the previous section.

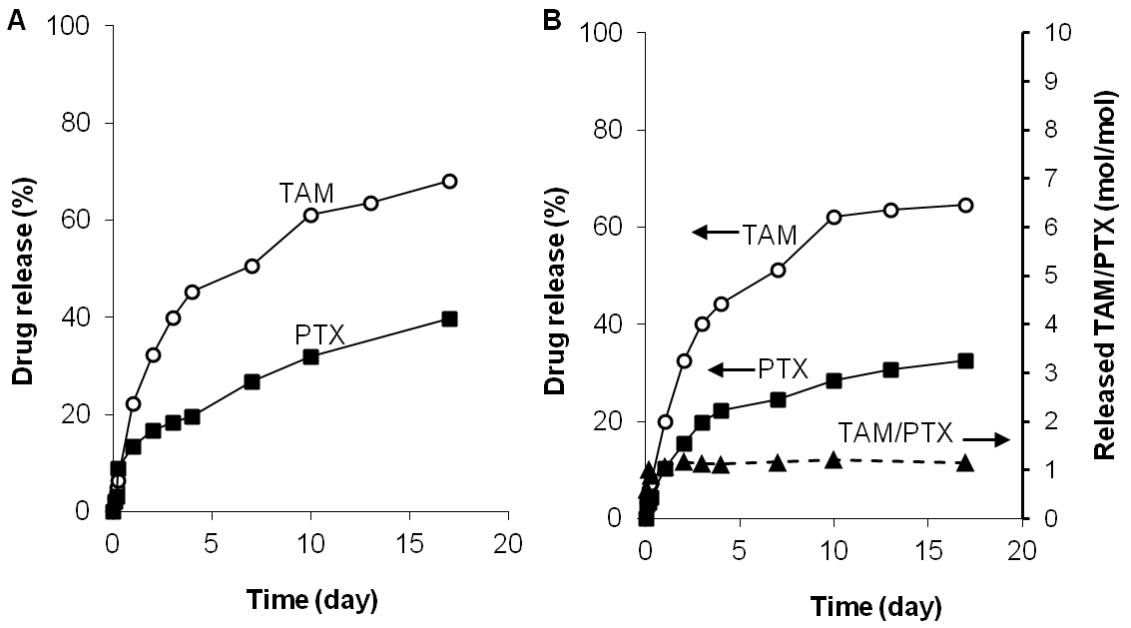

Figure 5.5 *In vitro* release profiles of TAM and PTX from (A) TAM-TAT/FOL micelles and PTX-TAT/FOL micelles, and (B) TAM/PTX(0/6/1)-TAT/FOL micelles in PBS (pH 7.4) at 37ºC. The experiments were conducted in triplicate. The standard deviation is less than 15%.

5.3.3 Enhancement of drug-loaded micelles with the surface modification using combined TAT and FOL

The modification of carrier's surface with FOL has demonstrated enhanced targeting property and cancer treatment effect [259, 275] including our previous study [257]. To further enhance the treatment efficiency, TAT peptide was utilized in this study since they are capable of transporting attached macromolecules from extracellular space through the cell membrane into cytoplasm in both *in vitro* and *in vivo* studies [138, 159, 172, 246]. The increase in cancer treatment efficacy of the drug-loaded micellar system with the modification of TAT and FOL was demonstrated by the comparison between non-modified micelles (prepared from PLGA-PEG copolymer) and TAT/FOL micelles

(prepared from 10% PLGA-PEG-TAT, 10% PLGA-PEG-FOL and 80% PLGA-PEG copolymers).

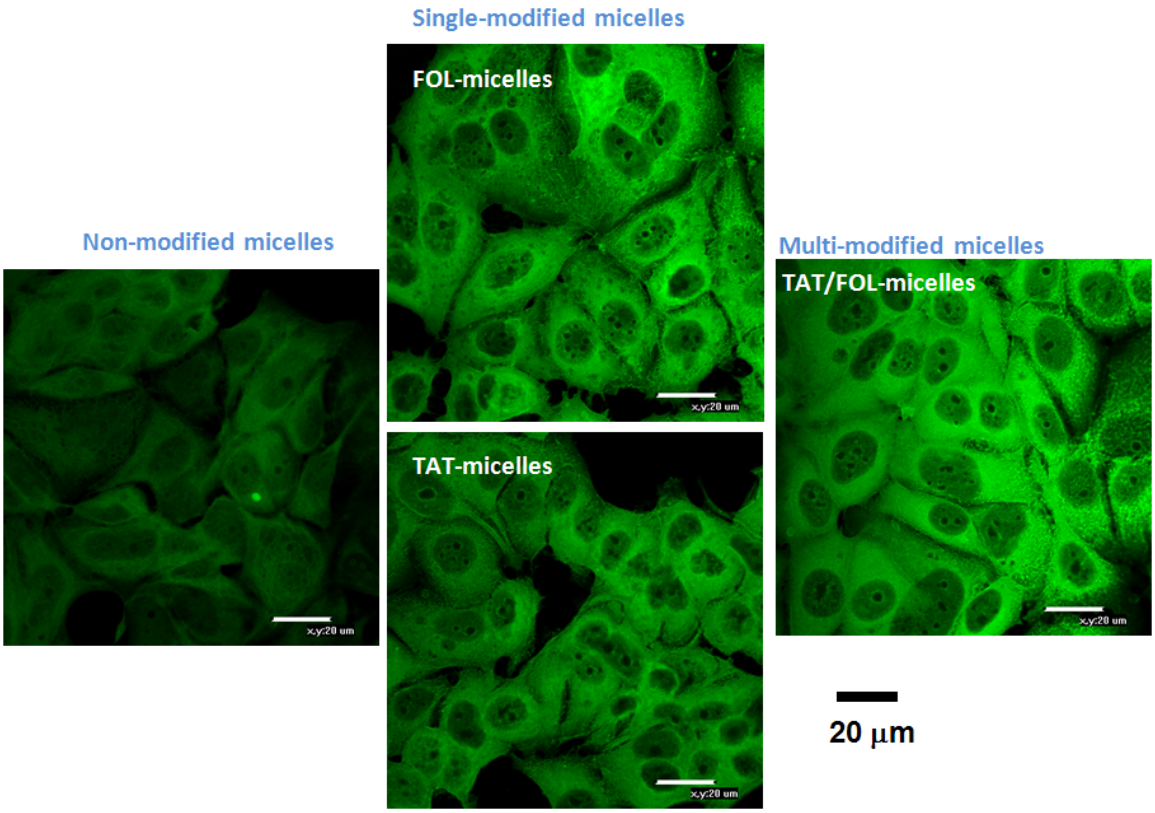

Figure 5.6 Confocal images of MCF-7 cells after incubation with various C6-loaded micellar systems.

First, in vitro cellular uptake of different surface modified micelles was observed in breast cancer cells (MCF-7). As shown in Figure 5.6, the fluorescence intensity in MCF-7 cells increases when micelles are modified with targeting (FOL) or penetrating (TAT) moiety. The strongest fluorescence intensity is observed for the cells treated with combined TAT and FOL modified micelles (TAT/FOL micelles). This observation indicates that the modification of micelles potentially improves the treatment efficacy of the drug delivery system. Multi-modification system may exhibit the highest treatment efficacy among these micellar systems.

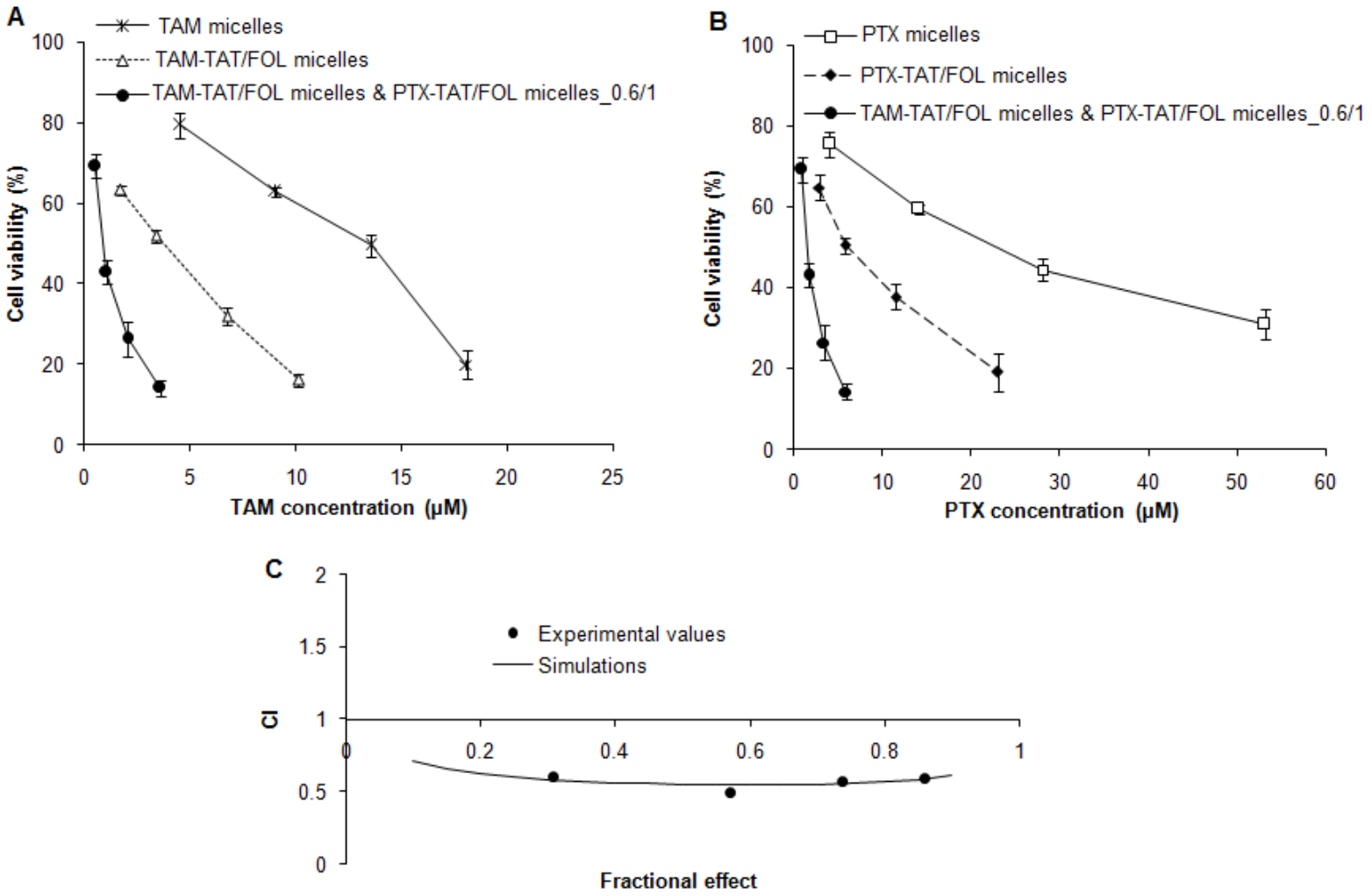

Figure 5.7 Comparisons of i*n vitro* MCF-7 cell viability that responds to the treatments with (A) TAM micelles, TAM- TAT/FOL micelles and co-delivery of TAM- TAT/FOL micelles & PTX-TAT/FOL micelles_0.6/1; (B) PTX micelles, PTX-TAT/FOL micelles and co-delivery of TAM- TAT/FOL micelles & PTX-TAT/FOL micelles_0.6/1. The synergistic effect of co-delivery of TAM-TAT/FOL micelles & PTX-TAT/FOL micelles_0.6/1 compared to TAM- TAT/FOL micellar or PTX-TAT/FOL micellar treatments was demonstrated as the CI values < 1 (C).

Furthermore, *in vitro* cytotoxicity study was carried out to investigate the anticancer effect of combined TAT/FOL micelles onto MCF-7 cells. The toxicity of all blank micelles was measured at a concentration of 2.0 mg/mL. The polymer concentration used in the blank micelle tests was higher than the concentration of polymers in all cytotoxicity tests with the presence of drug(s). Blank micelle tests indicate that micelles at concentration of 2.0 mg/mL were practically non-toxic to MCF-7 cells. Cell viability after non-modified micellar treatments (TAM micelles and PTX micelles) and TAT/FOL-modified micellar treatments (TAM-TAT/FOL micelles and PTX-TAT/FOL micelles) are shown in Figure 5.7A and 5.7B. It is obviously that the treatment with TAM-TAT/FOL micelles or PTX-TAT/FOL micelles is more efficient than the treatments with TAM micelles or PTX micelles as the much lower cell viability is observed at the same treatment concentration.

Table 5.3 IC_{50} values of different micellar systems to MCF-7 cells.

Treatment		IC_{50} (μM)
Single treatment	TAM micelles	10.61
	PTX micelles	20.70
	TAM -TAT/FOL micelles	3.01
	PTX-TAT/FOL micelles	5.93
Co-delivery treatment	TAM-TAT/FOL micelles & PTX-TAT/FOL micelles_0.6/1	0.90/1.50
Dual encapsulated treatment	TAM/PTX(0.6/1)-TAT/FOL micelles	0.85/1.41

As shown in Table 5.3, the IC_{50} of TAM micelles and PTX micelles are 10.61 μM and 20.70 μM respectively. With the addition of TAT and FOL onto the carrier surface, these

values are reduced to 3.01 μM and 5.93 μM, which is approximate 3.5 times lower than the IC_{50} of TAM micelles and PTX micelles. Compared with previous studies using TAT for micellar surface modification [137, 271] that exhibited less than 2 times enhancement compared to the non-modified micelles. The TAT/FOL modified micelles in this study performs better in promoting the effectiveness of the drug-loaded micelles.

5.3.4 Synergistic effect of the co-delivery of TAM-TAT/FOL micelles and PTX-TAT/FOL micelles

The preliminary studies in Sections 5.3.1 and 5.3.3 show that: (1) the treatment with the combination of two drugs TAM and PTX at ratio of 1/1 gives synergistic effect and (2) drug-loaded TAT/FOL micelles are more efficient than drug-loaded non-modified micelles. By utilizing the advantages of both mentioned methods, the co-delivery of TAM-TAT/FOL micelles and PTX-TAT/FOL micelles (Figure 5.3A) at the molar ratio of TAM/PTX of 0.6/1 (presented as TAM-TAT/FOL micelles & PTX-TAT/FOL micelles_0.6/1) was investigated. TAM-TAT/FOL micelles & PTX-TAT/FOL micelles was co-delivered at the ratio of 0.6/1 because this co-delivery ratio could provide the release amount of TAM/PTX of 1/1 to the breast cancer cells as discussed in Section 5.3.2.

The treatment effect of this system was compared with the TAM-TAT/FOL micellar or PTX-TAT/FOL micellar systems by *in vitro* cytotoxicity study. The required TAM and PTX concentrations of TAM-TAT/FOL micelles & PTX-TAT/FOL micelles_0.6/1 are lower than that of TAM-TAT/FOL micelles (Figure 5.6A) and PTX-TAT/FOL micelles (Figure 5.6B) to provide the same treatment efficacy respectively. Quantitatively, IC_{50}

values of TAM of co-delivered TAM-TAT/FOL micelles & PTX-TAT/FOL_0.6/1 is 0.9 μM and 3.3 times lower than that of TAM-TAT/FOL micelles (3.01 μM) (Table 5.3). Similarly, IC_{50} value of PTX of co-delivered TAM-TAT/FOL micelles & PTX-TAT/FOL_0.6/1 is approximate one quarter of that of PTX-TAT/FOL micelles. To further confirm the synergistic effect of this treatment method, the CI values of the treatment was calculated from the *in vitro* cytotoxicity experimental data of TAM-TAT/FOL micellar treatment, PTX-TAT/FOL micellar treatment and co-delivered TAM-TAT/FOL micelles & PTX-TAT/FOL_0.6/1 treatment using the Calcusyn software. From Figure 5.6C, the Cl values of less than 1 for all the fractional effect prove the synergistic effect of this co-delivery system compared with the TAM-TAT/FOL micellar and PTX-TAT/FOL micellar systems.

5.3.5 Synergistic effect of dual drugs-loaded micelles (TAM/PTX-TAT/FOL micelles)

In this section, we tested the enhancement potential of co-encapsulating TAM and PTX into the same TAT/FOL micelle, a dual drugs-loaded micelle system. Similar to the TAM-TAT/FOL micelles & PTX-TAT/FOL micelles_0.6/1 system shown in Section 5.3.4, the two drugs were loaded into this dual drugs micellar system at the TAM/PTX molar ratio of 0.6/1 (presented as TAM/PTX(0.6/1)-TAT/FOL micelles).

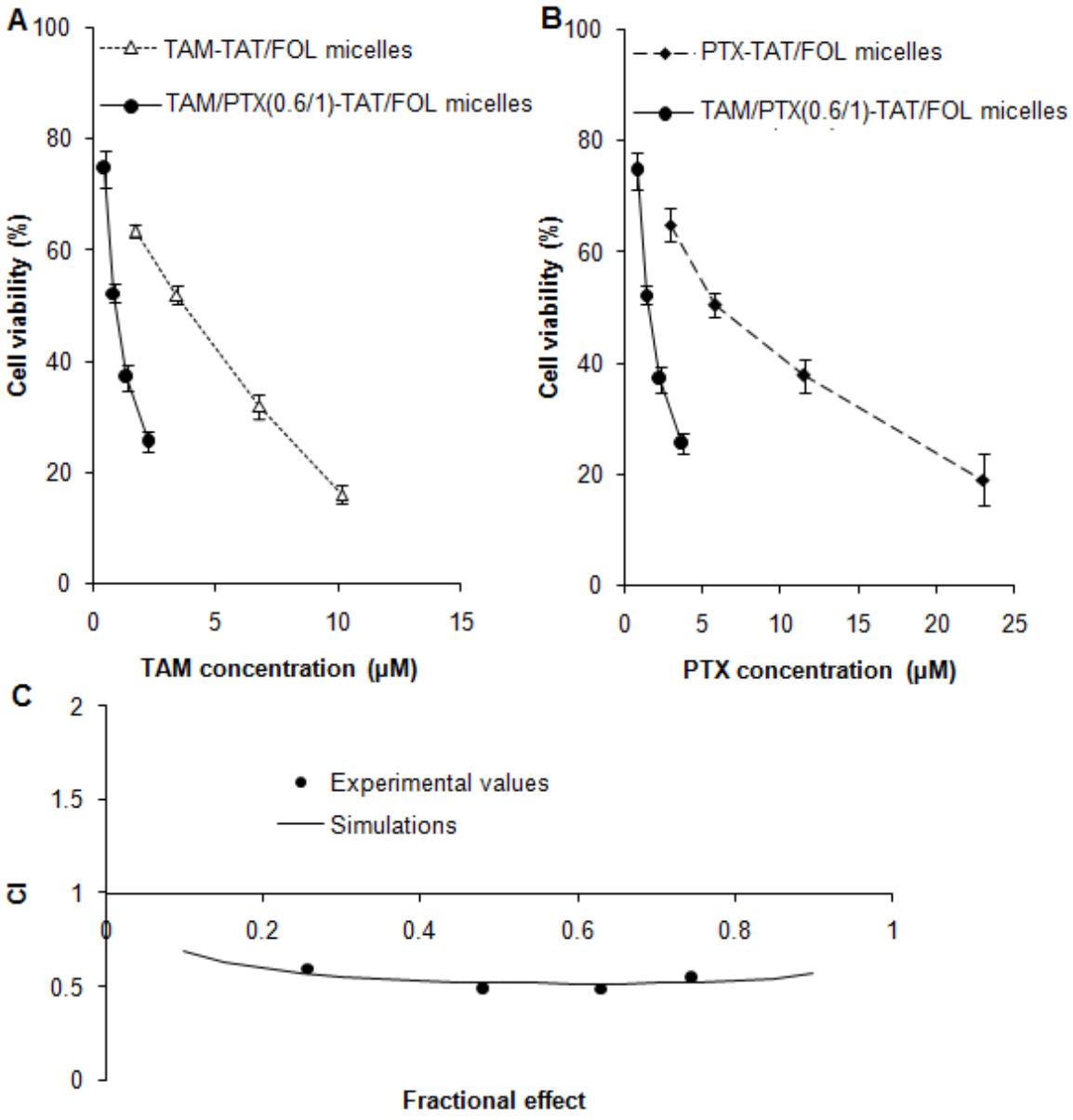

Figure 5.8 Comparisons of i*n vitro* MCF-7 cell viability that responds to the treatments with (TAM-TAT/FOL micelles and dual encapsulated TAM/PTX(0.6/1)-TAT/FOL micelles; (B) PTX-TAT/FOL micelles and dual encapsulated TAM/PTX(0.6/1)-TAT/FOL micelles. The synergistic effect of the dual encapsulated treatment compared to TAM-TAT/FOL micellar or PTX-TAT/FOL micellar treatments was demonstrated as the CI values < 1 (C).

The effects of the TAM/PTX(0.6/1)-TAT/FOL-micelles compared with TAM-TAT/FOL micelles and PTX-TAT/FOL micelles were firstly shown as the cell viability after treatment at different treatment concentrations of TAM (Figure 5.7A) and PTX (Figure

5.7B). From the two figures, the synergistic effects are observed from the lower cell viability of TAM/PTX(0.6/1)-TAT/FOL-micelles compared with that of TAM-TAT/FOL or PTX-TAT/FOL at the same TAM or PTX treatment concentration respectively. In Table 3, the IC_{50} of TAM/PTX(0.6/1)-TAT/FOL-micelles are 0.85 µM of TAM and 1.41 µM of PTX, approximately 3.5 and 5.2 times lower than the IC_{50} of TAM- TAT/FOL micelles and PTX-TAT/FOL micelles respectively. Moreover, Fig. 7C shows that all the CI values of TAM/PTX(0.6/1)-TAT/FOL-micelles are below 1, indicating the synergistic effect of the dual treatment as proven in previous studies [11, 219]. By utilizing the advantages of dual drugs-treatment and TAT/FOL modification, this newly developed system, TAM/PTX(0.6/1)-TAT/FOL micelles, shows much higher efficacy to MCF-7 treatment at IC_{50} of 0.85 µM T/1.41 µM PTX compared with the IC_{50} of traditional treatments of free TAM (7.74 µM) or free PTX (9.16 µM), or the single drug-loaded non-modified TAM (10.61 µM) micelles or PTX micelles (20.70 µM).

In this research work, we have demonstrated two systems, the co-delivery of two single drug-loaded micelles (TAM-TAT/FOL micelles & PTX-TAT/FOL_0.6/1) and the dual drugs-loaded micelles (TAM/PTX(0.6/1)-TAT/FOL micelles). The co-delivery of two single drug-loaded micelles is a flexible system for various treatments required different drug ratios. In contrast, the drug ratio of the dual drugs-loaded micelles is fixed. I*n vitro* cytotoxicity results show that exhibit the same synergistic effect to MCF-7 cells. However, the effect of the two methods may be different *in vivo* application as the micelles are circulated in the body's blood vessel before being delivered to the targeted tumors. The co-delivery of two single drug-loaded micelles may leads to the change in

the designed drug ratio at the targeted tumors. However, the dual drugs-loaded micelles have higher possibility in maintaining the initial drug ratio at the targeted tumors because the two drugs are encapsulated at the synergistic ratio into the same carrier. Therefore, the dual-drug loaded micelle system with FOL and TAT modifications is a better method for cancer treatment.

5.4 Conclusions

This study demonstrated the synergistic effect of the combined TAM and PTX at the ratio of 1/1 to breast cancer treatment. Further studies based on micellar technology for drug delivery were carried out to utilize (1) the synergistic effect of the combined TAM and PTX, (2) the advantage of micellar system to reduce the side-effects and control the release, and (3) the increase in penetrating and targeting efficacy of TAT/FOL modified system. Therefore, two newly developed systems were investigated in this work for breast cancer treatment: co-delivery of two single drug-loaded TAT/FOL modified micelles (TAM-TAT/FOL micelles & PTX-TAT/FOL micelles_0.6/1) and dual drugs-loaded TAT/FOL modified micelles (TAM/PTX(0.6/1)-TAT/FOL micelles). The two methods show the same synergistic effect but they contain their own advantage and limitation. For the co-delivery of two single drug-loaded micelles, the combination ratio could be easily varied for specific treatment with the limitation of maintaining the designed ratio in vivo treatment. The dual drugs-loaded micelles have higher possibility in maintaining the initial drug ratio for in vivo application which could overcome the limitation of the co-delivery of two single-drug-loaded micelles. However, the variation of drug ratios of the two drugs in the dual drugs-loaded micelles would be the limitation

for this system. Therefore, further optimization needs to be carried for specific applications.

Chapter 4 and Chapter 5 have demonstrated the co-encapsulation and co-delivery of synergistic hydrophobic drug combinations into micellar systems. To prove that micelles are not only able to co-encapsulate hydrophobic drugs. But they would be able to carry hydrophilic drugs if the suitable polymers are used to obtain strong interaction between drugs and polymers. Next chapter describes the co-encapsulation of cisplatin (CDDP) and DOX (in hydrophilic form DOX.HCl). The work in the next chapter addresses objective 4 in Chapter 1.

CHAPTER 6. Targeting delivery of a synergistic combination of doxorubicin and cisplatin with polymer-drug complex micellar systems

6.1 Introduction

Cisplatin (CDDP) is a first generation an platinum (Pt)-based anticancer drug that was first invented in 1965 [30]. CDDP has been demonstrated as a successful drug in inhibiting the growth of various types of cancers such as lung, ovarian, bladder, breast, testicular, head and neck cancers. Despite the high anticancer activity of CDDP, its application is limited due to the serious side effects including acute and chronic nephrotoxicity, myelosuppression [13]. In addition, CDDP exhibits some other unfavorable properties including poor water solubility, fast clearance [276], intrinsic or acquired tumor resistance [277]. Due to the rapid development of drug resistance in the tumor cells against CDDP, the combined therapy using CDDP (a platinum-based class) and non-platinum-based drugs are frequently used to archive higher chemotherapy efficacy [278-281]. Among many non-platinum-based drugs, doxorubicin (DOX), which works by binding to DNA and inhibiting nucleic acid synthesis of cells, has been commonly used together with CDDP in the combination therapy. Although the combined CDDP and DOX therapy has been demonstrated in phase III clinical trials as a synergistic cancer treatment, the side effects of this combination are still unfavorable [278, 281].

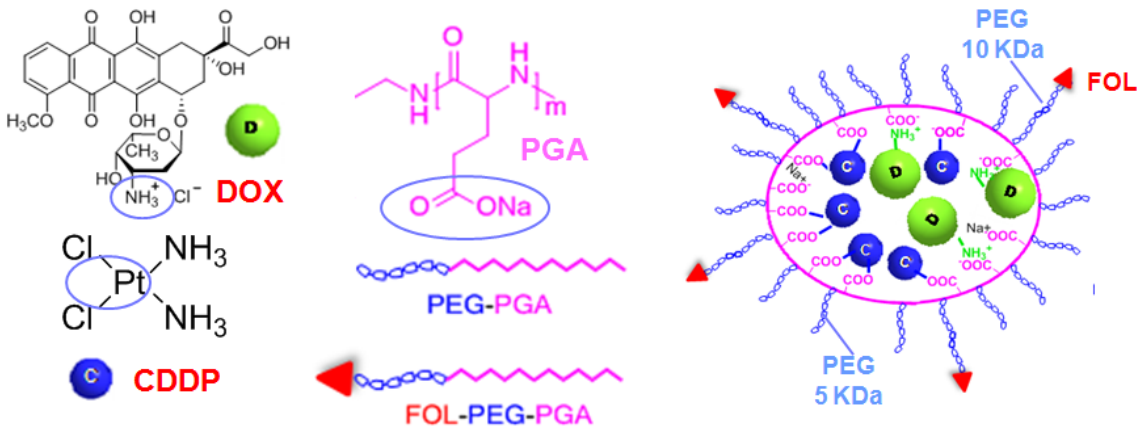

Figure 6.1 Formation of polymer-drug complex micelle between the glutamic acid groups of co-polymers (PEG-PLA and FOL-PEG-PLA) and two anticancer drugs DOX and CDDP.

To overcome the limitation caused by the side effects of CDDP and DOX, various methods have been studied to deliver CDDP and DOX to tumor tissues with lesser side effects by encapsulating drugs into carriers. Micelles, liposomes and nanoparticles are commonly used carriers for the delivery of a single drug CDDP [105, 282-285] or DOX [286, 287], or dual drugs CDDP/DOX [288]. A recent study has demonstrated that the combination therapy of DOX and CDDP using a nano-carrier system could improve the efficacy of advanced breast cancers while decreased clinical toxicity compared with the combined free DOX and CDDP treatment *in vivo* [289]. In addition to the delivery of drugs using a nano-carrier system, the therapeutic efficacy can be further improved by modifying the delivery carrier with a ligand that is able to target to specific cancer cells of interest. Folate (FOL) is a targeting ligand having high binding affinity to folate receptors overexpressed in ovarian, breast, brain, lung, colorectal cancer cells [253-255] and has widely been used to modify many delivery carriers such as nanoparticles [87], liposomes [256], micelles [257-260].

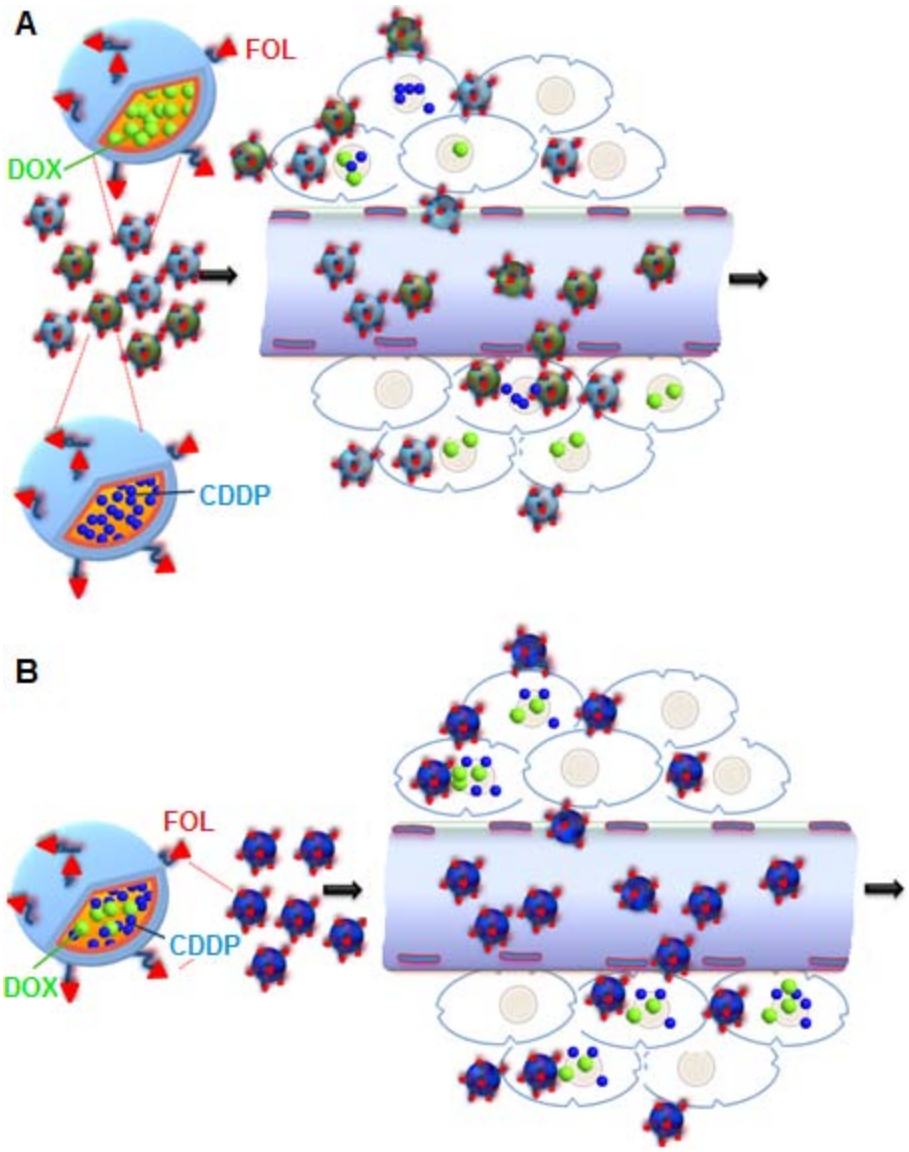

Figure 6.2 Active targeting co-delivery of DOX and CDDP to cancer cells by the modification of carriers with FOL which has high binding affinity to cancer cells by two methods: (A) injection of DOX- FOL micelles and CDDP-FOL micelles; (B) injection of CDDP/DOX-FOL micelles which encapsulate both CDDP and DOX at the designed ratio in a micelle.

Herein, our approach was to investigate CDDP and DOX delivery systems utilizing the benefits of (1) combined CDDP and DOX treatment, (2) delivery of drugs using micellar carriers, and (3) modification of carrier's surface with FOL targeting ligand. In addition, to obtain high encapsulation amount of CDDP and DOX, poly(ethylene glycol)-

poly(glutamic acid) (PEG-PGA) and folate-PEG-PGA (FOL-PEG-PGA) polymers were chosen to form drug carriers for this study (Fig. 1). The polymer-drug complex formation between PEG-PGA/FOL-PEG-PGA polymers and drugs CDDP or DOX was due to the ligand substitution reaction at platinum atoms of CDDP and carboxylic groups of PGA block [105], and the electrostatic interaction of the negatively charged PGA block and the cationic drug DOX [109, 286] respectively (Figure 6.1). *In vitro* cytotoxicity studies were carried out based on the three methods of CDDP/DOX delivery. Firstly, the effects of different free drug combinations (CDDP/DOX) on cancer cells was investigated to find out the combination that exhibits good synergy over a wide treatment concentration range for subsequent drug-encapsulating studies. Secondly, co-delivery of two single drug-loaded micelles using FOL modified system (CDDP-FOL micelles & DOX-FOL micelles) in Figure 6.2A. Finally, dual drugs-encapsulated micelles with FOL modification (Figure 6.2B) were evaluated.

6.2 Experimental section

6.2.1 Materials

Poly(ethylene glycol) bis(amine) (PEG-diamine, Mw:10,000) were purchased from Laysan Bio Inc (USA). Bis(trichloromethyl) carbonate (triphosgene), β-benzyl l-glutamate, poly(ethylene glycol)-amine (PEG-amine, Mw: 5,000), N-hydroxysuccinimide (NHS), dicyclohexyl carbodiimide (DCC), folic acid, cis-diamminedichloroplatinum (II) (cisplatin, CDDP), 3-[4,5-dimethylthiazolyl-2]-2,5-diphenyl tetrazolium bromide (MTT), hydrochloric acid (HCl) and platinum (Pt) standard solution 1000 mg/L in 5% hydrochloric acid were all purchased from Sigma-Aldrich (USA). Doxorubicin (DOX)

was obtained from Boryung (Korea). Pyridine, chloroform, dichloromethane (DCM), N,N-dimethylformamide (DMF), dimethyl sulfoxide (DMSO), anhydrous tetrahydrofuran (THF), methanol, 2-propanol, diethyl ether and hexane were purchased from Tedia (USA). Folate-free RPMI 1640 medium, fetal bovine serum (FBS), Trypsin-EDTA and penicillin-streptomycin were obtained from Invitrogen (USA). All chemicals were used directly without further purification. KB human oral cavity carcinoma cell line was purchased from ATCC (USA).

6.2.2 Synthesis and characterization of polymers

6.2.2.1 Synthesis of polymers

Two block copolymers, poly(ethylene glycol)-poly(glutamic acid) (PEG-PGA) and folate-PEG-PGA (FOL-PEG-PGA) were used in this study as carrier materials.

PEG-PGA was synthesized using a three-step protocol as insulated in Figure 6.3 [105]. Firstly, the N-carboxy anhydride of β-benzyl l-glutamate was synthesized using an equivalent of triphosgene in THF at 50°C in the N_2 atmosphere. The reaction took 3 hours to get a completely homogeneous solution of N-carboxy anhydride of β-benzyl l-glutamate which was then poured into ice-cold hexane and stored at -20°C overnight to assure complete crystallization. The crystallized N-carboxy anhydride of β-benzyl l-glutamate was collected and dried in the vacuum oven at room temperature to remove the residual solvent completely.

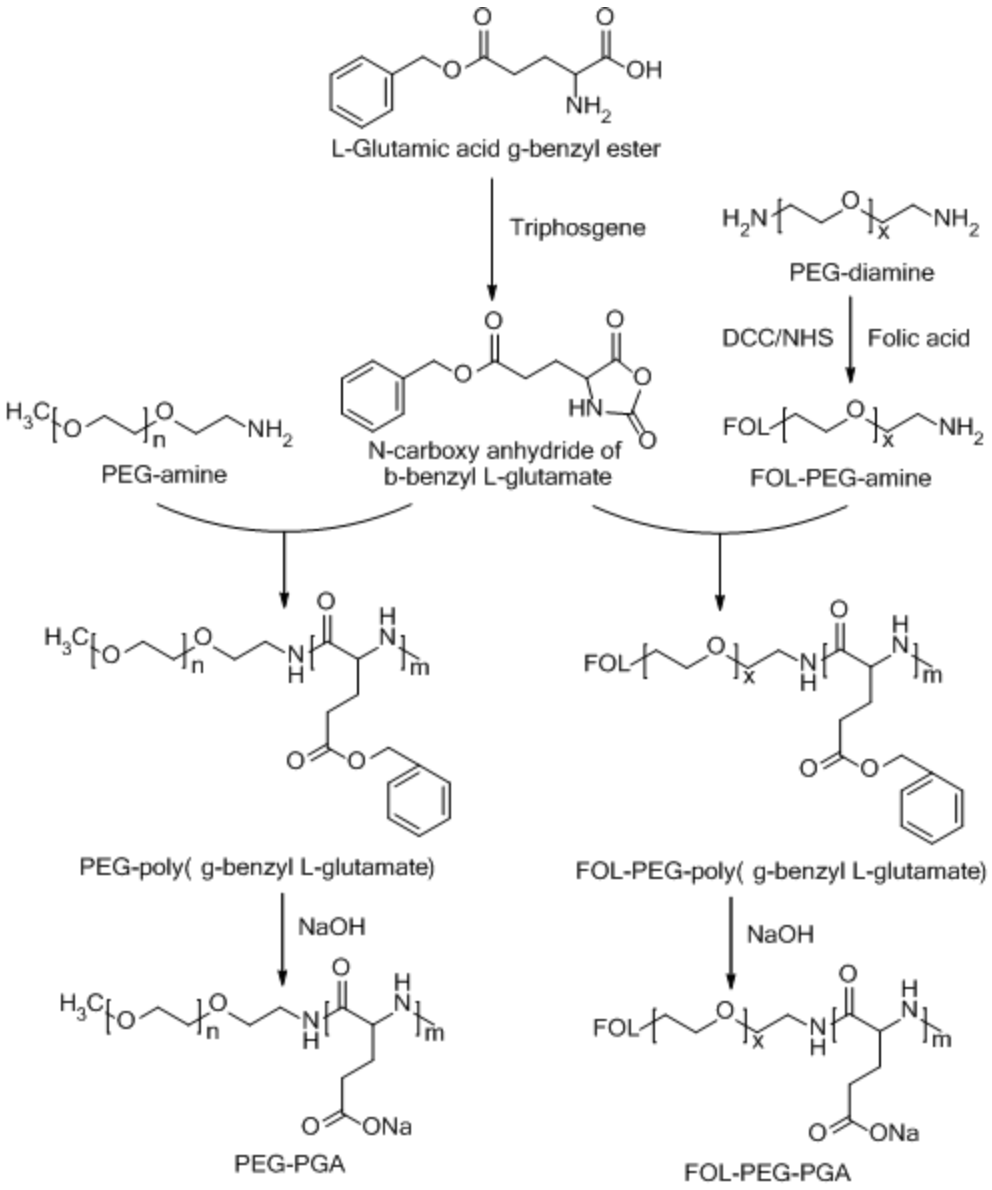

Figure 6.3 Schematic of PEG-PGA and FOL-PEG-PGA synthesis.

Secondly, PEG-poly(g-benzyl L-glutamate) was synthesized by the ring opening polymerization reaction of N-carboxy anhydride of β-benzyl l-glutamate with PEG-amine as the initiator in DMF/chloroform at 35°C in N_2 atmosphere for 3 days. The resultant solution was dropped into ice-cold diethyl ether to precipitate PEG-poly(β-benzyl L-glutamate) and the product was dried in a vacuum oven. Finally, PEG-PGA was

produced by the deprotection of the benzyl groups of PEG-poly(β-benzyl l-glutamate) in 0.5 M NaOH in a mixture of water/methanol/2-propanol at volume ratio of 1/2/2 at 0°C for 15 min [36]. The solution was poured into ice-cold diethyl ether to precipitate PEG-PGA. The precipitant was dissolved in DI water and dialyzed against DI water for two days and freeze-dried.

FOL-PEG-PGA was synthesized from the polymerization reaction between FOL-PEG-amine and N-carboxy anhydride of β-benzyl l-glutamate and followed by the deprotection of the benzyl groups. The synthesis of FOL-PEG-PGA was in the same mechanism with PEG-PGA synthesis with the additional of the coupling reaction of FOL to PEG before the polymerization reaction [257]. First, FOL was conjugated to PEG-diamine (Mw: 10,000) using DCC/NHS (molar ratio of PEG-diamine:folic acid:DCC:NHS = 1:1:2:2) in DMSO in the presence of pyridine for 10 h in the dark. The resultant solution was purified by being diluted with de-ionized (DI) water and centrifuged to remove the insoluble by-product dicyclohexylurea (DCU). The supernatant was further filtered to obtain clear yellow solution before being dialyzed against DI water for 2 days (MWCO: 1000) to remove DMSO and unreacted FOL and freeze-dried. The trace amount of unreacted PEG-diamine was then removed by batch adsorption with cellulose phosphate cation exchange resin using 5 mM phosphate buffer pH 7.0 as the start buffer. PEG-FOL was further purified by a DEAE sephadex anion exchange column with 20 mM Tris-HCl pH 8.0 as the start buffer to remove FOL-PEG-FOL by-products. The final product was precipitated twice in ice-cold diethyl ether, dissolved in DMSO for dialysis against DI water for 2 days (MWCO: 10,000), centrifuged, and then freeze-dried.

6.2.2.2 Characterization of polymers

The synthesized co-polymers, PEG-PGA and FOL-PEG-PGA, were characterized by gel permeation chromatography (GPC) and ^{1}H nuclear magnetic resonance (^{1}H NMR). GPC analysis was performed in an Agilent HPLC 1200 equipped with a TSK GEL G4000PW$_{XL}$ (4.6 mm × 300 mm, 10 μm) column and a refractive index (RI) detector. 100 mM NaCl in PBS was used as a mobile phase at the flow rate of 1 mL/min at 40°C. ^{1}H NMR was carried on in a Bruker AMX 500 at 80°C using D_2O as a solvent.

6.2.3 Preparation and characterization of cisplatin (CDDP) and doxorubicin (DOX) micelles

The micelles were prepared by dissolving polymers (PEG-PGA, FOL-PEG-PGA) and drugs (CDDP and DOX) in DI water to obtain a concentration of 5 mmol/L glutamic acid (GA). The molar ratio of drugs and polymers were kept at [molar of drugs]/[molar of GA] = 1/1 followed the previous study's protocol [105]. The solutions of polymers and drugs were kept at 37°C for 3 days under shaking condition for the formation of the polymer-drug complex micelles as shown in Fig. 1. The micelles were purified by dialyzing against DI water for 6 h to remove untrapped drugs.

The hydrodynamic size and zeta potential of polymeric micelles were measured at 25°C by a NanoSizer (Malvern Instruments, UK). Aqueous micelle solutions were prepared using deionized water. The concentration of polymeric micelles was kept at 1 mg/ml. The micelle solutions were filtered through a 0.80 μm cellulose membrane filter before measurements. The average values were calculated from at least 3 measurements

performed on each samples. The CDDP loading content in the micelles was determined by dissolving the micelles in 5% HCl and measuring the Pt concentration of the solution using an inductively coupled plasma-mass spectrometer (ICP-MS; Perkin-Elmer, Elan 6100). The DOX loading content in the micelles was estimated with a UV-vis spectrophotometry at 480 nm by dissolving 1 mg of DOX- loaded micelles in 1 ml DMSO.

6.2.4 *In vitro* release study

Micelle solutions (1 mg in 1 ml of PBS, pH 7.4) were transferred to dialysis tube (MWCO: 2,000 Da) and dialyzed against 3 ml PBS in a tube at 37°C with shaking at 100 rev/min. To measure the release of drugs at different time intervals, PBS solution in the tube was all withdrawn and replaced with 3 ml fresh PBS. To determine the released amount of CDDP, 10% HCl was added into the withdrawn solution to obtain the solution with 5% HCl and measured by ICP-MS. The released amount of DOX in the withdrawn solutions was transferred into a 96-well plate and analyzed by a microplate reader with excitation wavelength at 480 nm and emission wavelength at 570 nm. The drug release studies were performed in triplicate for each of the samples.

6.2.5 *In vitro* cytotoxicity study

The ability of various treatments to inhibit cell proliferation was evaluated using human carcinoma KB cell line with MTT viability assay. Cells cultured in free folic RPMI media supplemented with 10% FBS and 1% penicillin-streptomycin at 37°C in humidified environment of 5% CO_2 were seeded onto 96-well plates at a seeding density

of 10,000 cells/well and incubated for 2 days to permit cell attachment. The cells were then treated with free drugs or micelles at different concentrations for 3 days. Afterwards, the cell viability was determined by MTT assay following the method as described in Chapter 4. The combination index of the combined treatments was determined by Chou and Talalay's principle as mentioned in Chapter 2 and 4. The toxicity of all blank micelles was tested at a high concentration of 2.0 mg/mL and exhibited non-toxic to KB cells. This observation is in agreement with previous studies and indicates the suitability of the micellar system for carrying anticancer drugs.

6.3 Results and discussion

6.3.1 Characterization of polymers

The two polymers, PEG-PGA and FOL-PEG-PGA, were prepared by alkaline hydrolysis of PEG- or FOL-PEG-poly(g-benzyl L-glutamate), which were the products of the polymerization of N-carboxy anhydride of β-benzyl l-glutamate with amine initiators (PEG-amine or FOL-PEG-amine). Therefore, the degree of polymerization of the PGA blocks of PEG-PGA and FOL-PEG-PGA were determined by the changes in the molecular weight of PEG-PGA and FOL-PEG-PGA compared to that of PEG and FOL-PEG respectively. From GPC results (Figure 6.4A and 6.4C), the polymerization degrees of PGA blocks of PEG-PGA and FOL-PEG-PGA are estimated at 60 and 53 respectively. After the polymerization and alkaline hydrolysis to deprotect the benzyl group, the resultant polymers were purified to remove unreacted PEG or FOL-PEG and other small molecules such as monomer, solvents. The GPC spectra in Figure 6.4A and 6.4C show that the purification steps are able to remove completely unreacted PEG or FOL-PEG

from the products. However, there is a trace amount of small molecule impurities in the final products. From the ^{1}H NMR spectra, the protons of PGA block are observed at δ = 4.67, 2.20, 1.80-1.98 ppm [290], the protons of the PEG block are at δ = 3.5-3.7 ppm [291], and peaks at δ 6.6 and δ 7.6 are from FOL [257]. The absence of the residual benzyl group (δ = 7.3 pmm) in the ^{1}H NMR spectra of the synthesized polymers (Figure 6.4B and 6.4D) confirms the completion of the alkaline hydrolysis reaction. The above analysis results indicate that PEG-PGA and FOL-PEG-PGA were successfully prepared.

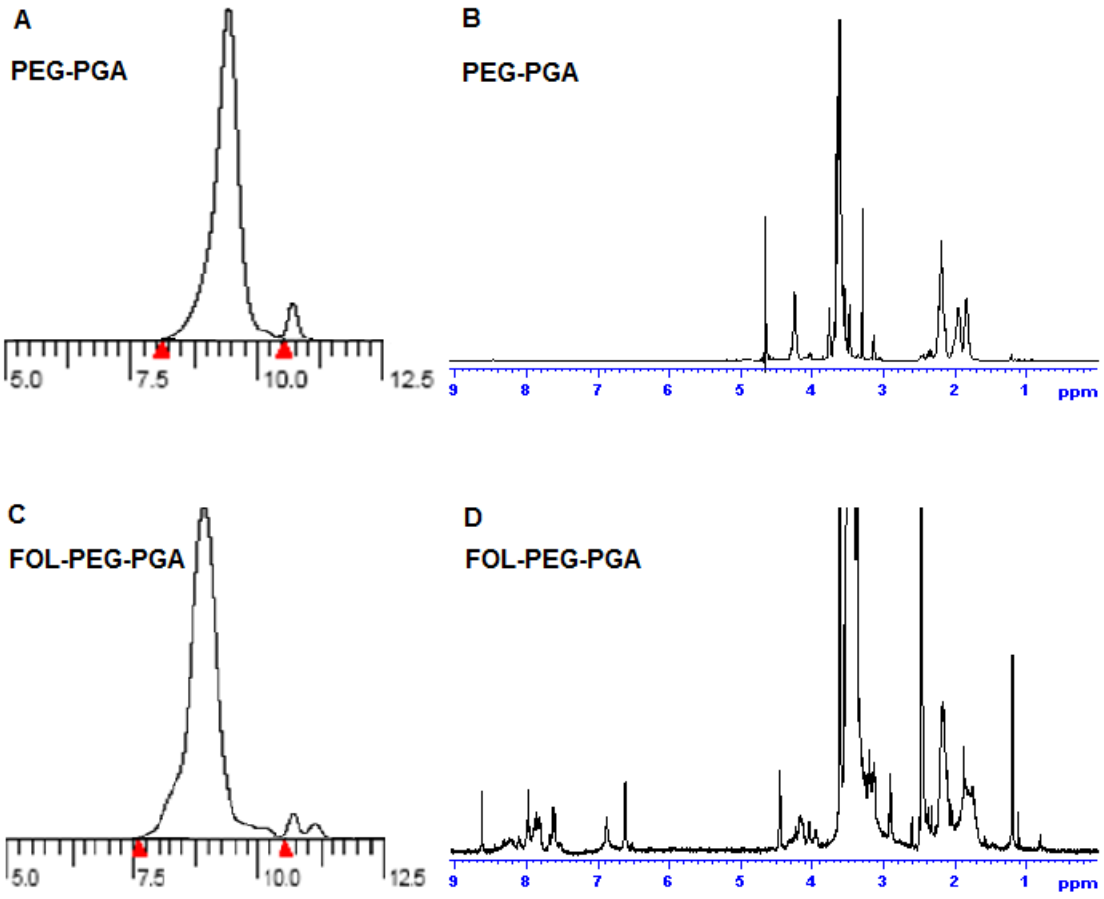

Figure 6.4 GPC and ^{1}H NMR spectra of PEG-PGA (A and B respectively) and FOL-PEG-PGA (C and D respectively).

6.3.2 *In vitro* cytotoxicity interaction between free cisplatin (CDDP) and free doxorubicin (DOX)

This study was designed for the investigation of the delivery system for CDDP and DOX at the synergistic ratio. Therefore, the combined effects of free CDDP and free DOX cancer cells at various ratios were firstly studied to obtain the synergistic ratio that was subsequently used for drug delivery studies. KB cell line was used as a model for all experiments. The combinations of free CDDP and free DOX are presented as CDDP/DOX_x/y while x/y is the molar ratio of CDDP/DOX in the combination.

Table 6.1 IC_{50} of different treatment compositions of free drugs, CDDP and DOX

Treatment compositions	IC_{50} (μM)
CDDP	9.158
CDDP/DOX_1/1	0.322/0.322
CDDP/DOX_10/1	1.538/0.154
CDDP/DOX_20/1	1.782/0.089
CDDP/DOX_40/1	2.582/0.065
CDDP/DOX_60/1	2.942/0.049
DOX	0.286

As shown in Figure 6.5A, the cell viability is gradually decreased as the increase of CDDP/DOX ratio from 1/1 to 40/1. However, the cell viability is almost unchanged when the CDDP/DOX ratio increases to 60/1, and this indicates that CDDP/DOX_60/1 treatment may not provide better synergistic effect than CDDP/DOX_40/1 treatment. From the IC_{50} values (the required dose to kill 50% cells) in Table 6.1, the treatment with

higher CDDP/DOX ratio results in lower IC_{50} of DOX but higher IC_{50} of CDDP. Therefore, it is impossible to determine the synergistic regimes from the data in Figure 6.5A and Table 6.1. Therefore, further analysis needs to be carried on these cytotoxicity results to obtain the more quantitative data using Calcusyn software that has been commonly used to study the effect of combined drug treatments by calculating the CI values of combinations at fixed ratios as a function of the cell viability [219, 272, 288]. The effect of combination treatments is considered as a synergistic combination with CI values below 1 for all treatment concentrations that provide the cell viability from 5% to 95%. From Figure 6.5B, CI values of CDDP/DOX_1/1 and CDDP/DOX_60/1 show synergistic effect at low treatment doses but antagonistic effect (CI > 1) at high treatment doses. Therefore, these two treatment combinations are not considered as synergistic regimes in this study. Three combinations at CDDP/DOX ratios of 10/1, 20/1 and 40/1 show synergistic effect for all treatment doses. Comparing among these three synergistic regimes, the CDDP/DOX_10/1 shows the highest CI values which indicate the lowest synergistic effect of CDDP/DOX_10/1. Between CDDP/DOX_20/1 and CDDP/DOX_40/1, the treatment with CDDP/DOX_20/1 exhibits higher synergistic effect at low treatment doses while the treatments with CDDP/DOX_40/1 at high doses show better synergistic effect. IC_{50} values of the two treatments in Table 6.1 show that the treatment with CDDP/DOX_20/1 reduces 45% required dose of CDDP compared to the treatment with CDDP/DOX_40/1 to kill 50% cancer cells. Therefore, the combination of CDDP and DOX at the composition of CDDP/DOX_20/1 is more favorable to the treatment of KB cells with good synergistic effect and low severe side effects caused by CDDP [13].

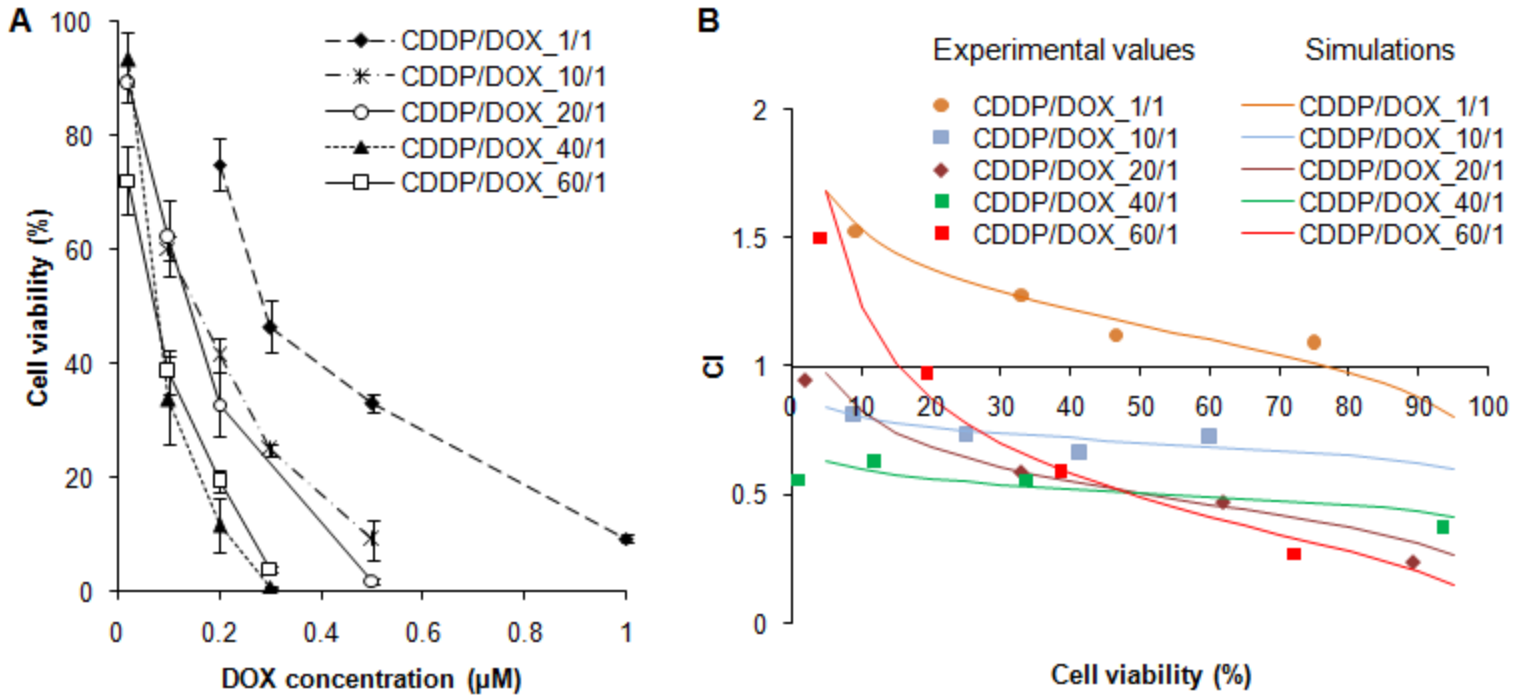

Figure 6.5 The combined effects of various CDDP/DOX ratios as presented by (A) the cytotoxicity respond of KB cells vs DOX concentration and (B) CI values as the function of cell viability.

6.3.3 Characterization of drug-loaded micelles

Two classes of polymer-drug complex micelles, single drug-loaded micelles (CDDP-micelles, CDDP-FOL micelles, DOX- micelles, DOX- FOL micelles) and dual drugs-loaded micelles (CDDP/DOX(20/1)-FOL micelles) were prepared for this study. CDDP/DOX(20/1)-FOL micelles indicate that this dual encapsulated system contains both CDDP and DOX in a micelle at the molar ratio of CDDP/DOX of 20/1.

Table 6.2 Characterization of polymeric micelles.

Micelles	DLC (%)	EE (%)	Size (nm)	Zeta potential (mV)
CDDP-micelles	26.1	52.6	167.0	-16.8
CDDP-FOL micelles	23.8	48.1	181.0	-14.5
DOX-micelles	48.4	65.0	190.7	-4.6
DOX-FOL micelles	45.5	61.2	205.6	-4.12
CDDP/DOX(20/1)-FOL micelles	20.1	33.2 (CDDP) 66.0 (DOX)	192.1	-3.5

Table 6.2 shows that the encapsulation of CDDP and DOX using this method can produce polymer-drug complex micelles with very high drug loading content (DLC) up to 26 % and 48% for CDDP and DOX encapsulation respectively. DLC of DOX is higher than that of CDDP can be due to the additional strong π-π interaction of DOX molecules besides the electrostatic interaction between DOX and PGA. Compared with recently reported CDDP and DOX-loaded systems such as systems from poly(γ, L-glutamic acid)-citric acid-cisplatin with the loading of CDDP at 20% [292], folate-poly(ethylene glycol)-poly(ε-caprolactone) with the loading of DOX at 4.6 – 13% [293], and mPEGylated

peptide dendron–DOX with the loading of DOX at 14% [294], the systems in this study are more favorable in term of DLC. All drug-loaded micelles in this study have the size from 167 nm to 205.6 nm with negative zeta potentials of approximately -5 to -15 mV (Table 6.2). The slightly negative zeta potentials of drug-loaded micelles can prevent the non-specific binding between the micelles and the cells due to the negative zeta potentials of most biological cells [295]. In addition, the modification of micelles with FOL moiety allows the drug-loaded micelles to accumulate specifically into the cancer cells via receptor-mediated interaction. These properties indicate the suitability of these systems for drug delivery application [273, 274].

6.3.4 *In vitro* drug release study

The release rates of CDDP and DOX from the polymer-drug complex micelles in PBS, pH 7.4 at 37°C are shown in Figure 6.6. Clearly, CDDP releases faster than DOX in all formulations due to the additional π-π interaction of DOX molecules besides the electrostactic interaction between DOX and PGA. The drug release profiles CDDP or DOX of singe-drug loaded micelles without FOL (CDDP-micelles and DOX- micelles) in Figure 6.6A and with FOL modification (CDDP-FOL micelles and DOX- FOL micelles) in Figure 6.6B are quite similar. However, DOX releases faster in the dual CDDP/DOX(20/1)-FOL micelles while CDDP releasing rate remains similar to that of CDDP-FOL micelles. The faster release rate of DOX in the dual system may due to the disruption of π-π interaction between DOX molecules by the presence of CDDP.

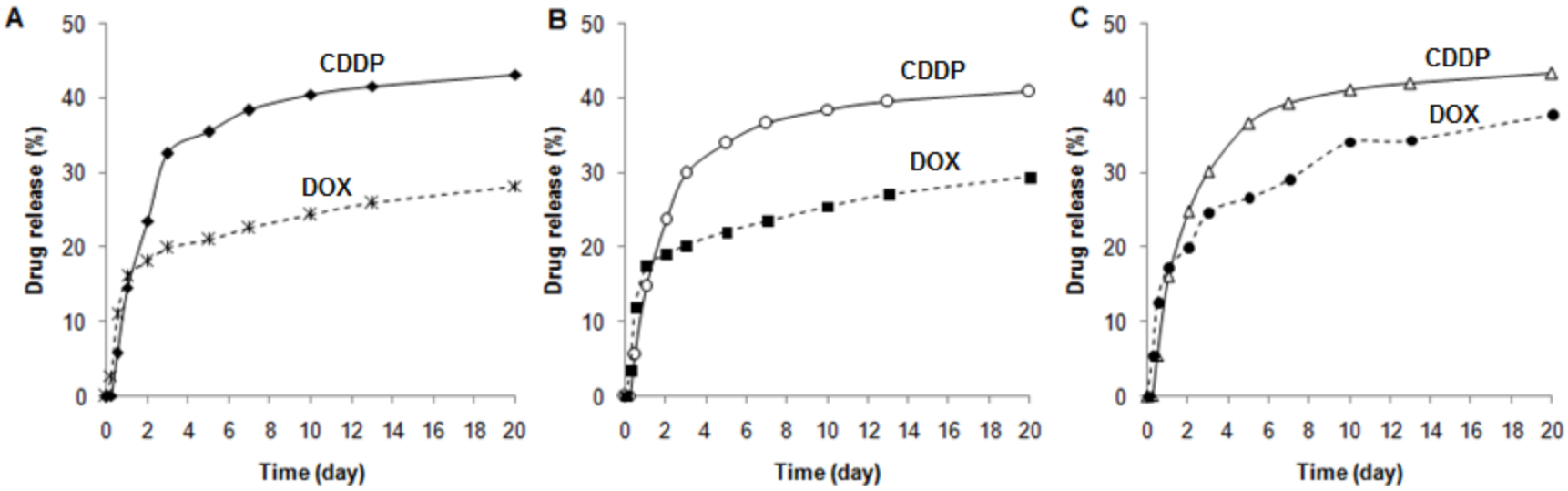

Figure 6.6 *In vitro* drug release of CDDP and DOX from: (A) CDDP-micelles and DOX- micelles, (B) CDDP-FOL micelles and DOX- FOL micelles, and (CDDP) CDDP/DOX(20/1)-FOL micelles. The experiments were conducted in triplicate. The standard deviation is less than 10%.

After the first 72 h of release, approximately less than 35% and 25% of CDDP and DOX are released respectively. Compare with recently reported studies as mentioned above (Section 6.3.3), the poly(γ, L-glutamic acid)-citric acid-cisplatin system with 50% CDDP release within first 72 h [292], folate-poly(ethylene glycol)-poly(ε-caprolactone) with 42% DOX release within the first 24 h [293], and mPEGylated peptide dendron–doxorubicin with 20% DOX release in the first 24 h [294], the micellar systems in this study show better sustainable release.

6.3.5 Cytotoxicity enhancement of drug-loaded micelles with the addition of FOL on the micelle surface

Table 6.3 IC_{50} of different micellar treatments: (1) delivery of single drug-loaded micelles, (2) co-delivery of two singe drug-loaded micelles at the ratio of CDDP/DOX at 20/1, and (3) delivery of dual drugs-loaded micelles at the ratio of CDDP/DOX at 20/1.

Treatment	IC_{50} (μM)
(1) Delivery of single drug-loaded micelles:	
CDDP-micelles	8.467
CDDP-FOL micelles	3.511
DOX-micelles	0.364
DOX-FOL micelles	0.170
(2) Co-delivery of two single drug-loaded micelles: CDDP-FOL micelles & DOX-FOL micelles_20/1	0.768/0.038
(3) Delivery of dual drugs-loaded micelles: CDDP/DOX(20/1)-FOL micelles	0.650/0.032

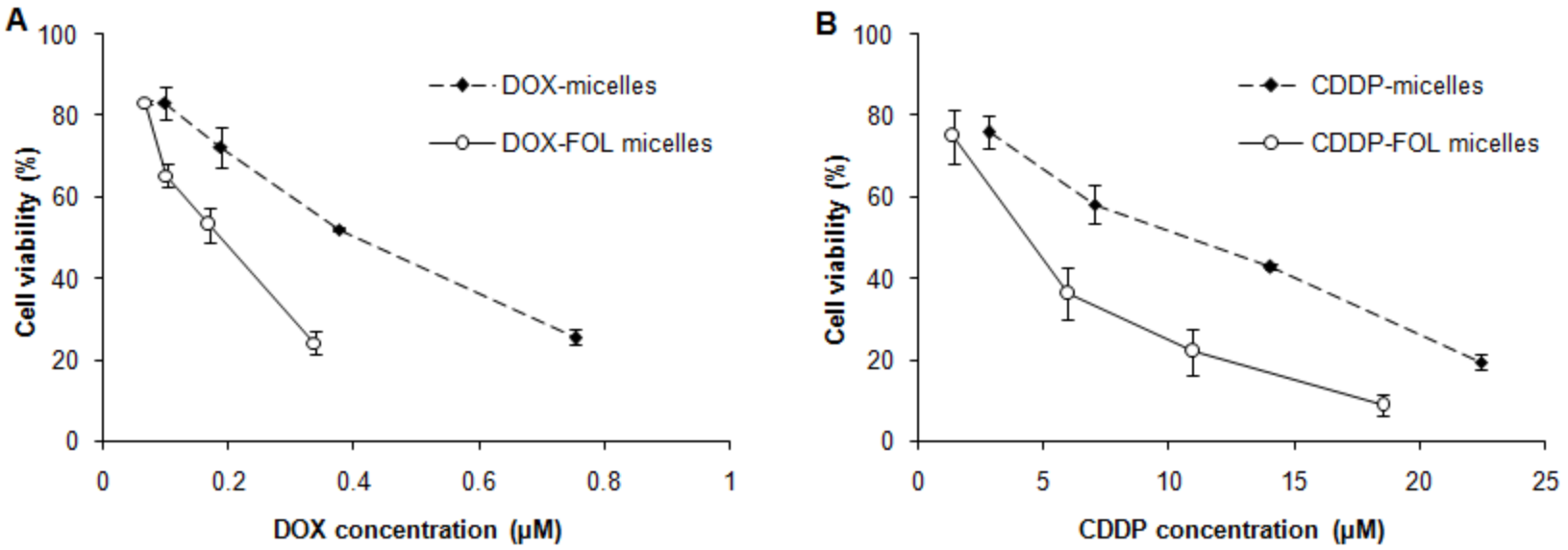

Figure 6.7 Effect of FOL modification on the treatment efficacy of CDDP and DOX loaded micelles to KB cells as investigated using (A) DOX- loaded micelles and (B) CDDP-loaded micelles.

The enhancement effect of FOL modification onto the treatment efficacy of drug-loaded micelles was investigated using single drug-loaded micelles of both anticancer drugs CDDP and DOX on KB cells. Figure 6.7 show that the FOL modified micelles (CDDP-FOL micelles and DOX- FOL micelles) exhibit lower degree of cancer cell viability than that of non-modified micelles (CDDP-micelles and DOX- micelles). Based on the IC_{50} values (Table 6.3), FOL-modified micelles show more than 2 times higher therapy efficacy than non-modified micelles. The high binding affinity of FOL with cancer cells can increase cellular uptake of FOL-modified into cancer cells (Figure 6.8) and results in higher cancer treatment efficacy. From the IC_{50} values, it can be seen that the enhancement in therapy efficacy of CDDP-FOL micelles versus free CDDP is approximate 2.6 times while that enhancement of DOX- FOL micelles versus free DOX is only approximate 1.7 times. It means that the FOL-micellar system is more effective for the treatment using free CDDP than that of free DOX. This observation is in agreement with the rapid development of CDDP resistance to cancer cells compared with other non-platinum based drugs as observed by previous studies [277].

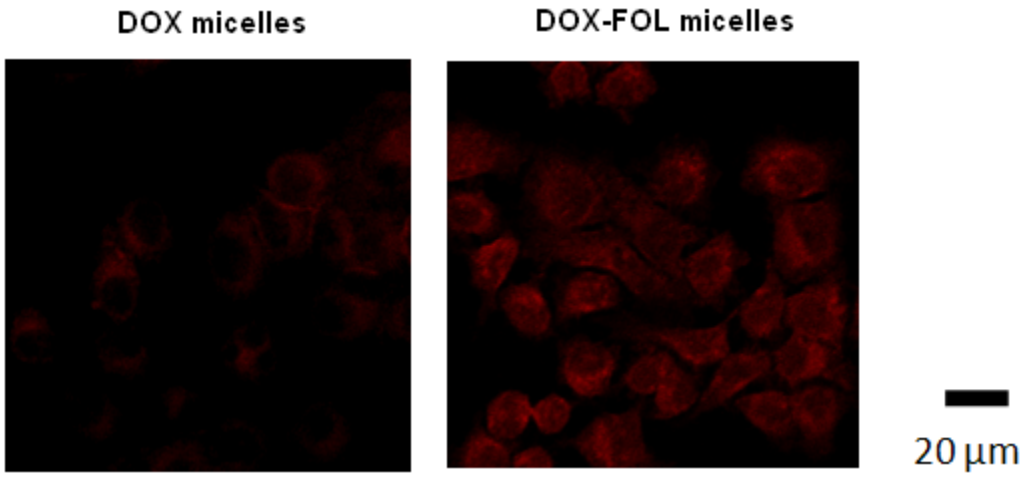

Figure 6.8 In vitro cellular uptake of DOX micelles and DOX-FOL micelles into KB cells.

6.3.6 Synergistic effect of the co-delivery of CDDP-loaded micelles and DOX- loaded micelles

Based on the preliminary study of free CDDP and free DOX combinations, the CDDP/DOX combinations at molar ratios from 20/1 to 40/1 show synergistic effect for the treatment doses that result in 5-95% cell viability. In addition, the FOL-modified micelles demonstrates higher cancer treatment efficacy than non-modified micelles as shown in Section 6.3.5. In this section, co-delivery of two single drug-loaded micelles was conducted using CDDP-FOL micelles & DOX-FOL micelles (Figure 6.2A) at the molar ratio of drugs in the two micellar systems of 20/1 (CDDP/DOX). This co-delivery system is noted as CDDP-FOL micelles & DOX-FOL micelles_20/1.

The higher cancer treatment efficacy of CDDP-FOL micelles & DOX-FOL micelles_20/1 compared to single-drug loaded micellar treatment is shown as the lower required treatment dose at the same treatment effect (Figure 6.9A and 6.9B). From Tables 6.3, the required dose to kill 50% KB cells (IC_{50}) of the CDDP-FOL micelles & DOX-FOL micelles_20/1 system is approximately 11 and 9.6 times lower than that of CDDP-micelles & DOX-micelles respectively. In quantitative comparison between the treatment efficacy of co-delivery system (CDDP-FOL micelles & DOX-FOL micelles_20/1) and single drug-loaded FOL micelles (CDDP-FOL micelles and DOX-FOL micelles), the CI values of the co-delivery system as the function of cell viability are presented in Figure 6.9C. Obviously, co-delivery of single drug-loaded micelle system is a synergistic treatment with all CI values < 1 for the wide range of treatment concentrations which is the same phenomenon as observed in the CDDP and DOX combination (Section 6.3.1).

This co-delivery of two single drug-loaded micellar system can potentially be a more flexible method to obtain the synergistic treatment compared with the delivery of dual drugs-loaded micelles (Figure 6.2B). Because the combined ratios in the co-delivery of two single drug-loaded micelle system can be easily varied for specific treatment.

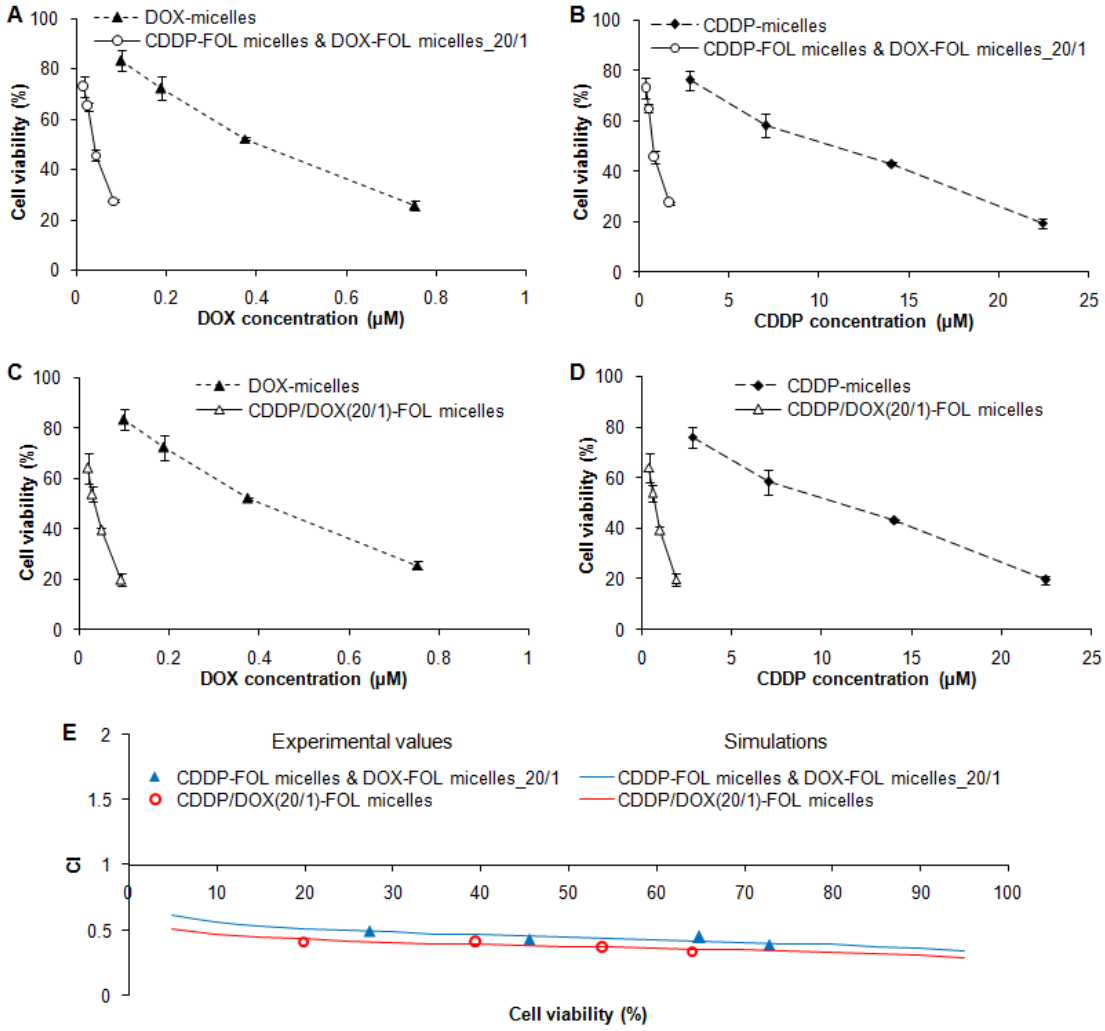

Figure 6.9 Cytotoxicity dose response of KB cells with various CDDP/DOX delivery strategies: (A-B) the co-delivery of two single drug-loaded FOL micelles (Figure 6.2A) at CDDP/DOX ratio of 20/1 compared to DOX- micelles and CDDP-micelles, respectively; and (CDDP-D) the dual drugs-encapsulated FOL micelles (Figure 6.2B) at the encapsulated CDDP/DOX ratio of 20/1 compared to DOX- micelles and CDDP-micelles respectively. Synergistic effects of the co-delivery of CDDP-FOL micelles & DOX- FOL micelles and the dual CDDP/DOX-FOL micelles treatment at the molar ratio of CDDP/DOX of 20/1 were presented as the CI values as the function of cell viability.

6.3.7 Synergistic effect of dual drugs-loaded micelles

CDDP-FOL micelles & DOX- FOL micelles_20/1 has been demonstrated as a synergistic co-delivery system for KB cell treatment. Therefore, a dual drugs-loaded FOL system at the molar ratio of CDDP/DOX of 20/1 has been fabricated to study its synergistic effect as well as to compare with the co-delivery system (CDDP-FOL micelles & DOX- FOL micelles_20/1). The dual drugs-loaded FOL system is presented as CDDP/DOX(20/1)-FOL micelles with the molar ratio of CDDP/DOX in a micelle of 20/1. As shown in Figure 6.9B, dual CDDP/DOX micelles with FOL modification show the higher cancer treatment efficiency than CDDP- or DOX- micelles. This phenomenon is similar to the co-delivery system as shown in Figure 6.9A. The IC_{50} values of CDDP-FOL micelles & DOX- FOL micelles_20/1 system and CDDP/DOX(20/1)-FOL micelle system are 0.768 μM (CDDP)/0.038 μM (DOX), 0.650 μM (CDDP)/0.032 μM (DOX) respectively as tabulated in Table 6.3. Based on the IC_{50} values and the CI values (Figure 6.9C) of the two systems, the dual drugs-loaded system seems slightly better than the co-delivery of two single drug-loaded system. This observation can be due to the faster release of DOX from the dual drugs-loaded system (Figure 6.6C) as well as the higher possibility of synergistic ratio of accumulated drugs in cancer cells using the dual drugs-loaded system.

Between the co-delivery system (CDDP-FOL micelles & DOX-FOL micelles_20/1, Figure 6.2A) and the dual system (CDDP/DOX_20/1-FOL micelles, Figure 6.2B), the dual system exhibits better delivery and treatment efficacy properties due to its higher ability in delivering the designed combination of therapeutic agents to the targeted tumors. Therefore, the dual system is more favorable for most cancer treatments.

However some special cases need special combined regimes, the co-delivery system may be applied as the combination ratio can be varied easily.

6.4 Conclusions

This study has demonstrated that the encapsulation of CDDP and DOX using PEG-PGA/FOL-PEG-PGA polymers as carrier materials provides polymer-drug complex micelles with high drug loading content of up to 26% (CDDP) and 48% (DOX) at sustained drug release. Combined synergistic CDDP/DOX treatments have been demonstrated using three methods: simultaneously delivery of free CDDP and free D, co-delivery of two single drug-loaded FOL micelles (CDDP-FOL micelles & DOX- FOL micelles_20/1) and dual drugs-loaded FOL micelles (CDDP/DOX(20/1)-FOL micelles. The combined treatments via FOL-micellar systems exhibit higher efficacy than free CDDP/DOX treatment due to the high binding affinity of the FOL to the cancer cells. The two combined methods via micellar systems (co-delivery and dual) show quite similar synergistic effect with slightly higher efficacy in the dual system. Although the co-delivery of two single drug-loaded FOL micelles and the dual drugs-loaded FOL micelles show slightly different *in vitro* studies, they contain their own advantage and limitation. For the co-delivery of two single drug-loaded micelles, the combination ratio could be easily varied for specific treatment with the limitation of maintaining the designed ratio *in vivo* treatment. The dual drugs-loaded micelles have higher possibility in maintaining the initial drug ratio for *in vivo* application which could overcome the limitation of the co-delivery of two single drug-loaded micelles. However, the variation

of drug ratios of the two drugs in the dual drugs-loaded micelles would require further optimization for specific applications.

CHAPTER 7. Conclusions and Recommendations

7.1 Conclusions

This thesis has been investigated the application of targeted nanotechnology for drug delivery in cancer therapy. Targeting micellar systems from biocompatible and biodegradable polymers have been designed to deliver different types of anticancer drugs in single-drug therapeutic or combined-drugs therapeutic methods. This thesis has three main duties: (i) synthesis of block copolymers as the materials for micellar formations, (ii) demonstration of surface modified polymeric micellar systems as the drug delivery carriers for the enhancement of targeting ability and cellular uptake, and (iii) demonstration of the synergistic therapeutic effect of combined chemotherapy based on two anticancer drugs via targeting micellar carriers.

This thesis has been studied different micellar systems for various drug delivery applications. Various micellar systems have been investigated to demonstrate the targeting delivery of (i) hydrophobic drugs based on hydrophobiCDDP-hydrophobic interaction, (ii) platinum-based drugs based on the polymer-metal complexation, and (iii) positive charged-drugs via the electrostatic interaction. In order to achieve the above aims, two block copolymer systems PLGA-PEG and PEG-PGA have been synthesized. PLGA-PEG polymer has been used to deliver hydrophobic drugs via the hydrophobic interaction between PLGA block and hydrophobic drugs. For delivering of platinum-based drugs or positive charged-drugs, PEG-PGA polymer has been applied due to the polymer-metal complexation between platinum-based drugs and carboxylic groups of

PGA block or electrostatic interaction between the negative charged carboxylic groups and positive charged-drugs. Moreover, the two polymer systems have been modified with FOL or TAT so that the resultant micelles exhibit cancer targeting ability and high cellular uptake. The results of this study show that the presence of FOL on the carrier surface can enhance the cellular uptake of the drug-loaded carriers into the cancer cells that leads to the higher cancer treatment efficacy. Besides FOL modification, this study also proves that the efficacy of the drug delivery systems can be further improve by multi-modifying the carrier surface with both FOL and TAT.

To utilize the synergistic effect of combined-anticancer drugs and the advanced targeting drug delivery systems that mentioned above, combined-anticancer drug treatments using surface modified micelles have been studied for delivering of two anticancer drugs in a micellar system (called as dual-drugs loaded micellar system) or in two separated micellar systems (called as co-delivery of two single drug-loaded micelle system). Three pairs of anticancer drugs including combination of two chemo-drugs DOX/PTX, combination of a chemo-drug and a hormone drug P/T, and combination of a platinum-based drug and a non-platinum-based drug CDDP/DOX have been studied for treatments of solid tumors, breast cancer, and solid tumors respectively. This study has demonstrated the enhancement of cancer treatment efficacy of the designed systems, which combine the advantages of micellar systems, targeting ability and uptake ability of ligands, and combined treatment of two different mechanism anticancer drugs, compared to the common delivery method using single drug delivery systems. This study also demonstrated and discussed the differences of the combined treatments between a dual-

drugs loaded micellar system and a co-delivery of two single drug-loaded micelle system. Due to the variation of cancer disease, the chemotherapeutic drugs are varied case by case based on the specific cancer and the patient respond. Therefore, the co-delivery system contributes its value to the cancer treatment due to its flexibility in turning the treatment combinations.

7.2 Recommendations

As proven in this work, the targeted dual drugs-loaded system shows promising data for cancer treatments. The targeting delivery of dual drugs-loaded technology may be further developed and move forward for clinical use. The author would like to make some recommendations for future studies.

Having developed the multi-modified carriers, the next phase of this study can investigate the structure of the polymers which will further increase the pharmacodynamics properties of these drug delivery systems. This should be achievable by tuning different parameters such as the purity, the ratio of hydrophilic/hydrophobic block, and the molecular weight of copolymers.

It is well known that the behavior of treatment systems may not always be similar between *in vitro* and *in vivo* studies. Therefore, *in vivo* studies should be carried out for further evaluations of this developed technology. First, tissue distribution of combination agents needs to be investigated to evaluate the efficiency of the co-delivery system and the dual system in delivery of combination drugs at designed regimes. Second, *in vivo*

antitumor efficacy should be study against various treatment technologies such as single drug-loaded system, co-delivery of two single-drug loaded system, dual drugs-loaded system. Body weight and mortality should also be monitored.

In this work, the micellar carriers have promisingly been demonstrated for simultaneously therapeutic drug delivery but they are only potential to co-encapsulate hydrophobic drug molecules or hydrophilic/hydrophobic drugs which exhibit special chemical interactions with polymers. As such, this property may limit some applications of micelles especially in the combined-drug treatments using drugs with different chemical/physical properties. Therefore, the author would recommend using polymersomes as carriers for delivery of anticancer drugs.

Polymersomes have recently been studied as new type of carriers for drug delivery because they act as stable polymer systems that can carry both hydrophilic and hydrophobic drugs. Polymersomes are composed of synthetic amphiphilic polymers and have similar vesicle structure to liposomes (Figure 7.1).

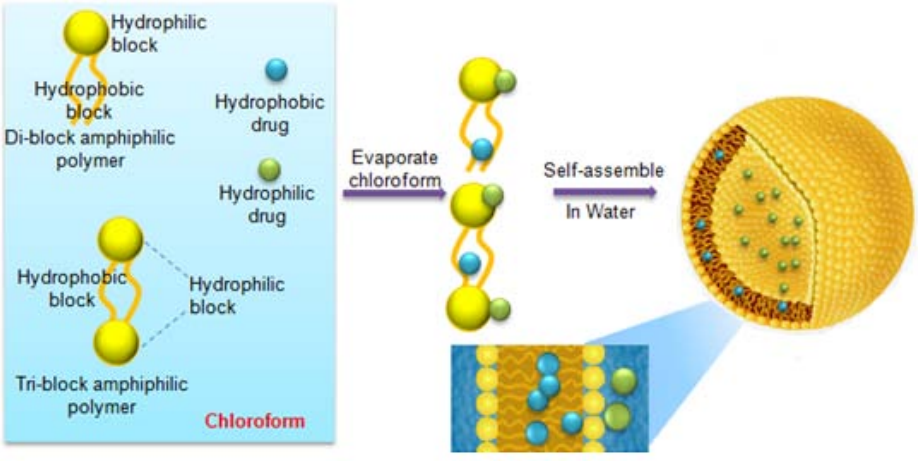

Figure 7.1 Schematic of preparation of drug-loaded polymersomes.

Compared to liposomes, polymersomes have been shown superior properties, including higher stability, larger storage capability, and sustained drug circulation time [296]. Moreover, the surface of polymersomes can be easily functionalized as block copolymer chemistries can be tailored via the synthesis processes. Besides, the above mentioned advantages of polymersomes, their drug loading capability in the shell can easily be tailored by varying the molecular weight (MW) of the hydrophobic block in the copolymer (Figure 7.2). Therefore, this new drug delivery technique has attached researchers recently [297-299].

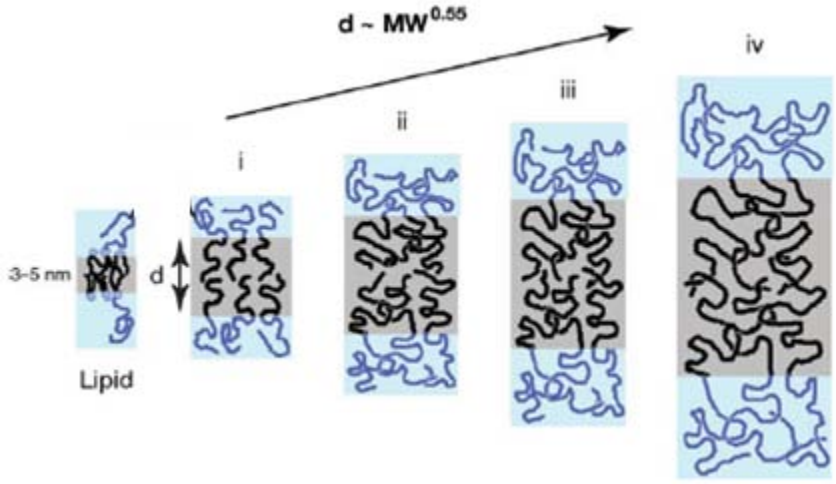

Figure 7.2 Schematic scaling of polymersome membrane thickness with copolymer molecular weight (MW) [300].

The vesicle morphologies of polymersomes are determined by the volume fraction of each block in copolymers. Generally, polymersomes are formed when the ratio of hydrophilic block to total polymer mass of approximately $\leq 35 \pm 10$ (%) as illustrated in Figure 7.3. Micelles or inverted microstructures are formed if that ratio is greater than 45% or less than 25% respectively.

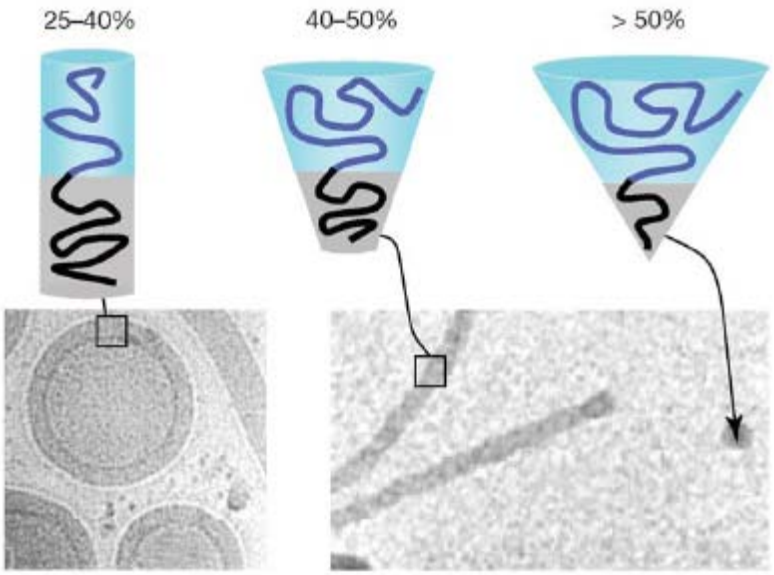

Figure 7.3 Schematics of self-assemble structures of block copolymer at various ratios of hydrophilic to total copolymer mass [300].

Polymersomes present as more advantage delivery systems when compared to micelles because they can simultaneously encapsulate hydrophobic drugs within their membrane and hydrophilic drugs in their aqueous interior. Despite of their superior properties, the development of polymersome drug delivery systems is still limited to *in vivo* study because of the difficulty in controlling their size, structure and surface modifications.

REFERENCES

[1] *World Cancer Report 2008*: International Agency for Reserch on Cancer, 2008.

[2] Arrowsmith, J., *From the analyst's couch: a decade of change* Nat Rev Drug Discov, 2012. 11: p. 17-18.

[3] Siegel, R., D. Naishadham, and A. Jemal, *Cancer statistics, 2012.* CA-Cancer J Clin, 2012. 62(1): p. 10-29.

[4] *Cancer survival in Singapore 1968-2007*: National Registry of Diseases Office, 2007.

[5] Lim, G.H., K.Y. Chow, and H.P. Lee, *Singapore cancer trends in the last decade.* Singap Med J, 2012. 53(1): p. 3-10.

[6] Jang, S.H., M.G. Wientjes, D. Lu , and J.L.S. Au, *Drug delivery and transport to solid tumors.* Pharm Res, 2003. 20: p. 1337-1350.

[7] Vasir, J.K. and V. Labhasetwar, *Targeted drug delivery in cancer therapy.* Technol Cancer Res T, 2005. 4: p. 363-374.

[8] Bourzac, K., *Nanotechnology carrying drugs.* Nature, 2012. 491: p. S58-S60.

[9] Bae, Y. and K. Kataoka, *Polymer assemblies: intelligent block copolymer micelles for the programmed delivery of drugs and genes, Polymeric Drug Delivery Systems*, G.S. Kwon, Editor 2005, Taylor & Francis. p. 652.

[10] Seymour, L., R. Duncan, J. Strohalm, and J. Kopecek, *Effect of molecular weight (Mw) of N-(2-hydroxypropyl)methacrylamide copolymers on body distribution and rate of excretion after subcutaneous, intraperitoneal, and intravenous adminustration to rats.* Drugs Pharmaceut Sci, 2005. 148: p. 1341-1358.

[11] Kirk, J., S.K. Syed, A.L. Harris, et al., *Reversal of P-glycoprotein-mediated multidrug resistance by pure anti- oestrogens and novel tamoxifen derivatives.* Biochem Pharmacol, 1994. 48(2): p. 277-285.

[12] Murphy, C.G. and A.D. Seidman, *Evolving approaches to metastatic breast cancer previously treated with anthracyclines and taxanes.* Clin Breast Cancer, 2009. 9, Supplement 2(0): p. S58-S65.

[13] Pinzani, V., F. Bressolle, I.J. Haug, et al., *Cisplatin-induced renal toxicity and toxicity-modulating strategies: a review.* Cancer Chemoth Pharm, 1994. 35(1): p. 1-9.

[14] Sahai, E., *Illuminating the metastatic process.* Nat Rev Cancer, 2007. 7(10): p. 737-749.

[15] Widakowich, C., E. de Azambuja, T. Gil, et al., *Molecular targeted therapies in breast cancer: Where are we now?* Int J Biochem Cell B, 2007. 39: p. 1375-1387.

[16] Lim, S., S. Lee, J. Han, et al., *Prolonged clinical benefit from the maintenance hormone therapy in patients with metastatic breast cancer.* Breast, 2013.

[17] Al-Mubarak, M., A.G. Sacher, A. Ocana, et al., *Fulvestrant for advanced breast cancer: a meta-analysis.* Cancer Treat Rev, 2013. 39(7): p. 753-758.

[18] Ijichi, N., T. Shigekawa, K. Ikeda, et al., *Association of positive EBAG9 immunoreactivity with unfavorable prognosis in breast cancer patients treated with tamoxifen.* Clin Breast Cancer, 2013.

[19] Vogel, V.G., *Raloxifene: A selective estrogen receptor modulator for reducing the risk of invasive breast cancer in postmenopausal women.* Womens Health, 2007. 3(2): p. 139-153.

[20] Bevers, T.B., *Raloxifene: An agent for breast cancer prevention.* Expert Rev Obstet Gynecol, 2008. 3(3): p. 277-285.

[21] Morad, S.A.F., J.C. Levin, S.F. Tan, et al., *Novel off-target effect of tamoxifen - Inhibition of acid ceramidase activity in cancer cells.* BBA - Mol Cell Biol L, 2013. 1831(12): p. 1657-1664.

[22] Kumar, R., V. Verma, A. Sarswat, et al., *Selective estrogen receptor modulators regulate stromal proliferation in human benign prostatic hyperplasia by multiple beneficial mechanisms - Action of two new agents.* Invest New Drug, 2012. 30(2): p. 582-593.

[23] Iijima, M., H. Uhara, Y. Ide, et al., *Estrogen-receptor-alpha-positive extramammary Paget's disease treated with hormonal therapy.* Dermatology, 2006. 213(2): p. 144-146.

[24] Prakash, S., M. Malhotra, W. Shao, C. Tomaro-Duchesneau, and S. Abbasi, *Polymeric nanohybrids and functionalized carbon nanotubes as drug delivery carriers for cancer therapy.* Adv Drug Deliv Rev, 2011. 63(14-15): p. 1340-1351.

[25] De Keulenaer, G.W., K. Doggen, and K. Lemmens, *The vulnerability of the heart as a pluricellular paracrine organ: Lessons from unexpected triggers of heart failure in targeted ErbB2 anticancer therapy.* Circ Res, 2010. 106(1): p. 35-46.

[26] Yao, X., K. Panichpisal, N. Kurtzman, and K. Nugent, *Cisplatin nephrotoxicity: a review.* Am J Med Sci, 2007. 334(2): p. 115-124.

[27] Rybak, L.P., *Mechanisms of cisplatin ototoxicity and progress in otoprotection.* Curr Opin Otolaryngo, 2007. 15(5): p. 364-369.

[28] Lukenbill, J. and M. Kalaycio, *Fludarabine: a review of the clear benefits and potential harms.* Leukemia Res, 2013. 37(9): p. 986-994.

[29] Pavlidis, E.T. and T.E. Pavlidis, *Role of bevacizumab in colorectal cancer growth and its adverse effects: A review.* World J Gastroentero, 2013. 19(31): p. 5051-5060.

[30] Rosenberg, B., L. Van Camp, and T. Krigas, *Inhibition of cell division in Escherichia coli by electrolysis products from a platinum electrode [17].* Nature, 1965. 205(4972): p. 698-699.

[31] Lammers, T., F. Kiessling, W.E. Hennink, and G. Storm, *Drug targeting to tumors: principles, pitfalls and (pre-) clinical progress.* J Control Release, 2012. 161(2): p. 175-187.

[32] Hu, C.M.J. and L. Zhang, *Nanoparticle-based combination therapy toward overcoming drug resistance in cancer.* Biochem Pharmacol, 2012. 83(8): p. 1104-1111.

[33] Kataoka, K., A. Harada, and Y. Nagasaki, *Block copolymer micelles for drug delivery: design, characterization and biological significance.* Adv Drug Deliv Rev, 2012. 64(SUPPL.): p. 37-48.

[34] Danhier, F., E. Ansorena, J.M. Silva, et al., *PLGA-based nanoparticles: An overview of biomedical applications.* J Control Release, 2012. 161(2): p. 505-522.

[35] Shapira, A., Y.D. Livney, H.J. Broxterman, and Y.G. Assaraf, *Nanomedicine for targeted cancer therapy: Towards the overcoming of drug resistance.* Drug Resist Updat, 2011. 14(3): p. 150-163.

[36] Yokoyama, M., S. Inoue, K. Kataoka, et al., *Molecular design for missile drug: Synthesis of adriamycin conjugated with immunoglobulin G using poly(ethylene glycol)-block-poly(aspartic acid) as intermediate carrier.* Makromol Chem, 1989. 190: p. 2041-2054.

[37] Duncan, R., M.J. Vicent, F. Greco, and R.I. Nicholson, *Polymer-drug conjugates: Towards a novel approach for the treatment of endrocine-related cancer.* Endocr-Relat Cancer, 2005. 12(SUPPL. 1): p. S189-S199.

[38] Ferrari, M., *Cancer nanotechnology: Opportunities and challenges.* Nat Rev Cancer, 2005. 5(3): p. 161-171.

[39] Tang, L. and J. Cheng, *Nonporous silica nanoparticles for nanomedicine application.* Nano Today, 2013. 8(3): p. 290-312.

[40] Brannon-Peppas, L. and J.O. Blanchette, *Nanoparticle and targeted systems for cancer therapy.* Adv Drug Deliv Rev, 2004. 56(11): p. 1649-1659.

[41] Matsumura, Y. and H. Maeda, *A new concept for macromolecular therapeutics in cancer chemotherapy: Mechanism of tumoritropic accumulation of proteins and the antitumor agent smancs.* Cancer Res, 1986. 46(12 I): p. 6387-6392.

[42] Peer, D., J.M. Karp, S. Hong, et al., *Nanocarriers as an emerging platform for cancer therapy.* Nat Nanotechnol, 2007. 2(12): p. 751-760.

[43] Maeda, H., *The enhanced permeability and retention (EPR) effect in tumor vasculature: the key role of tumor-selective macromolecular drug targeting.* Adv Enzyme Regul, 2001. 41(1): p. 189-207.

[44] Maeda, H., J. Wu, T. Sawa, Y. Matsumura, and K. Hori, *Tumor vascular permeability and the EPR effect in macromolecular therapeutics: a review.* J Control Release, 2000. 65(1–2): p. 271-284.

[45] Torchilin, V.P., *Passive and active drug targeting: Drug delivery to tumors as an example, Drug Deliv* 2010. p. 3-53.

[46] Harris, L., G. Batist, R. Belt, et al., *Liposome-encapsulated doxorubicin compared with conventional doxorubicin in a randomized multicenter trial as first-line therapy of metastatic breast carcinoma.* Cancer, 2002. 94(1): p. 25-36.

[47] Marty, M., *Liposomal doxorubicin (Myocet™) and conventional anthracyclines: a comparison.* Breast, 2001. 10(SUPPL. 2): p. 28-33.

[48] Forssen, E.A., *The design and development of DaunoXome® for solid tumor targeting in vivo.* Adv Drug Deliv Rev, 1997. 24(2-3): p. 133-150.

[49] Phuphanich, S., B. Maria, R. Braeckman, and M. Chamberlain, *A pharmacokinetic study of intra-CSF administered encapsulated cytarabine (DepoCyt®) for the treatment of neoplastic meningitis in patients with leukemia, lymphoma,or solid tumors as part of a phase III study.* J Neuro-Oncol, 2007. 81(2): p. 201-208.

[50] Gordon, A.N., J.T. Fleagle, D. Guthrie, et al., *Recurrent epithelial ovarian carcinoma: A randomized phase III study of pegylated liposomal doxorubicin versus topotecan.* J Clin Oncol, 2001. 19(14): p. 3312-3322.

[51] Muggia, F. and A. Hamilton, *Phase III data on Caelyx® in ovarian cancer.* Eur J Cancer, 2001. 37(SUPPL. 9): p. S15-S18.

[52] Matsumura, Y., M. Gotoh, K. Muro, et al., *Phase I and pharmacokinetic study of MCC-465, a doxorubicin (DXR) encapsulated in PEG immunoliposome, in patients with metastatic stomach cancer.* Ann Oncol, 2004. 15(3): p. 517-525.

[53] Infante, J.R., V.L. Keedy, S.F. Jones, et al., *Phase I and pharmacokinetic study of IHL-305 (PEGylated liposomal irinotecan) in patients with advanced solid tumors.* Cancer Chemoth Pharm, 2012. 70(5): p. 699-705.

[54] Mylonopouloua, E., C.D. Arvanitisa, M. Bazan-Peregrinoa, M. Arora, and C.C. Coussios. *Ultrasonic activation of thermally sensitive liposomes*. 2010. Aix-en-Provence.

[55] May, J.P. and S.D. Li, *Thermosensitive liposomes in cancer therapy.* Recent Pat Biomed Eng, 2012. 5(2): p. 148-158.

[56] Saul, J.M., A. Annapragada, J.V. Natarajan, and R.V. Bellamkonda, *Controlled targeting of liposomal doxorubicin via the folate receptor in vitro.* J Control Release, 2003. 92(1-2): p. 49-67.

[57] Mamasheva, E., C. O'Donnell, A. Bandekar, and S. Sofou, *Heterogeneous liposome membranes with pH-triggered permeability enhance the in vitro antitumor activity of folate-receptor targeted liposomal doxorubicin.* Mol Pharm, 2011. 8(6): p. 2224-2232.

[58] Kawano, K. and Y. Maitani, *Effects of polyethylene glycol spacer length and ligand density on folate receptor targeting of liposomal doxorubicin in vitro.* J Drug Deliv, 2011. 2011.

[59] Gao, W., B. Xiang, T.T. Meng, F. Liu, and X.R. Qi, *Chemotherapeutic drug delivery to cancer cells using a combination of folate targeting and tumor microenvironment-sensitive polypeptides.* Biomaterials, 2013. 34(16): p. 4137-4149.

[60] Saad, M., O.B. Garbuzenko, E. Ber, et al., *Receptor targeted polymers, dendrimers, liposomes: Which nanocarrier is the most efficient for tumor-specific treatment and imaging?* J Control Release, 2008. 130(2): p. 107-114.

[61] Molavi, O., X.B. Xiong, D. Douglas, et al., *Anti-CD30 antibody conjugated liposomal doxorubicin with significantly improved therapeutic efficacy against anaplastic large cell lymphoma.* Biomaterials, 2013. 34(34): p. 8718-8725.

[62] Zhang, Q., J. Tang, L. Fu, et al., *A pH-responsive α-helical cell penetrating peptide-mediated liposomal delivery system.* Biomaterials, 2013. 34(32): p. 7980-7993.

[63] Shahin, M., R. Soudy, H. El-Sikhry, et al., *Engineered peptides for the development of actively tumor targeted liposomal carriers of doxorubicin.* Cancer Lett, 2013. 334(2): p. 284-292.

[64] Gregoriadis, G. and B.E. Ryman, *Liposomes as carriers of enzymes or drugs: a new approach to the treatment of storage diseases.* Biochem J, 1971. 124(5).

[65] Klibanov, A.L., K. Maruyama, V.P. Torchilin, and L. Huang, *Amphipathic polyethyleneglycols effectively prolong the circulation time of liposomes.* FEBS Letters, 1990. 268(1): p. 235-237.

[66] Allen, T.M., C. Hansen, F. Martin, C. Redemann, and A. Yau-Young, *Liposomes containing synthetic lipid derivatives of poly(ethylene glycol) show prolonged circulation half-lives in vivo.* Biochim Biophys Acta 1991. 1066(1): p. 29-36.

[67] Blume, G. and G. Cevc, *Liposomes for the sustained drug release in vivo.* Biochim Biophys Acta, 1990. 1029(1): p. 91-97.

[68] Allen, T.M. and P.R. Cullis, *Liposomal drug delivery systems: from concept to clinical applications.* Adv Drug Deliv Rev, 2013. 65(1): p. 36-48.

[69] O'Hare, K.B., R. Duncan, J. Strohalm, K. Ulbrich, and P. Kopeckova, *Polymeric drug-carriers containing doxorubicin and melanocyte-stimulating hormone: In vitro and in vivo evaluation against murine melanoma.* J Drug Target, 1993. 1(3): p. 217-229.

[70] Duncan, R., *The dawning era of polymer therapeutics.* Nat Rev Drug Discov, 2003. 2(5): p. 347-360.

[71] Hoes, C.J.T., W. Potman, W. van Heeswijk, et al., *Optimization of macromolecular prodrugs of the antitumor antibiotic adriamycin.* J Control Release, 1985. 2: p. 205-213.

[72] Duncan, R., P. Kopeckova-Rejmanova, J. Strohalm, et al., *Anticancer agents coupled to N-(2-hydroxypropyl)methacrylamide copolymers* Br J Cancer, 1987. 55: p. 165-174.

[73] Zunino, F., G. Pratesi, and A. Micheloni, *Poly(carboxylic acid) polymers as carriers for anthracyclines.* J Control Release, 1989. 10: p. 65-73.

[74] Singer, J.W., R. Bhatt, J. Tulinsky, et al., *Water-soluble poly-(L-glutamic acid)-Gly-camptothecin conjugates enhance camptothecin stability and efficacy in vivo.* J Control Release, 2001. 74(1-3): p. 243-247.

[75] Homsi, J., G.R. Simon, C.R. Garrett, et al., *Phase I trial of poly-L-glutamate camptothecin (CT-2106) administered weekly in patients with advanced solid malignancies.* Clin Cancer Res, 2007. 13(19): p. 5855-5861.

[76] Singer, J.W., R. Bhatt, J. Tulinsky, et al., *Water-soluble poly-(l-glutamic acid)–Gly-camptothecin conjugates enhance camptothecin stability and efficacy in vivo.* J Control Release, 2001. 74(1–3): p. 243-247.

[77] Langer, C.J., *CT-2103: a novel macromolecular taxane with potential advantages compared with conventional taxanes.* Clin Lung Cancer, 2004. 6(SUPPL. 2): p. S85-S88.

[78] Langer, C.J., *CT-2103: emerging utility and therapy for solid tumours.* Expert Opin Inv Drug, 2004. 13(11): p. 1501-1508.

[79] Mita, M., A. Mita, J. Sarantopoulos, et al., *Phase i study of paclitaxel poliglumex administered weekly for patients with advanced solid malignancies.* Cancer Chemoth Pharm, 2009. 64(2): p. 287-295.

[80] Dinndorf, P.A., J. Gootenberg, M.H. Cohen, P. Keegan, and R. Pazdur, *FDA drug approval summary: pegaspargase (Oncaspar®) for the first-line treatment of children with acute lymphoblastic leukemia (ALL).* Oncologist, 2007. 12(8): p. 991-998.

[81] Van Der Schoot, S.C., B. Nuijen, P. Sood, et al., *Pharmaceutical development, quality control, stability and compatibility of a parenteral lyophilized formulation*

of the investigational polymer-conjugated platinum antineoplastic agent AP5346. Pharmazie, 2006. 61(10): p. 835-844.

[82] Campone, M., J.M. Rademaker-Lakhai, J. Bennouna, et al., *Phase I and pharmacokinetic trial of AP5346, a DACH-platinum-polymer conjugate, administered weekly for three out of every 4 weeks to advanced solid tumor patients.* Cancer Chemoth Pharm, 2007. 60(4): p. 523-533.

[83] Nowotnik, D.P. and E. Cvitkovic, *ProLindac™ (AP5346): A review of the development of an HPMA DACH platinum Polymer Therapeutic.* Adv Drug Deliv Rev, 2009. 61(13): p. 1214-1219.

[84] Nowotnik, D.P., *AP5346 (ProLindac™), a dach platinum polymer conjugate in Phase II trials against ovarian cancer.* Curr Bioact Compd, 2011. 7(1): p. 21-26.

[85] Seymour, L.W., D.R. Ferry, D.J. Kerr, et al., *Phase II studies of polymer-doxorubicin (PK1, FCE28068) in the treatment of breast, lung and colorectal cancer.* Int J Oncol, 2009. 34(6): p. 1629-1636.

[86] Davis, M.E., Z. Chen, and D.M. Shin, *Nanoparticle therapeutics: An emerging treatment modality for cancer.* Nat Rev Drug Discov, 2008. 7(9): p. 771-782.

[87] Zhang, Z., S. Huey Lee, and S.S. Feng, *Folate-decorated poly(lactide-co-glycolide)-vitamin E TPGS nanoparticles for targeted drug delivery.* Biomaterials, 2007. 28(10): p. 1889-1899.

[88] Cheng, J., B.A. Teply, I. Sherifi, et al., *Formulation of functionalized PLGA–PEG nanoparticles for in vivo targeted drug delivery.* Biomaterials, 2007. 28(5): p. 869-876.

[89] Jeevitha, D. and K. Amarnath, *Chitosan/PLA nanoparticles as a novel carrier for the delivery of anthraquinone: Synthesis, characterization and in vitro cytotoxicity evaluation.* Colloid Surface B, 2013. 101: p. 126-134.

[90] Miele, E., G.P. Spinelli, F. Tomao, and S. Tomao, *Albumin-bound formulation of paclitaxel (Abraxane® ABI-007) in the treatment of breast cancer.* Int J Nanomed, 2009. 4(1): p. 99-105.

[91] Jin, C., L. Bai, H. Wu, F. Tian, and G. Guo, *Radiosensitization of paclitaxel, etanidazole and paclitaxel+etanidazole nanoparticles on hypoxic human tumor cells in vitro.* Biomaterials, 2007. 28(25): p. 3724-3730.

[92] Dong, Y. and S.S. Feng, *Poly(d,l-lactide-co-glycolide) (PLGA) nanoparticles prepared by high pressure homogenization for paclitaxel chemotherapy.* Int J Pharm, 2007. 342(1-2): p. 208-214.

[93] Svenson, S., M. Wolfgang, J. Hwang, J. Ryan, and S. Eliasof, *Preclinical to clinical development of the novel camptothecin nanopharmaceutical CRLX101.* J Control Release, 2011. 153(1): p. 49-55.

[94] Young, C., T. Schluep, J. Hwang, and S. Eliasof, *CRLX101 (formerly IT-101)-A novel nanopharmaceutical of camptothecin in clinical development.* Curr Bioact Compd, 2011. 7(1): p. 8-14.

[95] Gaur, S., L. Chen, T. Yen, et al., *Preclinical study of the cyclodextrin-polymer conjugate of camptothecin CRLX101 for the treatment of gastric cancer.* Nanomed-Nanotechnol, 2012. 8(5): p. 721-730.

[96] Wang, H., Y. Zhao, Y. Wu, et al., *Enhanced anti-tumor efficacy by co-delivery of doxorubicin and paclitaxel with amphiphilic methoxy PEG-PLGA copolymer nanoparticles.* Biomaterials, 2011. 32(32): p. 8281-8290.

[97] Wang, H., Y. Wu, R. Zhao, and G. Nie, *Engineering the assemblies of biomaterial nanocarriers for delivery of multiple theranostic agents with enhanced antitumor efficacy.* Adv Mater, 2013. 25(11): p. 1616-1622.

[98] Pan, J. and S.S. Feng, *Targeted delivery of paclitaxel using folate-decorated poly(lactide)-vitamin E TPGS nanoparticles.* Biomaterials, 2008. 29(17): p. 2663-2672.

[99] Sun, B., B. Ranganathan, and S.S. Feng, *Multifunctional poly(d,l-lactide-co-glycolide)/montmorillonite (PLGA/MMT) nanoparticles decorated by Trastuzumab for targeted chemotherapy of breast cancer.* Biomaterials, 2008. 29(4): p. 475-486.

[100] Liu, C., F. Liu, L. Feng, et al., *The targeted co-delivery of DNA and doxorubicin to tumor cells via multifunctional PEI-PEG based nanoparticles.* Biomaterials, 2013. 34(10): p. 2547-2564.

[101] Kim, E., Y. Jung, H. Choi, et al., *Prostate cancer cell death produced by the co-delivery of Bcl-xL shRNA and doxorubicin using an aptamer-conjugated polyplex.* Biomaterials, 2010. 31(16): p. 4592-4599.

[102] Hu, Q., X. Gao, T. Kang, et al., *CGKRK-modified nanoparticles for dual-targeting drug delivery to tumor cells and angiogenic blood vessels.* Biomaterials, 2013. 34(37): p. 9496-9508.

[103] Swaminathan, S.K., E. Roger, U. Toti, et al., *CD133-targeted paclitaxel delivery inhibits local tumor recurrence in a mouse model of breast cancer.* J Control Release, 2013.

[104] Sant, S., S. Poulin, and P. Hildgen, *Effect of polymer architecture on surface properties, plasma protein adsorption, and cellular interactions of pegylated nanoparticles.* J Biomed Mater Res, 2008. 87A(4): p. 885-895.

[105] Nishiyama, N., S. Okazaki, H. Cabral, et al., *Novel Cisplatin-Incorporated Polymeric Micelles Can Eradicate Solid Tumors in Mice.* Cancer Res, 2003. 63(24): p. 8977-8983.

[106] Uchino, H., Y. Matsumura, T. Negishi, et al., *Cisplatin-incorporating polymeric micelles (NC-6004) can reduce nephrotoxicity and neurotoxicity of cisplatin in rats.* Br J Cancer, 2005. 93(6): p. 678-687.

[107] Rafi, M., H. Cabral, M.R. Kano, et al., *Polymeric micelles incorporating (1,2-diaminocyclohexane)platinum (II) suppress the growth of orthotopic scirrhous gastric tumors and their lymph node metastasis.* J Control Release, 2012. 159(2): p. 189-196.

[108] Cabral, H., N. Nishiyama, and K. Kataoka, *Optimization of (1,2-diamino-cyclohexane)platinum(II)-loaded polymeric micelles directed to improved tumor targeting and enhanced antitumor activity.* J Control Release, 2007. 121: p. 146-155.

[109] Akao, T., T. Kimura, Y.S. Hirofuji, et al., *A poly(γ-glutamic acid)amphiphile complex as a novel nanovehicle for drug delivery system.* J Drug Target, 2010. 18(7): p. 550-556.

[110] Yoo, H.S. and T.G. Park, *Biodegradable polymeric micelles composed of doxorubicin conjugated PLGA-PEG block copolymer.* J Control Release, 2001. 70(1-2): p. 63-70.

[111] Kim, T.Y., D.W. Kim, J.Y. Chung, et al., *Phase I and pharmacokinetic study of Genexol-PM, a Cremophor-free, polymeric micelle-formulated paclitaxel, in patients with advanced malignancies* Clin Cancer Res, 2004. 10(11): p. 3708-3716.

[112] Lee, K.S., H.C. Chung, S.A. Im, et al., *Multicenter phase II trial of Genexol-PM, a Cremophor-free, polymeric micelle formulation of paclitaxel, in patients with metastatic breast cancer.* Breast Cancer Res Tr, 2008. 108(2): p. 241-250.

[113] Shin, H.-C., A.W.G. Alani, D.A. Rao, N.C. Rockich, and G.S. Kwon, *Multi-drug loaded polymeric micelles for simultaneous delivery of poorly soluble anticancer drugs.* J Control Release, 2009. 140(3): p. 294-300.

[114] Plummer, R., R.H. Wilson, H. Calvert, et al., *A Phase i clinical study of cisplatin-incorporated polymeric micelles (NC-6004) in patients with solid tumours.* Br J Cancer, 2011. 104(4): p. 593-598.

[115] Hamaguchi, T., T. Doi, T. Eguchi-Nakajima, et al., *Phase I study of NK012, a novel SN-38-incorporating micellar nanoparticle, in adult patients with solid tumors.* Clin Cancer Res, 2010. 16(20): p. 5058-5066.

[116] Koizumi, F., M. Kitagawa, T. Negishi, et al., *Novel SN-38-incorporating polymeric micelles, NK012, eradicate vascular endothelial growth factor-secreting bulky tumors.* Cancer Res, 2006. 66(20): p. 10048-10056.

[117] Matsumura, Y., T. Hamaguchi, T. Ura, et al., *Phase I clinical trial and pharmacokinetic evaluation of NK911, a micelle-encapsulated doxorubicin* Br J Cancer, 2004. 91: p. 1775-1781.

[118] Nishiyama, N. and K. Kataoka, *Preparation and characterization of size-controlled polymeric micelle containing cis-dichlorodiammineplatinum(II) in the core.* J Control Release, 2001. 74: p. 83-94.

[119] Gao, X., B. Wang, X. Wei, et al., *Preparation, characterization and application of star-shaped PCL/PEG micelles for the delivery of doxorubicin in the treatment of colon cancer.* Int J Nanomed, 2013. 8: p. 971-982.

[120] Cho, H., T.C. Lai, and G.S. Kwon, *Poly(ethylene glycol)-block-poly(ε-caprolactone) micelles for combination drug delivery: Evaluation of paclitaxel, cyclopamine and gossypol in intraperitoneal xenograft models of ovarian cancer.* J Control Release, 2013. 166(1): p. 1-9.

[121] Hamaguchi, T., Y. Matsumura, M. Suzuki, et al., *NK105, a paclitaxel-incorporating micellar nanoparticle formulation, can extend in vivo antitumour activity and reduce the neurotoxicity of paclitaxel.* Br J Cancer, 2005. 92(7): p. 1240-1246.

[122] Hamaguchi, T., K. Kato, H. Yasui, et al., *A phase I and pharmacokinetic study of NK105, a paclitaxel-incorporating micellar nanoparticle formulation.* Br J Cancer, 2007. 97(2): p. 170-176.

[123] Negishi, T., F. Koizumi, H. Uchino, et al., *NK105, a paclitaxel-incorporating micellar nanoparticle, is a more potent radiosensitising agent compared to free paclitaxel.* Br J Cancer, 2006. 95(5): p. 601-606.

[124] Lee, A.L.Z., Y. Wang, H.Y. Cheng, S. Pervaiz, and Y.Y. Yang, *The co-delivery of paclitaxel and herceptin using cationic micellar nanoparticles.* Biomaterials, 2009. 30(5): p. 919-927.

[125] Alakhov, V., E. Klinski, S. Li, et al., *Block copolymer-based formulation of doxorubicin. From cell screen to clinical trials.* Colloid Surface B, 1999. 16(1-4): p. 113-134.

[126] Valle, J.W., A. Armstrong, C. Newman, et al., *A phase 2 study of SP1049C, doxorubicin in P-glycoprotein-targeting pluronics, in patients with advanced adenocarcinoma of the esophagus and gastroesophageal junction.* Invest New Drug, 2011. 29(5): p. 1029-1037.

[127] Ebrahim Attia, A.B., C. Yang, J.P.K. Tan, et al., *The effect of kinetic stability on biodistribution and anti-tumor efficacy of drug-loaded biodegradable polymeric micelles.* Biomaterials, 2013. 34(12): p. 3132-3140.

[128] Danquah, M., T. Fujiwara, and R.I. Mahato, *Self-assembling methoxypoly(ethylene glycol)-b-poly(carbonate-co-l-lactide) block copolymers for drug delivery.* Biomaterials, 2010. 31(8): p. 2358-2370.

[129] Yu, H., Z. Xu, D. Wang, et al., *Intracellular pH-activated PEG-b-PDPA wormlike micelles for hydrophobic drug delivery.* Polym Chem, 2013. 4(19): p. 5052-5055.

[130] Wang, H., F. Xu, Y. Wang, et al., *pH-responsive and biodegradable polymeric micelles based on poly([small beta]-amino ester)-graft-phosphorylcholine for doxorubicin delivery.* Polym Chem, 2013. 4(10): p. 3012-3019.

[131] Huang, H., Y. Li, C. Li, et al., *A novel anti-VEGF targeting and MRI-visible smart drug delivery system for specific diagnosis and therapy of liver cancer.* Macromol Biosci, 2013. 13(10): p. 1358-1368.

[132] Zhao, H. and L.Y.L. Yung, *Selectivity of folate conjugated polymer micelles against different tumor cells.* Int J Pharm, 2008. 349(1–2): p. 256-268.

[133] Zhao, H., H.H.P. Duong, and L.Y.L. Yung, *Folate-conjugated polymer micelles with pH-triggered drug release properties.* Macromol Rapid Commun, 2010. 31(13): p. 1163-1169.

[134] Qiu, L.-Y., L. Yan, L. Zhang, Y.-M. Jin, and Q.-H. Zhao, *Folate-modified poly(2-ethyl-2-oxazoline) as hydrophilic corona in polymeric micelles for enhanced intracellular doxorubicin delivery.* Int J Pharm, 2013. 456(2): p. 315-324.

[135] Hrkach, J., D.V. Hoff, M.M. Ali, et al., *Preclinical development and clinical translation of a PSMA-targeted docetaxel nanoparticle with a differentiated pharmacological profile* Sci Transl Med, 2012. 4(128ra39): p. 1-11.

[136] Xu, W., I.A. Siddiqui, M. Nihal, et al., *Aptamer-conjugated and doxorubicin-loaded unimolecular micelles for targeted therapy of prostate cancer.* Biomaterials, 2013. 34(21): p. 5244-5253.

[137] Sawant, R.R. and V.P. Torchilin, *Enhanced cytotoxicity of TATp-bearing paclitaxel-loaded micelles in vitro and in vivo.* Int J Pharm, 2009. 374(1–2): p. 114-118.

[138] Liu, L., K. Guo, J. Lu, et al., *Biologically active core/shell nanoparticles self-assembled from cholesterol-terminated PEG-TAT for drug delivery across the blood-brain barrier.* Biomaterials, 2008. 29(10): p. 1509-1517.

[139] Liu, L., S.S. Venkatraman, Y.Y. Yang, et al., *Polymeric micelles anchored with TAT for delivery of antibiotics across the blood-brain barrier.* Biopolymers Pept Sci 2008. 90(5): p. 617-623.

[140] Li, X., M. Wang, C. Liu, X. Jing, and Y. Huang, *TAT-modified mixed micelles as biodegradable targeting and delivering system for cancer therapeutics.* J Appl Polym Sci, 2013. 130(6): p. 4598-4607.

[141] Sethuraman, V.A., M.C. Lee, and Y.H. Bae, *A biodegradable pH-sensitive micelle system for targeting acidic solid tumors.* Pharm Res, 2008. 25(3): p. 657-666.

[142] Mu, L., T.A. Elbayoumi, and V.P. Torchilin, *Mixed micelles made of poly(ethylene glycol)-phosphatidylethanolamine conjugate and D-a-tocopheryl polyethylene glycol 1000 succinate* Int J Pharm, 2005. 306: p. 142-149.

[143] Jain, R.K., L.L. Munn, and D. Fukumura, *Dissecting tumour pathophysiology using intravital microscopy.* Nat Rev Cancer, 2002. 2: p. 266-276.

[144] Calderara F, H.Z., Hurtrez G, Lerch J-P, Nugay T, Riess G, *Investigation of olystryrene-poly(ethylene oxide) block copolymer micelles formation in organic and aqueous solutions by nonradiadiative energy transfer experiments.* Marcromolecules, 1994. 27: p. 1210-1215.

[145] Wang Y, K.C.-M., Chun M, Quirk R-P, Mattice WL, *Exchange of chains between micelles of labeled polystyrene-block-poly(oxyethylene) as monitored by nonradiatice singlet enery transfer.* Marcromolecules, 1995. 28: p. 904-911.

[146] Steven D. Weitman, R.H.L., Leslie R. Coney, Daniel W. Fort, Verna Frasca, Vincent R. Zurawski, Jr., and Barton A. Kamen *Distribution of the Folate Receptor GP38 in Normal and Malignant Cell Lines and Tissues* Cancer Research, 1992. 52(12).

[147] M. Jules Mattes, P.P.M., David M. Goldenberg, Arnold S. Dion, Robert V. P. Hutter, and Kenneth M. Klein *Patterns of Antigen Distribution in Human Carcinomas* Cancer Research, 1990. 50: p. 880S-884S.

[148] Steven D. Weitman, A.G.W., Leslie R. Coney, Vincent R. Zurawski, Debra S. Jennings, and Barton A. Kamen *Cellular Localization of the Folate Receptor: Potential Role in Drug Toxicity and Folate Homeostasis* Cancer Research, 1992. 52(23): p. 6708-6711.

[149] Leamon, C.P. and P.S. Low, *Receptor-mediated drug delivery, Drug Delivery Principles and Application*, B. Wang, T. Siahaan, and R.A. Soltero, Editors. 2005, Wiley-Interscience. p. 448.

[150] Borsi, L., E. Balza, M. Bestagno, et al., *Selective targeting of tumoral vasculature: Comparison of different formats of an antibody (l19) to the ED-B domain of fibronectin.* Int J Cancer, 2002. 102(1): p. 75-85.

[151] Neri, D. and R. Bicknell, *Tumour vascular targeting.* Nat Rev Cancer, 2005. 5(6): p. 436-446.

[152] Temming, K., R.M. Schiffelers, G. Molema, and R.J. Kok, *RGD-based strategies for selective delivery of therapeutics and imaging agents to the tumour vasculature.* Drug Resist Updat, 2005. 8(6): p. 381-402.

[153] Mitra, A., J. Mulholland, A. Nan, et al., *Targeting tumor angiogenic vasculature using polymer-RGD conjugates.* J Control Release, 2005. 102(1): p. 191-201.

[154] Arap, W., R. Pasqualini, and E. Ruoslahti, *Cancer treatment by targeted drug delivery to tumor vasculature in a mouse model.* Science, 1998. 279(5349): p. 377-380.

[155] Green, M. and P.M. Loewenstein, *Autonomous functional domains of chemically synthesized human immunodeficiency virus tat trans-activator protein.* Cell, 1988. 55(6): p. 1179-1188.

[156] Frankel, A.D. and C.O. Pabo, *Cellular uptake of the tat protein from human immunodeficiency virus.* Cell, 1988. 55(6): p. 1189-1193.

[157] Grunwald, J., T. Rejtar, R. Sawant, Z. Wang, and V.P. Torchilin, *TAT peptide and its conjugates: proteolytic stability.* Bioconjugate Chem, 2009. 20(8): p. 1531-1537.

[158] Levchenko, T.S., R. Rammohan, N. Volodina, and V.P. Torchilin, *Tat Peptide-Mediated Intracellular Delivery of Liposomes*, 2003. p. 339-349.

[159] Rao, K.S., M.K. Reddy, J.L. Horning, and V. Labhasetwar, *TAT-conjugated nanoparticles for the CNS delivery of anti-HIV drugs.* Biomaterials, 2008. 29(33): p. 4429-4438.

[160] Qin, Y., H. Chen, Q. Zhang, et al., *Liposome formulated with TAT-modified cholesterol for improving brain delivery and therapeutic efficacy on brain glioma in animals.* Int J Pharm, 2011. 420(2): p. 304-312.

[161] Niu, R., P. Zhao, H. Wang, et al., *Preparation, characterization, and antitumor activity of paclitaxel-loaded folic acid modified and TAT peptide conjugated PEGylated polymeric liposomes.* J Drug Target, 2011. 19(5): p. 373-381.

[162] Ignatovich, I.A., E.B. Dizhe, A.V. Pavlotskaya, et al., *Complexes of plasmid DNA with basic domain 47-57 of the HIV-1 Tat protein are transferred to mammalian cells by endocytosis-mediated pathways.* J Biol Chem, 2003. 278(43): p. 42625-42636.

[163] Zhao, P., H. Wang, M. Yu, et al., *Paclitaxel-loaded, folic-acid-targeted and TAT-peptide-conjugated polymeric liposomes: In vitro and in vivo evaluation.* Pharm Res, 2010. 27(9): p. 1914-1926.

[164] Koren, E., A. Apte, A. Jani, and V.P. Torchilin, *Multifunctional PEGylated 2C5-immunoliposomes containing pH-sensitive bonds and TAT peptide for enhanced tumor cell internalization and cytotoxicity.* J Control Release, 2012. 160(2): p. 264-273.

[165] Wang, H., W. Su, S. Wang, et al., *Smart multifunctional core-shell nanospheres with drug and gene co-loaded for enhancing the therapeutic effect in a rat intracranial tumor model.* Nanoscale, 2012. 4(20): p. 6501-6508.

[166] Tanaka, K., T. Kanazawa, Y. Shibata, et al., *Development of cell-penetrating peptide-modified MPEG-PCL diblock copolymeric nanoparticles for systemic gene delivery.* Int J Pharm, 2010. 396(1–2): p. 229-238.

[167] Sun, Q., J. Xiong, J. Lu, et al., *Secretory TAT-peptide-mediated protein transduction of LIF receptor α-chain distal cytoplasmic motifs into human myeloid HL-60 cells.* Braz J Med Biol Res, 2012. 45(10): p. 913-920.

[168] Malhotra, M., C. Tomaro-Duchesneau, and S. Prakash, *Synthesis of TAT peptide-tagged PEGylated chitosan nanoparticles for siRNA delivery targeting neurodegenerative diseases.* Biomaterials, 2013. 34(4): p. 1270-1280.

[169] Moschos, S.A., S.W. Jones, M.M. Perry, et al., *Lung delivery studies using siRNA conjugated to TAT(48-60) and penetratin reveal peptide induced reduction in gene expression and induction of innate immunity.* Bioconjugate Chem, 2007. 18(5): p. 1450-1459.

[170] Futaki, S., T. Suzuki, W. Ohashi, et al., *Arginine-rich peptides. An abundant source of membrane-permeable peptides having potential as carriers for intracellular protein delivery.* J Biol Chem, 2001. 276(8): p. 5836-5840.

[171] Snyder, E.L. and S.F. Dowdy, *Recent advances in the use of protein transduction domains for the delivery of peptides, proteins and nucleic acids in vivo.* Expert Opin Drug Deliv, 2005. 2(1): p. 43-51.

[172] Schwarze, S.R., A. Ho, A. Vocero-Akbani, and S.F. Dowdy, *In vivo protein transduction: delivery of a biologically active protein into the mouse.* Science, 1999. 285(5433): p. 1569-1572.

[173] Sethuraman, V.A. and Y.H. Bae, *TAT peptide-based micelle system for potential active targeting of anti-cancer agents to acidic solid tumors.* J Control Release, 2007. 118(2): p. 216-224.

[174] Liu, L., J. Yang, J. Xie, et al., *The potent antimicrobial properties of cell penetrating peptide-conjugated silver nanoparticles with excellent selectivity for Gram-positive bacteria over erythrocytes.* Nanoscale, 2013. 5(9): p. 3834-3840.

[175] Zhang, K., H. Fang, Z. Chen, J.S.A. Taylor, and K.L. Wooley, *Shape effects of nanoparticles conjugated with cell-penetrating peptides (HIV Tat PTD) on CHO cell uptake.* Bioconjugate Chem, 2008. 19(9): p. 1880-1887.

[176] Joliot, A. and A. Prochiantz, *Transduction peptides: from technology to physiology.* Nat Cell Biol, 2004. 6(3): p. 189-196.

[177] Pooga, M., C. Kut, M. Kihlmark, et al., *Cellular translocation of proteins by transportan.* FASEB J, 2001. 15(8): p. 1451-1453.

[178] Morris, M.C., S. Deshayes, F. Heitz, and G. Divita, *Cell-penetrating peptides: from molecular mechanisms to therapeutics.* Biol Cell, 2008. 100(4): p. 201-217.

[179] Gros, E., S. Deshayes, M.C. Morris, et al., *A non-covalent peptide-based strategy for protein and peptide nucleic acid transduction.* Biochim Biophys Acta 2006. 1758(3): p. 384-393.

[180] Kenien, R., J.L. Zaro, and W.C. Shen, *MAP-mediated nuclear delivery of a cargo protein.* J Drug Target, 2012. 20(4): p. 329-337.

[181] Pujals, S., J. Fernández-Carneado, C. López-Iglesias, M.J. Kogan, and E. Giralt, *Mechanistic aspects of CPP-mediated intracellular drug delivery: Relevance of CPP self-assembly.* Biochim Biophys Acta, 2006. 1758(3): p. 264-279.

[182] Rousselle, C., M. Smirnova, P. Clair, et al., *Enhanced delivery of doxorubicin into the brain via a peptide-vector-mediated strategy: Saturation kinetics and specificity.* J Pharmacol Exp Ther, 2001. 296(1): p. 124-131.

[183] Veldhoen, S., S.D. Laufer, A. Trampe, and T. Restle, *Cellular delivery of small interfering RNA by a non-covalently attached cell-penetrating peptide: Quantitative analysis of uptake and biological effect.* Nucleic Acids Res, 2006. 34(22): p. 6561-6573.

[184] Moghimi, S.M., P. Symonds, J.C. Murray, et al., *A two-stage poly(ethylenimine)-mediated cytotoxicity: Implications for gene transfer/therapy.* Mol Ther, 2005. 11(6): p. 990-995.

[185] Nasrollahi, S.A., C. Taghibiglou, E. Azizi, and E.S. Farboud, *Cell-penetrating peptides as a novel transdermal drug delivery system.* Chem Biol Drug Des, 2012. 80(5): p. 639-646.

[186] Rothbard, J.B., S. Garlington, Q. Lin, et al., *Conjugation of arginine oligomers to cyclosporin A facilitates topical delivery and inhibition of inflammation.* Nat Med, 2000. 6(11): p. 1253-1257.

[187] Lindgren, M., K. Rosenthal-Aizman, K. Saar, et al., *Overcoming methotrexate resistance in breast cancer tumour cells by the use of a new cell-penetrating peptide.* Biochem Pharmacol, 2006. 71(4): p. 416-425.

[188] Liang, J.F. and V.C. Yang, *Synthesis of doxorubicin-peptide conjugate with multidrug resistant tumor cell killing activity.* Bioorg Med Chem Lett, 2005. 15(22): p. 5071-5075.

[189] Mazel, M., P. Clair, C. Rousselle, et al., *Doxorubicin-peptide conjugates overcome multidrug resistance.* Anti-Cancer Drugs, 2001. 12(2): p. 107-116.

[190] Fritzer, M., T. Szekeres, V. Szüts, H.N. Jarayam, and H. Goldenberg, *Cytotoxic effects of a doxorubicin-transferrin conjugate in multidrug-resistant KB cells.* Biochem Pharmacol, 1996. 51(4): p. 489-493.

[191] Fawell, S., J. Seery, Y. Daikh, et al., *Tat-mediated delivery of heterologous proteins into cells.* Proc Natl Acad Sci U S A, 1994. 91(2): p. 664-668.

[192] Aarts, M., Y. Liu, L. Liu, et al., *Treatment of ischemic brain damage by perturbing NMDA receptor-PSD-95 protein interactions.* Science, 2002. 298(5594): p. 846-850.

[193] Rapoport, M. and H. Lorberboum-Galski, *TAT-based drug delivery system - New directions in protein delivery for new hopes?* Expert Opin Drug Deliv, 2009. 6(5): p. 453-463.

[194] Wadia, J.S., R.V. Stan, and S.F. Dowdy, *Transducible TAT-HA fusogenic peptide enhances escape of TAT-fusion proteins after lipid raft macropinocytosis.* Nat Med, 2004. 10(3): p. 310-315.

[195] Morris, M.C., J. Depollier, J. Mery, F. Heitz, and G. Divita, *A peptide carrier for the delivery of biologically active proteins into mammalian cells.* Nat Biotechnol, 2001. 19(12): p. 1173-1176.

[196] Wolf, Y., S. Pritz, S. Abes, et al., *Structural requirements for cellular uptake and antisense activity of peptide nucleic acids conjugated with various peptides.* Biochemistry, 2006. 45(50): p. 14944-14954.

[197] Nakase, I., G. Tanaka, and S. Futaki, *Cell-penetrating peptides (CPPs) as a vector for the delivery of siRNAs into cells.* Mol BioSyst, 2013. 9(5): p. 855-861.

[198] Nakase, I., H. Akita, K. Kogure, et al., *Efficient intracellular delivery of nucleic acid pharmaceuticals using cell-penetrating peptides.* Acc Chem Res, 2012. 45(7): p. 1132-1139.

[199] Tang, J., L. Zhang, Y. Liu, et al., *Synergistic targeted delivery of payload into tumor cells by dual-ligand liposomes co-modified with cholesterol anchored transferrin and TAT.* Int J Pharm, 2013. 454(1): p. 31-40.

[200] Sharma, G., A. Modgil, B. Layek, et al., *Cell penetrating peptide tethered bi-ligand liposomes for delivery to brain in vivo: Biodistribution and transfection.* J Control Release, 2013. 167(1): p. 1-10.

[201] Zhao, B.X., Y. Zhao, Y. Huang, et al., *The efficiency of tumor-specific pH-responsive peptide-modified polymeric micelles containing paclitaxel.* Biomaterials, 2012. 33(8): p. 2508-2520.

[202] Duong, H.H.P. and L.Y.L. Yung, *Synergistic co-delivery of doxorubicin and paclitaxel using multi-functional micelles for cancer treatment.* Int J Pharm, 2013. 454(1): p. 486-495.

[203] Torchilin, V.P., *Cell penetrating peptide-modified pharmaceutical nanocarriers for intracellular drug and gene delivery.* Biopolymers, 2008. 90(5): p. 604-610.

[204] Chen, J., S. Li, and Q. Shen, *Folic acid and cell-penetrating peptide conjugated PLGA-PEG bifunctional nanoparticles for vincristine sulfate delivery.* Eur J Pharm Sci, 2012. 47(2): p. 430-443.

[205] Berry, C.C., *Intracellular delivery of nanoparticles via the HIV-1 tat peptide.* Nanomedicine, 2008. 3(3): p. 357-365.

[206] Heitz, F., M.C. Morris, and G. Divita, *Twenty years of cell-penetrating peptides: from molecular mechanisms to therapeutics.* Br J Pharmacol, 2009. 157(2): p. 195-206.

[207] Vives, E., *Cellular utake of the Tat peptide: an endocytosis mechanism following ionic interactions.* J Mol Recog, 2003. 16(5): p. 265-271.

[208] Brooks, H., B. Lebleu, and E. Vivès, *Tat peptide-mediated cellular delivery: back to basics.* Adv Drug Deliv Rev, 2005. 57(4 SPEC.ISS.): p. 559-577.

[209] Kaplan, I.M., J.S. Wadia, and S.F. Dowdy, *Cationic TAT peptide transduction domain enters cells by macropinocytosis.* J Control Release, 2005. 102(1): p. 247-253.

[210] Chung, S.K., K.K. Maiti, and W.S. Lee, *Recent advances in cell-penetrating, non-peptide molecular carriers.* Int J Pharm, 2008. 354(1-2): p. 16-22.

[211] Tünnemann, G., R.M. Martin, S. Haupt, et al., *Cargo-dependent mode of uptake and bioavailability of TAT-containing proteins and peptides in living cells.* FASEB J, 2006. 20(11): p. 1775-1784.

[212] Nabholtz, J.-M.A. and A. Riva, *The choice of adjuvant combination therapies with taxanes: rationale and issues addressed in ongoing studies.* Clin Breast Cancer, 2001. 2, Supplement 1(0): p. S7-S14.

[213] Piccart-Gebhart, M., i.T. Burzykowsk, M. Buyse, et al., *Taxanes alone or in combination with anthracyclines as first-line therapy of patients with metastatic breast cancer.* J Clin Oncol, 2008. 26: p. 1980-6.

[214] Ganta, S. and M. Amiji, *Coadministration of paclitaxel and curcumin in nanoemulsion formulations to overcome multidrug resistance in tumor cells.* Mol Pharm, 2009. 6: p. 928-39.

[215] Lambert, L., N. Qiao, K. Hunt, et al., *Autophagy: a novel mechanism of synergistic cytotoxicity between doxorubicin and roscovitine in a sarcoma model.* Cancer Res, 2008. 68: p. 7966-74.

[216] Carrick, S., S. Parker, C.E. Thornton, et al., *Single agent versus combination chemotherapy for metastatic breast cancer.* Cochrane DB Syst Rev, 2009(2).

[217] Qi, W.X., L.n. Tang, A.n. He, Z. Shen, and Y. Yao, *Comparison between doublet agents versus single agent in metastatic breast cancer patients previously treated with an anthracycline and a taxane: A meta-analysis of four phase III trials.* Breast, 2012.

[218] Piccart-Gebhart, M., T. Burzykowski, M. Buyse, et al., *Taxanes alone or in combination with anthracyclines as first-line therapy of patients with metastatic breast cancer.* J Clin Oncol, 2008. 26: p. 1980-6.

[219] Webb, M.S., S. Johnstone, T.J. Morris, et al., *In vitro and in vivo characterization of a combination chemotherapy formulation consisting of vinorelbine and phosphatidylserine.* Eur J Pharm Biopharm, 2007. 65(3): p. 289-299.

[220] Tardi, P., T. Harasym, M. Webb, et al., *Compositions for delivery of drug combinations*, Celator Pharmaceuticals, Inc. 2003.

[221] *Cell cycle p21, depression, and neurogenesis and in the hippocampus*. 2010; Available from: http://scientopia.org.

[222] Mosmann, T., *Rapid colorimetric assay for cellular growth and survival: Application to proliferation and cytotoxicity assays.* J Immunol Methods, 1983. 65(1-2): p. 55-63.

[223] Bhuyan, B.K., B.E. Loughman, T.J. Fraser, and K.J. Day, *Comparison of different methods of determining cell viability after exposure to cytotoxic compounds.* Exp Cell Res, 1976. 97(2): p. 275-280.

[224] Mitchell, D., K. Santone, and D. Acosta, *Evaluation of cytotoxicity in cultured cells by enzyme leakage.* J Tissue Cult Meth, 1980. 6(3-4): p. 113-116.

[225] Nieminen, A.L., G.J. Gores, J.M. Bond, et al., *A novel cytotoxicity screening assay using a multiwell fluorescence scanner.* Toxicol Appl Pharmacol, 1992. 115(2): p. 147-155.

[226] Puck, T.T., P.I. Marcus, and S.J. Cieciura, *Clonal growth of mammalian cells in vitro; growth characteristics of colonies from single HeLa cells with and without a feeder layer.* J Exp Med, 1956. 103(2): p. 273-283.

[227] Johnson, L.V., M.L. Walsh, and L.B. Chen, *Localization of mitochondria in living cells with rhodamine 123.* Proc Natl Acad Sci U S A, 1980. 77(2 II): p. 990-994.

[228] Stoddart, M.J., *Cell viability assays: introduction.* Methods Mol Bio, 2011. 740: p. 1-6.

[229] Mayer, L.D. and A.S. Janoff, *Optimizing combination chemotherapy by controlling drug ratios.* Mol Interventions, 2007. 7(4): p. 216-223.

[230] Loewe, S., *The problem of synergism and antagonism of combined drugs.* Arzneim-Forsch, 1953. 3(6): p. 285-290.

[231] Tallarida, R.J., *Drug synergism: Its detection and applications.* J Pharmacol Exp Ther, 2001. 298(3): p. 865-872.

[232] Chou, T.-C. and P. Talalay, *Quantitative analysis of dose-effect relationships: the combined effects of multiple drugs or enzyme inhibitors.* Adv Enzyme Regul, 1984. 22(0): p. 27-55.

[233] Chou, T.-C. and P. Talalay, *Analysis of combined drug effects: a new look at a very old problem.* Trends Pharmacol Sci, 1983. 4(0): p. 450-454.

[234] Yokoyama, M., *Polymeric micelles as a new drug carrier system and their required considerations for clinical trials.* Expert Opin Drug Deliv, 2010. 7(2): p. 145-158.

[235] Bader, H., H. Ringsdorf, and B. Schmidt, *Watersoluble polymers in medicine.* Macromol. Mater. Eng., 1984.

[236] Yokoyama, M., T. Okano, Y. Sakurai, et al., *Selective delivery of adiramycin to a solid tumor using a polymeric micelle carrier system.* J. Drug. Target., 1999. 7(3): p. 171-186.

[237] Kwon, G., S. Suwa, M. Yokoyama, et al., *Enhanced tumor accumulation and prolonged circulation times of micelle-forming poly(ethylene oxide-aspartate) block copolymer-adriamycin conjugates.* J. Control. Release, 1994. 29(1-2): p. 17-23.

[238] Guo, X.D., F. Tandiono, N. Wiradharma, et al., *Cationic micelles self-assembled from cholesterol-conjugated oligopeptides as an efficient gene delivery vector.* Biomaterials, 2008. 29(36): p. 4838-4846.

[239] Matsumura, Y. and K. Kataoka, *Preclinical and clinical studies of anticancer agent-incorporating polymer micelles.* Cancer Sci, 2009. 100(4): p. 572-579.

[240] Matsumura, Y., *Polymeric micellar delivery systems in oncology.* Jpn J Clin Oncol, 2008. 38(12): p. 793-802.

[241] Matsumura, Y., *Poly (amino acid) micelle nanocarriers in preclinical and clinical studies.* Adv Drug Deliv Rev, 2008. 60(8): p. 899-914.

[242] Kim, D.W., S.Y. Kim, H.K. Kim, et al., *Multicenter phase II trial of Genexol-PM, a novel Cremophor-free, polymeric micelle formulation of paclitaxel, with cisplatin in patients with advanced non-small-cell lung cancer.* Ann Oncol, 2007. 18(12): p. 2009-2014.

[243] Xiong, X.B., A. Mahmud, H. Uludag, and A. Lavasanifar, *Multifunctional polymeric micelles for enhanced intracellular delivery of doxorubicin to metastatic cancer cells.* Pharm Res, 2008. 25(11): p. 2555-2566.

[244] Vives, E., J. Schmidt, and A. Pelegrin, *Cell-penetrating and cell-targeting peptides in drug delivery.* BBA- Rev Cancer, 2008. 1786(2): p. 126-138.

[245] Hansen, M., K. Kilk, and Ã. Langel, *Predicting cell-penetrating peptides.* Adv Drug Deliv Rev, 2008. 60(4-5): p. 572-579.

[246] Cao, G., W. Pei, H. Ge, et al., *In vivo delivery of a Bcl-xL fusion protein containing the TAT protein transduction domain protects against ischemic brain injury and neuronal apoptosis.* J Neurosci, 2002. 22(13): p. 5423-5431.

[247] Stewart, K.M., K.L. Horton, and S.O. Kelley, *Cell-penetrating peptides as delivery vehicles for biology and medicine.* Org Biomol Chem, 2008. 6(13): p. 2242-2255.

[248] Astriab-Fisher, A., D. Sergueev, M. Fisher, B. Ramsay Shaw, and R.L. Juliano, *Conjugates of antisense oligonucleotides with the Tat and antennapedia cell-*

penetrating peptides: effects on cellular uptake, binding to target sequences, and biologic actions. Pharm Res, 2002. 19(6): p. 744-754.

[249] Nori, A., K.D. Jensen, M. Tijerina, P. Kopeckova, and J. Kopecek, *Tat-conjugated synthetic macromolecules facilitate cytoplasmic drug delivery to human ovarian carcinoma cells.* Bioconjugate Chem, 2003. 14(1): p. 44-50.

[250] Torchilin, V.P., R. Rammohan, V. Weissig, and T.S. Levchenko, *TAT peptide on the surface of liposomes affords their efficient intracellular delivery even at low temperature and in the presence of metabolic inhibitors.* P Natl Acad Sci USA, 2001. 98(15): p. 8786-8791.

[251] Sugita, T., T. Yoshikawa, Y. Mukai, et al., *Comparative study on transduction and toxicity of protein transduction domains.* Br J Pharmacol, 2008. 153(6): p. 1143-1152.

[252] Toro, A., M. Paiva, C. Ackerley, and E. Grunebaum, *Intracellular delivery of purine nucleoside phosphorylase (PNP) fused to protein transduction domain corrects PNP deficiency in vitro.* Cell Immunol, 2006. 240(2): p. 107-115.

[253] Lu, Y., E. Sega, C.P. Leamon, and P.S. Low, *Folate receptor-targeted immunotherapy of cancer: Mechanism and therapeutic potential.* Adv Drug Deliv Rev, 2004. 56(8): p. 1161-1176.

[254] Leamon, C.P. and J.A. Reddy, *Folate-targeted chemotherapy.* Adv Drug Deliv Rev, 2004. 56(8): p. 1127-1141.

[255] Jhaveri, M.S., A.S. Rait, K.N. Chung, J.B. Trepel, and E.H. Chang, *Antisense oligonucleotides targeted to the human α folate receptor inhibit breast cancer cell growth and sensitize the cells to doxorubicin treatment.* Mol Cancer Ther, 2004. 3(12): p. 1505-1512.

[256] Lee, R.J. and P.S. Low, *Folate-mediated tumor cell targeting of liposome-entrapped doxorubicin in vitro.* BBA - Biomembranes, 1995. 1233(2): p. 134-144.

[257] Zhao, H. and L.Y.L. Yung, *Selectivity of folate conjugated polymer micelles against different tumor cells.* Int J Pharm, 2008. 349(1-2): p. 256-268.

[258] Kim, S.H., J.H. Jeong, C.O. Joe, and T.G. Park, *Folate receptor mediated intracellular protein delivery using PLL-PEG-FOL conjugate.* J Control Release, 2005. 103(3): p. 625-634.

[259] Park, E.K., S.Y. Kim, S.B. Lee, and Y.M. Lee, *Folate-conjugated methoxy poly(ethylene glycol)/poly(e-caprolactone) amphiphilic block copolymeric micelles for tumor-targeted drug delivery.* J Control Release, 2005. 109(1-3): p. 158-168.

[260] Yoo, H.S. and T.G. Park, *Folate receptor targeted biodegradable polymeric doxorubicin micelles.* J Control Release, 2004. 96(2): p. 273-283.

[261] Wolszczak, M. and J. Miller, *Characterization of non-ionic surfactant aggregates by fluorometric techniques.* J Photoch Photobio A 2002. 147(1): p. 45-54.

[262] Zhao, H.Z., E.C. Tan, and L.Y.L. Yung, *Potential use of cholecalciferol polyethylene glycol succinate as a novel pharmaceutical additive.* J Biomed Mater Res A, 2008. 84: p. 954-64.

[263] Lee, E.S., K. Na, and Y.H. Bae, *Doxorubicin loaded pH-sensitive polymeric micelles for reversal of resistant MCF-7 tumor.* J Control Release, 2005. 103(2): p. 405-418.

[264] Ziegler, A., P. Nervi, M. Durrenberger, and J. Seelig, *The cationic cell-penetrating peptide CPPTAT derived from the HIV-1 protein TAT is rapidly transported into living fibroblasts: Optical, biophysical, and metabolic evidence.* Biochemistry, 2005. 44(1): p. 138-148.

[265] Leane, M.M., R. Nankervis, A. Smith, and L. Illum, *Use of the ninhydrin assay to measure the release of chitosan from oral solid dosage forms.* Int J Pharm, 2004. 271(1–2): p. 241-249.

[266] Beletsi, A., L. Leontiadis, P. Klepetsanis, D.S. Ithakissios, and K. Avgoustakis, *Effect of preparative variables on the properties of poly(dl-lactide-co-glycolide)–methoxypoly(ethyleneglycol) copolymers related to their application in controlled drug delivery.* Int. J. Pharm., 1999. 182(2): p. 187-197.

[267] Silhol, M., M. Tyagi, M. Giacca, B. Lebleu, and E. Vives, *Different mechanisms for cellular internalization of the HIV-1 Tat-derived cell penetrating peptide and recombinant proteins fused to Tat.* Eur J Biochem, 2002. 269(2): p. 494-501.

[268] Hobbs, S.K., W.L. Monsky, F. Yuan, et al., *Regulation of transport pathways in tumor vessels: Role of tumor type and microenvironment.* P. Natl. Acad. Sci. USA, 1998. 95(8): p. 4607-4612.

[269] Carrstensen, H., R.H. Müller, and B.W. Müller, *Particle size, surface hydrophobicity and interaction with serum of parenteral fat emulsions and model drug carriers as parameters related to RES uptake.* Clinical. Nutrition., 1992. 11(5): p. 289-297.

[270] Liu, S.-Q., N. Wiradharma, S.-J. Gao, Y.W. Tong, and Y.-Y. Yang, *Bio-functional micelles self-assembled from a folate-conjugated block copolymer for targeted intracellular delivery of anticancer drugs.* Biomaterials, 2007. 28(7): p. 1423-1433.

[271] Sethuraman, V.A., M.C. Lee, and Y.H. Bae, *A biodegradable pH-sensitive micelles system for targeting acidic solid tumors.* Pharm Res, 2008. 25: p. 657-66.

[272] Reynolds, C.P. and B.J. Maurer, *Evaluating response to antineoplastic drug combinations in tissue culture models.* Methods Mol Med, 2005. 110: p. 173-183.

[273] Hobbs, S.K., W.L. Monsky, F. Yuan, et al., *Regulation of transport pathways in tumor vessels: Role of tumor type and microenvironment.* P Natl Acad Sci USA, 1998. 95(8): p. 4607-4612.

[274] Carrstensen, H., R.H. Müller, and B.W. Müller, *Particle size, surface hydrophobicity and interaction with serum of parenteral fat emulsions and model drug carriers as parameters related to RES uptake.* Clin Nutr, 1992. 11(5): p. 289-297.

[275] Liu, Y., K. Li, J. Pan, B. Liu, and S.S. Feng, *Folic acid conjugated nanoparticles of mixed lipid monolayer shell and biodegradable polymer core for targeted delivery of Docetaxel.* Biomaterials, 2010. 31(2): p. 330-338.

[276] Siddik, Z.H., D.R. Newell, F.E. Boxall, and K.R. Harrap, *The comparative pharmacokinetics of carboplatin and cisplatin in mice and rats.* Biochem Pharmacol, 1987. 36(12): p. 1925-1932.

[277] Giaccone, G., *Clinical perspectives on platinum resistance.* Drugs, 2000. 59(SUPPL. 4): p. 9-17.

[278] Tate Thigpen, J., M.F. Brady, H.D. Homesley, et al., *Phase III trial of doxorubicin with or without cisplatin in advanced endometrial carcinoma: A gynecologic oncology group study.* J Clin Oncol, 2004. 22(19): p. 3902-3908.

[279] Fleming, G.F., V.L. Brunetto, D. Cella, et al., *Phase III trial of doxorubicin plus cisplatin with or without paclitaxel plus filgrastim in advanced endometrial carcinoma: A gynecologic oncology group study.* J Clin Oncol, 2004. 22(11): p. 2159-2166.

[280] Long Iii, H.J., R.A. Nelimark, K.C. Podratz, et al., *Phase III comparison of methotrexate, vinblastine, doxorubicin, and cisplatin (MVAC) vs. doxorubicin and cisplatin (AC) in women with advanced primary or recurrent metastatic carcinoma of the uterine endometrium.* Gynecol Oncol, 2006. 100(3): p. 501-505.

[281] Homesley, H.D., V. Filiaci, S.K. Gibbons, et al., *A randomized phase III trial in advanced endometrial carcinoma of surgery and volume directed radiation followed by cisplatin and doxorubicin with or without paclitaxel: A Gynecologic Oncology Group study.* Gynecol Oncol, 2009. 112(3): p. 543-552.

[282] Yokoyama, M., T. Okano, Y. Sakurai, S. Suwa, and K. Kataoka, *Introduction of cisplatin into polymeric micelle.* J Control Release, 1996. 39(2-3): p. 351-356.

[283] Avgoustakis, K., A. Beletsi, Z. Panagi, et al., *PLGA-mPEG nanoparticles of cisplatin: In vitro nanoparticle degradation, in vitro drug release and in vivo drug residence in blood properties.* J Control Release, 2002. 79(1-3): p. 123-135.

[284] Dhar, S., F.X. Gu, R. Langer, O.C. Farokhza, and S.J. Lippard, *Targeted delivery of cisplatin to prostate cancer cells by aptamer functionalized Pt(IV) prodrug-PLGA - PEG nanoparticles.* Proc Nat Acad Sci USA, 2008. 105(45): p. 17356-17361.

[285] Mattheolabakis, G., E. Taoufik, S. Haralambous, M.L. Roberts, and K. Avgoustakis, *In vivo investigation of tolerance and antitumor activity of cisplatin-loaded PLGA-mPEG nanoparticles.* Eur J Pharm Biopharm, 2009. 71(2): p. 190-195.

[286] Margaritis, A. and B. Manocha, *Controlled release of doxorubicin from doxorubicin/γ-polyglutamic acid ionic complex.* J Nanomater, 2010. 2010.

[287] Tacar, O., P. Sriamornsak, and C.R. Dass, *Doxorubicin: an update on anticancer molecular action, toxicity and novel drug delivery systems.* J Pharm Pharmacol, 2013. 65(2): p. 157-170.

[288] Lee, S.M., T.V. O'Halloran, and S.T. Nguyen, *Polymer-caged nanobins for synergistic cisplatin-doxorubicin combination chemotherapy.* J AmChem Soc, 2010. 132(48): p. 17130-17138.

[289] Cohen, S.M., R. Mukerji, S. Cai, et al., *Subcutaneous delivery of nanoconjugated doxorubicin and cisplatin for locally advanced breast cancer demonstrates improved efficacy and decreased toxicity at lower doses than standard systemic combination therapy in vivo.* Am J Surg, 2011. 202(6): p. 646-653.

[290] Deng, C., G. Rong, H. Tian, et al., *Synthesis and characterization of poly(ethylene glycol)-b-poly (L-lactide)-b-poly(L-glutamic acid) triblock copolymer.* Polymer, 2005. 46(3): p. 653-659.

[291] Beletsi, A., L. Leontiadis, P. Klepetsanis, D.S. Ithakissios, and K. Avgoustakis, *Effect of preparative variables on the properties of poly(dl-lactide-co-glycolide)–methoxypoly(ethyleneglycol) copolymers related to their application in controlled drug delivery.* Int J Pharm, 1999. 182(2): p. 187-197.

[292] Xiong, Y., W. Jiang, Y. Shen, et al., *A Poly(γ, l-glutamic acid)-citric acid based nanoconjugate for cisplatin delivery.* Biomaterials, 2012. 33(29): p. 7182-7193.

[293] Cuong, N.V., Y.L. Li, and M.F. Hsieh, *Targeted delivery of doxorubicin to human breast cancers by folate-decorated star-shaped PEG-PCL micelle.* J Mater Chem, 2012. 22(3): p. 1006-1020.

[294] She, W., K. Luo, C. Zhang, et al., *The potential of self-assembled, pH-responsive nanoparticles of mPEGylated peptide dendron-doxorubicin conjugates for cancer therapy.* Biomaterials, 2013. 34(5): p. 1613-1623.

[295] Y, Z., Y. M, P. NG, et al., *Zeta potential: a surface electrical characteristic to probe the interaction of nanoparticles with normal and cancer human breast epithelial cells.* Biomed Microdevices, 2008. 10(2): p. 321-328.

[296] Levine, D.H., P.P. Ghoroghchian, J. Freudenberg, et al., *Polymersomes: A new multi-functional tool for cancer diagnosis and therapy.* Methods, 2008. 46(1): p. 25-32.

[297] Ahmed, F., R.I. Pakunlu, A. Brannan, et al., *Biodegradable polymersomes loaded with both paclitaxel and doxorubicin permeate and shrink tumors, inducing apoptosis in proportion to accumulated drug.* J Control Release, 2006. 116(2 SPEC. ISS.): p. 150-158.

[298] Du, Y., W. Chen, M. Zheng, F. Meng, and Z. Zhong, *PH-sensitive degradable chimaeric polymersomes for the intracellular release of doxorubicin hydrochloride.* Biomaterials, 2012. 33(29): p. 7291-7299.

[299] Liu, G.Y., C.J. Chen, and J. Ji, *Biocompatible and biodegradable polymersomes as delivery vehicles in biomedical applications.* Soft Matter, 2012. 8(34): p. 8811-8821.

[300] Discher, D.E. and F. Ahmed, *Polymersomes*, 2006. p. 323-341.